

Final Report • 16 February 2017

CO₂ CAPTURE FROM IGCC GAS STREAMS USING THE AC-ABC PROCESS

Final Report

Covering the period October 1, 2009 through September 30, 2016

SRI Project P19207 and P21321

Cooperative Agreement No.: DE-FE0000896

Principal Investigator: Anoop Nagar

Contributors: Elisabeth McLaughlin, Marc Hornbostel, Gopala Krishnan, Indira
Jayaweera, SRI International
Eli Gal, EIG, Inc.
Martin Taylor, BHTS, Inc.

Performing Organization: SRI International
333 Ravenswood Avenue
Menlo Park, CA 94025

Other Team Members: Bechtel Hydrocarbon Technology Solutions, Inc.
EIG, Inc.
National Carbon Capture Center

Prepared for: U.S. Department of Energy
National Energy Technology Center
3600 Collins Ferry Road
Morgantown, WV26505

DOE Project Manager: Steve Mascaro

DISCLAIMER

This report was prepared as an account of work sponsored by an agency of the United States Government. Neither the United States Government nor any agency thereof, nor any of their employees, makes any warranty, express or implied, or assumes any legal liability or responsibility for the accuracy, completeness, or usefulness of any information, apparatus, product, or process disclosed, or represents that its use would not infringe privately owned rights. Reference herein to any specific commercial product, process, or service by trade name, trademark, manufacturer, or otherwise does not necessarily constitute or imply endorsement, recommendation, or favoring by the United States Government or any agency thereof. The views and opinions of authors expressed herein do not necessarily state or reflect those of the United States Government or any agency thereof.

CONTENTS

DISCLAIMER	1
CONTENTS.....	2
LIST OF TABLES	3
LIST OF ILLUSTRATIONS	4
ABSTRACT.....	7
EXECUTIVE SUMMARY	8
INTRODUCTION	10
WORK PERFORMED	11
Budget Period 1.....	11
Bench-scale Test Unit Construction	11
Bench-scale Absorber Tests.....	14
Bench-scale Regenerator Testing	33
Bench-scale Test Data Analysis.....	42
Preliminary Process Modeling and Cost Economics	48
Budget Period 2	48
Small Pilot-Scale Design	48
Integrated Plant Operation – First Test Campaign	50
Analytical Testing.....	55
System Modification and Maintenance	60
CO ₂ / H ₂ S Separation Process.....	64
Second Test Campaign	66
Pilot-Plant Modification.....	67
Pilot-Plant Operation	69
Discussion of Results	71
Process Modelling.....	91
TECHNO-ECONOMIC ANALYSIS OF AC-ABC PROCESS: SUMMARY	101
IGCC Reference Case	102
IGCC Case with AC-ABC CO ₂ and H ₂ S Capture	104
Cost Estimating Methodology and Assumptions.....	107
AC-ABC Process Details and Assumptions	110
Plant Performance Summary with AC-ABC CO ₂ and H ₂ S Capture	116
Cost Advantages of AC-ABC Process.....	117
Sensitivity Analyses.....	119
APPENDIX A.....	123
Equipment Cost List for AC-ABC Process	123
Operating and Maintenance Cost Summary	125
CONCLUSIONS.....	130
REFERENCES	132

LIST OF TABLES

Table 1. Details of the initial absorber test conditions for a 50-SLPM test gas flow rate.	14
Table 2. Details of the absorber test conditions at 30°C.	19
Table 4. Residual NH ₃ partial pressures at varying temperature and CO ₂ loadings.	24
Table 5. Absorber test conditions to determine the H ₂ S capture efficiency.	26
Table 6. Solubility of gases in aqueous solutions at 20°C.	28
Table 7. Absorber test conditions to determine the H ₂ S capture efficiency in gas mixtures.	29
Table 8. Bench-scale absorber data for H ₂ S absorption under varying conditions.	30
Table 9. Test conditions and results from regenerator runs.	38
Table 10. Typical raw syngas stream composition from the lignite coal gasifier at NCCC.	70
Table 11. Regenerations #1-#4.	87
Table 12. Regenerations #5-#8.	87
Table 13. Near complete removal of sulfur in BPSC.	90
Table 14. Net power output and relative efficiency in CO ₂ capture.	100
Table 15. CO ₂ capture costs compared to IGCC base case (Case B5A).	101
Table 16. Capital cost comparison to IGCC base case (Case B5A).	101
Table 17. Stream tables: GEE IGCC with AC-ABC and BPSC.	106
Table 18. Factors for calculating BEC and TPC from delivered equipment cost.	108
Table 19. Difference in Selexol and AC-ABC total plant cost.	109
Table 20. AC-ABC process stream tables.	113
Table 21. Plant performance summary.	117
Table 22. Summary of sensitivity analysis results.	119
Table 23. Equipment costs for AC-ABC and BPSC process.	123
Table 24. GEE IGCC with AC-ABC/ BPSC: initial/annual operating and maintenance costs.	125
Table 25. DOE Case B5B: initial and annual operating and maintenance costs (NETL 2015).	127

LIST OF ILLUSTRATIONS

Figure 1. Schematic diagram of the bench-scale test unit.....	12
Figure 2. A photograph of the bench-scale test unit.	13
Figure 3. CO ₂ capture efficiency of a 4 M ammonia solution at 165 psig at 20° to 55°C.....	15
Figure 4. Variation of CO ₂ capture efficiency with temperature for 4 M ammonia solution at 165 psi at varying CO ₂ loadings.	16
Figure 5. CO ₂ capture efficiency of a 4 M ammonia solution at 165 and 265 psig at 20°C.....	17
Figure 6. Calculated CO ₂ loading at varying CO ₂ /NH ₃ ratios for 4, 6, and 10 M starting ammonia concentrations.	18
Figure 7. Observed CO ₂ capture as a function of the CO ₂ /NH ₃ ratio and the CO ₂ partial pressure at 30°C and 265 psia.	20
Figure 8. Observed CO ₂ loading for a 6 M ammonia solution as a function of CO ₂ partial pressure at 30 C and 265 psig.	20
Figure 9. CO ₂ capture efficiency of 4 and 8 M ammonia solutions at 265 psia at 30° to 60°C. .	22
Figure 10. CO ₂ capture rates of 4 and 8 M ammonia solutions at 265 psia at 43° to 60°C.....	23
Figure 11. CO ₂ capture rate of 4 and 8 M ammonia solutions at 265 psia at 33° to 60°C.	24
Figure 12. The relationship between calculated CO ₂ back pressure and the measured CO ₂ capture rate.....	25
Figure 13. Measured H ₂ S capture efficiency for 7.5 to 8 M ammonia solutions at 50°C.	27
Figure 14. CO ₂ and H ₂ S capture efficiencies of ammonia solutions at varying CO ₂ loadings....	29
Figure 15. Effect of gas flow rate and the scrubbing solution CO ₂ /NH ₃ ratio on H ₂ S absorption at 25°C.	31
Figure 16. Effect of gas flow rate and the liquid recirculation rate on H ₂ S absorption.....	32
Figure 17. Effect of liquid circulation to gas flow rate ratio on H ₂ S absorption.	32
Figure 18. Schematic diagram of the bench-scale regenerator unit.	34
Figure 19. Photograph of the regenerator.	35
Figure 20. Evolution of CO ₂ from the ammonium bicarbonate solution as a function of temperature.	36
Figure 21. Measured P-T curves for H ₂ S-H ₂ O-CO ₂ -NH ₃ from static experiments.	36
Figure 22. Equilibrium solubilities of H ₂ S in H ₂ S-H ₂ O-CO ₂ -NH ₃ system at a temperature of 50°C and pressures of 20 and 40 bar.	37
Figure 23. Variation of the R value (molar NH ₃ /CO ₂ ratio) in the regenerated solution as a function of regenerator temperature at 300 psig.	39
Figure 24. Effect of temperature and pressure on H ₂ S composition in the regenerator exit gas. 40	
Figure 25. Effect of pressure on H ₂ S composition in the regenerator exit gas at 120° and 165°C.	40
Figure 26. Variation of CO ₂ /H ₂ S ratio in the regenerator exit gas with pressure at 120° and 165°C.	41
Figure 27. Trace removal of hydrogen sulfide from the absorber exit gas.....	42

Figure 28. Partial pressure of CO ₂ at the top of the absorber column as a function of the scrubbing solution CO ₂ /NH ₃ ratio.	43
Figure 29. Estimated heat of reaction for CO ₂ absorption into an 8 M NH ₃ solution.	44
Figure 30. Gas mass-transfer coefficient for CO ₂ capture at 55°C and 20 bar.	46
Figure 31. Height of mass-transfer unit for CO ₂ absorption as a function of CO ₂ loading of the ammonia capture at 55°C and 20 bar.	47
Figure 32. Process flow diagram of the AC-ABC system.	50
Figure 33. CO ₂ concentration in syngas (Run #3).	51
Figure 34. CO ₂ capture efficiency (Run #3).	52
Figure 35. H ₂ S concentration in syngas (Run #3).	52
Figure 36. Absorber pressure (Run #3).	54
Figure 37. Regenerator pressure (Run #3).	55
Figure 38. CO ₂ loading (Run #3).	56
Figure 39. CO ₂ / NH ₃ loading (Run #3).	57
Figure 40. CO ₂ loading (Run #2).	57
Figure 41. NH ₃ & H ₂ S concentrations in regenerator gas.	58
Figure 42. Gas composition (dry basis) of regenerated gas stream.	59
Figure 43. Mass balance of hydrogen.	59
Figure 44. NH ₃ concentration in clean syngas.	60
Figure 46. X-ray fluorescence analysis of the syngas-entrained particles.	62
Figure 47. Semi-quantitative analysis by X-ray diffraction of syngas-entrained particles.	63
Figure 48. Sulfur in outlet plenum of reactor intercooler HX-04.	64
Figure 49. Close-up view of sulfur in outlet plenum of reactor intercooler HX-04.	65
Figure 50. Raw syngas availability.	70
Figure 51. Syngas availability during Run #10.	71
Figure 52. Raw syngas, clean syngas, and regenerated gas stream mass flow rate (Run #10).	72
Figure 53. Concentration of CO ₂ in raw and clean syngas (Run #10).	72
Figure 54. Concentration of H ₂ S in raw and clean syngas (Run #10).	73
Figure 55. Capture efficiency and CO ₂ loading in solvent (Run #10).	74
Figure 56. CO ₂ loading varied by changing solvent recirculation rate (Run #10).	75
Figure 57. Ammonia and sulfide concentrations in lean solution (Run #10).	76
Figure 58. CO ₂ loading in lean and rich solution (Run #10).	77
Figure 59. Ammonia in clean syngas from absorber (Run #10).	77
Figure 60. Absorber bottom-stage temperature profile (Run # 10).	78
Figure 61. Absorber and regenerator pressure (Run #10).	79
Figure 62. Reboiler temperature for thermal siphon (Run #10).	79
Figure 63. Regenerated gas stream main constituents.	80
Figure 64. Methane and carbon monoxide in the regenerated stream.	81

Figure 65. Hydrogen and argon in the regenerated gas stream.....	81
Figure 66. Gas mass balance (Run #10).	82
Figure 67. Energy input to reboiler (Run #10).....	83
Figure 68. BPSC diagram.	85
Figure 69. The graph shows good regeneration and different temperatures at various catalytic reactor locations. Multiple temperature levels (once stabilized) show significant heat loss from the reactor vessel.	89
Figure 70. Schematic of the Selexol process for 90% CO ₂ capture and sequestration at 2,200 psi; H ₂ S outlet is 10 ppm.	93
Figure 71. Schematic of the AC-ABC process for 90% CO ₂ capture and sequestration at 2,200 psi; the emissions at the H ₂ S outlet are 10 ppm.....	95
Figure 72. CO ₂ compressor power for compression of 500 st/h of CO ₂ to 2,215 psia.	96
Figure 73. Pump power for pumping lean solution to the CO ₂ absorber as a function of the CO ₂ stripper operating pressure (pump feed pressure).....	97
Figure 74. Saturated steam temperature required for the stripping of CO ₂	99
Figure 75. Case B5B block flow diagram.....	103
Figure 76. GEE IGCC block flow diagram with AC-ABC and BPSC.....	105
Figure 77. AC-ABC block flow diagram.....	112
Figure 78. Bechtel pressure-swing Claus process to convert H ₂ S to elemental sulfur.	115
Figure 79. A photograph of the AC-ABC pilot plant at the NCCC.....	128
Figure 80. A photograph of the AC-ABC process skids.....	128
Figure 81. A photograph of sulfur recovery reactors.....	129
Figure 82. A photograph of skid B-1 with sulfur condensers.....	129

ABSTRACT

The objective of this project was to develop a novel, low-cost CO₂ capture process from pre-combustion gas streams. The bench-scale work was conducted at the SRI International. A 0.15-MWe integrated pilot plant was constructed and operated for over 700 hours at the National Carbon Capture Center, Wilsonville, AL.

The AC-ABC (ammonium carbonate-ammonium bicarbonate) process for capture of CO₂ and H₂S from the pre-combustion gas stream offers many advantages over Selexol-based technology. The process relies on the simple chemistry of the NH₃-CO₂-H₂O-H₂S system and on the ability of the aqueous ammoniated solution to absorb CO₂ at near ambient temperatures and to release it as a high-purity, high-pressure gas at a moderately elevated regeneration temperature. It is estimated the increase in cost of electricity (COE) with the AC-ABC process will be ~ 30%, and the cost of CO₂ captured is projected to be less than \$27/metric ton of CO₂ while meeting 90% CO₂ capture goal.

The Bechtel Pressure Swing Claus (BPSC) is a complementary technology offered by Bechtel Hydrocarbon Technology Solutions, Inc. BPSC is a high-pressure, sub-dew-point Claus process that allows for nearly complete removal of H₂S from a gas stream. It operates at gasifier pressures and moderate temperatures and does not affect CO₂ content. When coupled with AC-ABC, the combined technologies allow a nearly pure CO₂ stream to be captured at high pressure, something which Selexol and other solvent-based technologies cannot achieve.

EXECUTIVE SUMMARY

Capturing CO₂ from coal-fired power plants is a critical step in carbon sequestration. In the integrated gasification combined cycle (IGCC) process, which generates electricity more efficiently than do pulverized coal (PC) combustion power plants, coal is reacted with steam and O₂ under pressure in the range of 300 to 1000 psi to form a fuel gas containing mainly CO, H₂, H₂S, CO₂, and residual steam. The current “best-case” option for carbon capture is using a liquid solvent such as Selexol or Rectisol to absorb CO₂ and H₂S at elevated pressures, and it is estimated that the cost of electricity (COE) will increase by more than 41% if CO₂ is captured by a Selexol-based process (NETL 2015).

The AC-ABC (ammonium carbonate-ammonium bicarbonate) process for capture of CO₂ and H₂S from the pre-combustion gas stream offers many advantages over Selexol-based technology. The process relies on the simple chemistry of the NH₃-CO₂-H₂O-H₂S system and on the ability of the aqueous ammoniated solution to absorb CO₂ at near ambient temperatures and to release it as a high-purity, high-pressure gas at a moderately elevated temperature. It is estimated the increase in COE with the AC-ABC process will be ~ 30%, and the cost of CO₂ captured is projected to be less than \$27/metric ton of CO₂ while meeting 90% CO₂ capture goal.

In Budget Period 1, we used a bench-scale absorber and determined the optimum operating conditions for absorption of CO₂ and H₂S from simulated fuel gas streams using ammoniated solutions at elevated pressures. A bench-scale reactor was also used to strip CO₂ and H₂S from loaded solutions containing carbonates and sulfides. A preliminary economic analysis was performed to estimate the COE for CO₂ capture using the AC-ABC process and compare it with a Selexol-based process. The results of this analysis showed that the AC-ABC process offers a significant reduction in the increase in the COE and has the potential to meet the DOE target.

Based on the bench-scale test results, a small-scale pilot plant (0.15 MWe) was designed to process 500 lb/hr of shifted syngas from an air blown gasifier at the National Carbon Capture Center (NCCC) in Wilsonville, Alabama during Budget Period 2. Bechtel Hydrocarbon Technologies, Inc. designed a sub-dew-point Claus process that was installed downstream to separate H₂S from CO₂ and convert the same to elemental sulfur.

The pilot plant was operated for over 700 hours in two test campaigns including a continuous 7-day (175 hr) run. Based on the results from the test runs and liquid and gas analysis, the following conclusions can be drawn:

- Ammoniated solution is very effective in rapid absorption of CO₂ with high CO₂ loading at elevated pressure. CO₂ capture efficiency greater than 99% was demonstrated, with 12% CO₂ effective loading.
- H₂S can be simultaneously absorbed along with CO₂ in a single absorber column. The H₂S capture efficiency was greater than 99%.
- The absorption and thus loss of fuel gas species like H₂, CO, and CH₄ was shown to be very low.
- Low ammonia loss from the system was demonstrated.
- Both the absorber and regenerator were operated at similar elevated pressure, thus reducing the need for pumping solvents across pressure boundaries.
- Simultaneous stripping of CO₂ and H₂S was demonstrated in a single column at elevated pressure and moderate temperature.
- The Bechtel Pressure-Swing Claus Process (BPSC) process demonstrated conversion of H₂S to high-purity elemental sulfur, and a clean CO₂ gas stream at elevated pressure was available for sequestration or transportation.
- Availability of regenerated CO₂ at elevated pressure significantly reduced the compressor requirements for CO₂ sequestration.
- A techno-economic analysis showed the cost of CO₂ capture using the AC-ABC / BPSC process from the IGCC gas stream is less than \$27/metric ton of CO₂.

INTRODUCTION

Capturing CO₂ from coal-fired power plants is a critical step in carbon sequestration. In the IGCC process, which generates electricity more efficiently than do pulverized coal (PC) combustion power plants, coal is reacted with steam and O₂ under pressure in the range of 300 to 1000 psi to form a fuel gas containing mainly CO, H₂, H₂S, CO₂, and residual steam. The CO in the gas stream is converted to CO₂ and H₂ by using the water-gas shift reaction at about 200° to 285°C. The gas stream leaving the water-gas shift reactor (WGSR) contains mainly H₂, CO₂, H₂S, and H₂O. An H₂-rich fuel gas suitable for combustion in a gas turbine is produced by condensing the steam and removing the CO₂ and H₂S. The current “best-case” option for carbon capture is using a liquid solvent such as Selexol or Rectisol to absorb CO₂ and H₂S at elevated pressures.

The AC-ABC process for capture of CO₂ and H₂S in the precombustion gas stream offers many advantages over solvent-based technology. The process relies on the simple chemistry of the NH₃-CO₂-H₂O-H₂S system and on the ability of the aqueous ammoniated solution to absorb CO₂ at near ambient temperatures and to release it as a high-pressure gas at a moderately elevated temperature.

Bechtel’s Pressure Swing Claus (BPSC) technology is used to recover sulfur from a high-pressure gas (CO₂, syngas, or hydrocarbons) as liquid sulfur using SO₂ as an oxidant. Multiple sub-dew-point reactors are used in rotation (Lead/Lag/Regeneration) similar to a molecular sieve dehydration unit (Mole-Sieve), a pressure swing absorption unit (PSA), or a low-pressure sub-dew-point Claus process.

The overall objective of the program was to develop, for IGCC-based power plants, an innovative, low-cost CO₂ capture technology based on absorption on a high-capacity and low-cost aqueous ammoniated solution. The specific objectives were to:

1. Test the technology on a bench-scale batch reactor to validate the concept and to determine the optimum operating conditions for a small pilot-scale reactor,
2. Design, build, and perform tests using a small pilot-scale reactor capable of continuous integrated operation, and
3. Perform a technical and economic evaluation on the technology.

The experimental program consisted of three tasks:

1. Bench-scale batch tests
2. Pilot-scale integrated, continuous tests
3. Project management

WORK PERFORMED

BUDGET PERIOD 1

The work performed in Budget Period 1 was mainly in Task 1. Task 1 consists of several subtasks:

1. Bench-scale test unit construction
2. Development of test plans
3. Absorber tests
4. Regenerator tests
5. Bench-scale test data analysis
6. Preliminary process modeling
7. Preliminary economic analysis

Bench-scale Test Unit Construction

We modified an existing high-pressure reactor to conduct absorption tests with simulated IGCC gas streams representative of those downstream of a WGSR. Figures 1 and 2 are a schematic diagram and photograph of the bench-scale unit, respectively. The high-pressure reactor or absorption column was constructed of stainless steel and is rated for operating up to 600 psi. It has an internal diameter (ID) of 4 in and a length of 48 in. A stainless steel structural packing (22-in long) with a packing density of $425 \text{ m}^2/\text{m}^3$ is placed inside the column to facilitate the gas-liquid contact. The ammonium carbonate feed solution is injected at the top of the column using a high-pressure metering pump. The test gas stream consisting of CO_2 , H_2 , H_2S , and N_2 is blended using pure or mixed gases and metered into the bottom of the column using mass flow controllers. The absorber solution is circulated through the column with a gear pump, and the liquid level inside the column is monitored with a level indicator that is capable of operating at elevated pressures. The heat generated by the absorption reaction is removed from the circulating solution with an external heat exchanger. The pressure, temperature, and flow rate of liquid and gas streams are monitored and recorded. The gas exiting the reactor is scrubbed to remove trace levels of H_2S and vented. The circulating liquid is withdrawn at a rate to maintain a constant level in the column and collected in the spent solution reservoir.

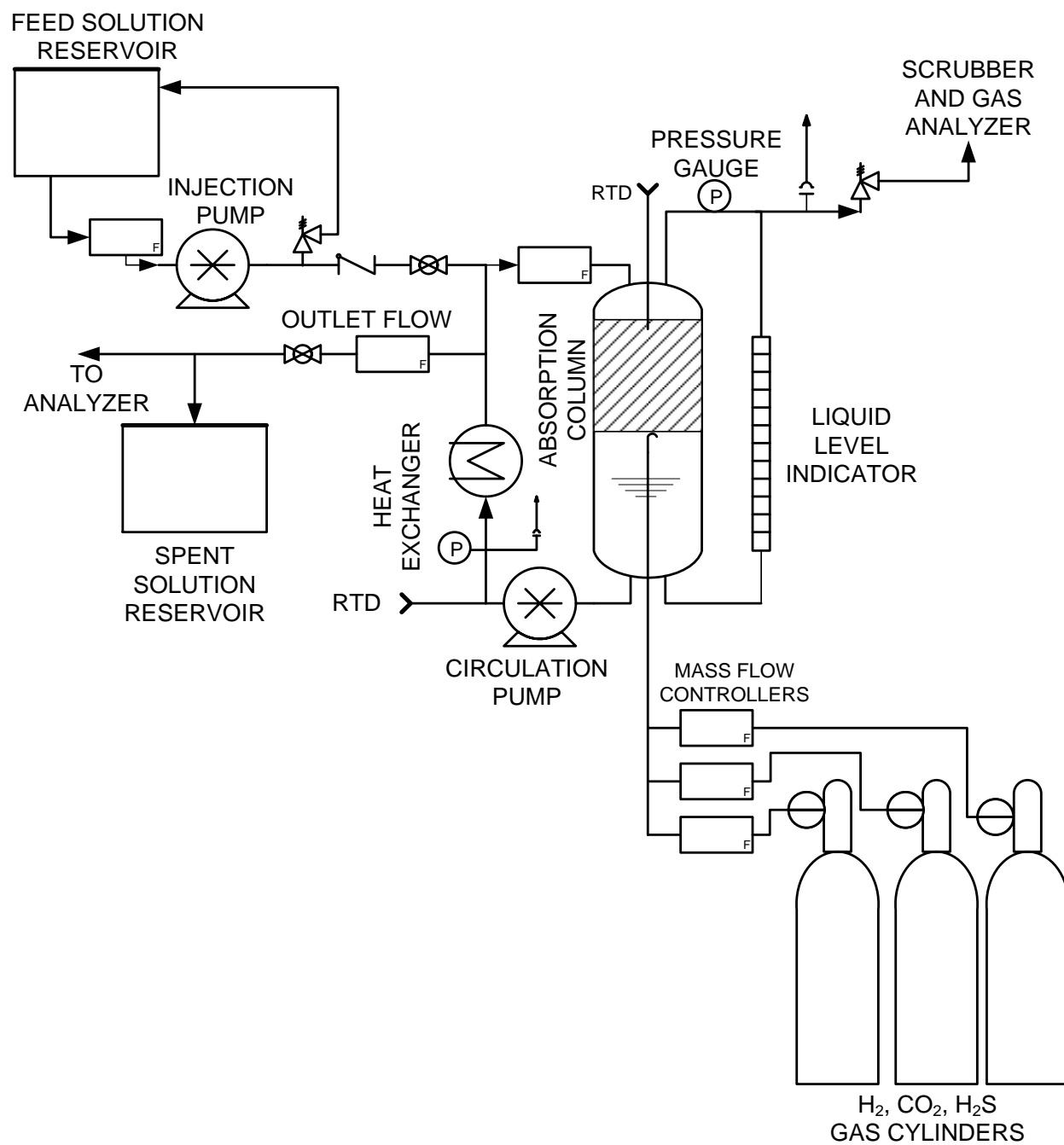


Figure 1. Schematic diagram of the bench-scale test unit.



Figure 2. A photograph of the bench-scale test unit.

The composition of the gas stream leaving the absorber was monitored by several techniques including an on-line infrared absorption CO₂ monitor, gas chromatography, and liquid chromatography depending on the nature of the component. Infrared absorption is a

standard technique for monitoring the CO₂ concentration in a gas mixture. The gas chromatography was used to determine the H₂ and H₂S concentrations in the gas stream. We determined the residual NH₃ concentration in the absorber exit gas by dissolving the gas in a dilute acid and measuring NH₃⁺ concentration with a liquid by ion chromatograph. The NH₃ and CO₂ levels in the solution were determined by titration.

Bench-scale Absorber Tests

CO₂ Absorption Rate Measurements: In the first series of tests (Test Series A), a 4 M ammonia solution was tested at two different pressure (165 and 265 psi) and four different temperatures (20°, 30°, 45°, and 55°C) to determine the effects of temperature and pressure on the CO₂ capture efficiency. Table 1 shows the test conditions. When conducting these tests, the reactor was filled initially with the predetermined amount of 4 M ammonia solution with known CO₂ loading followed by solution recycle through the packing and the heat exchanger at the set pressure; in most cases, N₂ is used to set the pressure to the desired test pressure. Once the system is equilibrated at a known temperature, pressure, and starting CO₂ loading, the gas mixture to be tested is introduced through the bottom of the absorber. The percentage of CO₂ capture efficiency of the ammonia solution for capturing CO₂ from the test gas stream is evaluated by measuring the inlet CO₂ concentration, and the outlet CO₂ concentration is measured using a Horiba infrared CO₂ analyzer.

Table 1. Details of the initial absorber test conditions for a 50-SLPM test gas flow rate.

Run Number	NH ₃ Concentration (M)	Starting CO ₂ Loading (CO ₂ /NH ₃ molar ratio)	CO ₂ -Feed Gas (%)	Temperature (°C)	Pressure (psi)
Run 3	4	0.14	50	20	165
Run 4	4	0.14	50	30	265
Run 5	4	0.14	50	20	165
Run 6	4	0.14	50	45	165
Run 7	4	0.14	50	55	165

Figure 3 shows the data from Runs #3, 4, 6, and 7 that compares the effect of temperature on the CO₂ capture efficiency at 165 psi pressure. A test gas stream with a 50% v/v inlet CO₂ at a gas feed flow rate of 50 SLPM was used in these tests. The operating liquid-to-gas ratio of the absorber was 50 kg/kg. The data shows that the capture efficiency is ~ 100% when the solution's CO₂/NH₃ ratio is less than 0.4, indicating that the absorption of CO₂ into the solution is rapid. As more CO₂ is absorbed into the solution, the rate of CO₂ capture decreases. At a CO₂/NH₃ ratio

(defined as R') of 1, no more CO_2 can be absorbed because the solution is saturated with ammonium bicarbonate (NH_4HCO_3). At a reactor pressure of 165 psig, the capture efficiency increases with increasing temperature from 20° to 45°C but decreases at higher temperatures. This effect of temperature on the rate of CO_2 capture can be understood from kinetic and equilibrium considerations as described below.

To understand the effect of temperature, we considered the equilibrium of the aqueous-phase $\text{NH}_3\text{-H}_2\text{O-CO}_2$ system. The well-known reaction mechanism between carbon dioxide and aqueous ammonia is as follows

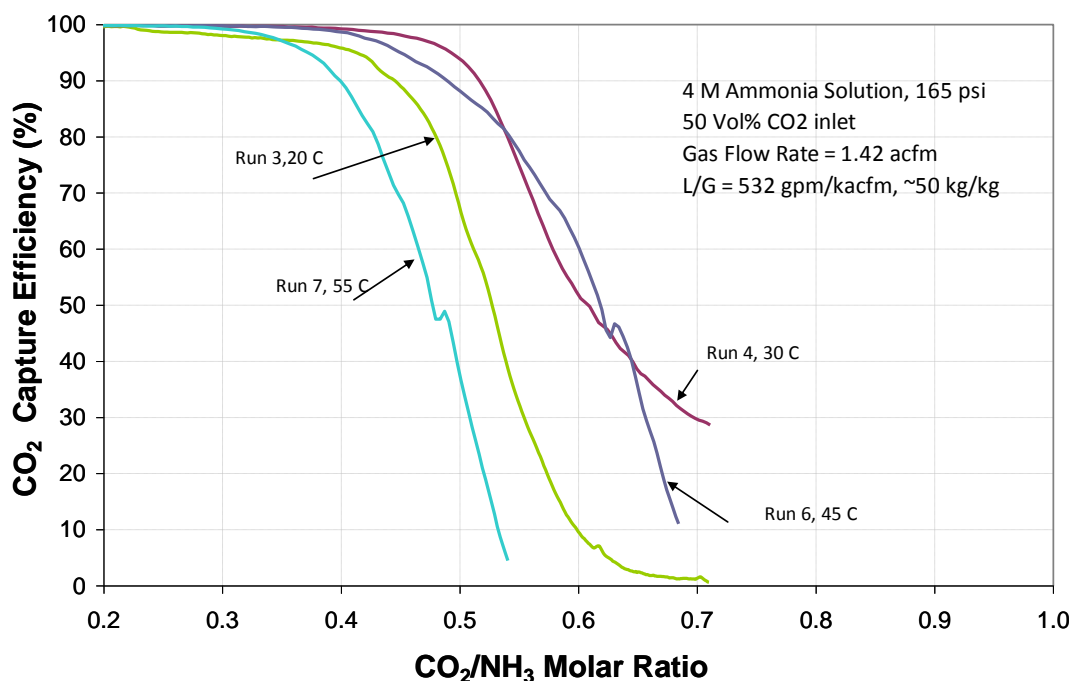
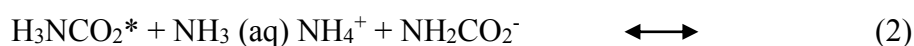


Figure 3. CO_2 capture efficiency of a 4 M ammonia solution at 165 psig at 20° to 55°C.

In dilute solutions, mostly bicarbonate (HCO_3^-) and carbonate (CO_3^{2-}) ions are formed; in concentrated solutions, and the reaction product is mainly carbamate (H_3NCO_2^*). As more CO_2 is absorbed in the solution, CO_2 loading (defined as CO_2/NH_3 ratio) increases. Note that CO_2

loadings of 1 and 0.5 correspond to NH_4HCO_3 and $(\text{NH}_4)_2\text{CO}_3$ compounds, respectively. Ammonium bicarbonate solids precipitate when the CO_2 loading increases above a certain value, depending on the ammonia molarity of the solution and temperature. The above-discussed tests were conducted at CO_2 loading values below the precipitation point.

Figure 4 illustrates the measured CO_2 capture efficiency as a function of temperatures for various CO_2 loadings. The data indicates that the capture efficiency increases with temperatures up to a 35°C as the reaction kinetics increase. At a higher temperature, the partial pressure of CO_2 in equilibrium with the solution also increases, providing a backpressure for absorption, and the rate of CO_2 capture decreases.

Figure 5 compares the effect of pressure on CO_2 capture efficiency using the data from Runs #3 and 5. This data indicates that the CO_2 capture efficiency increases with increasing absorber pressure from 165 psi to 265 psi, as expected for a gas-liquid reaction. We believe that at a given temperature, the rate of CO_2 capture will continue to increase with the pressure.

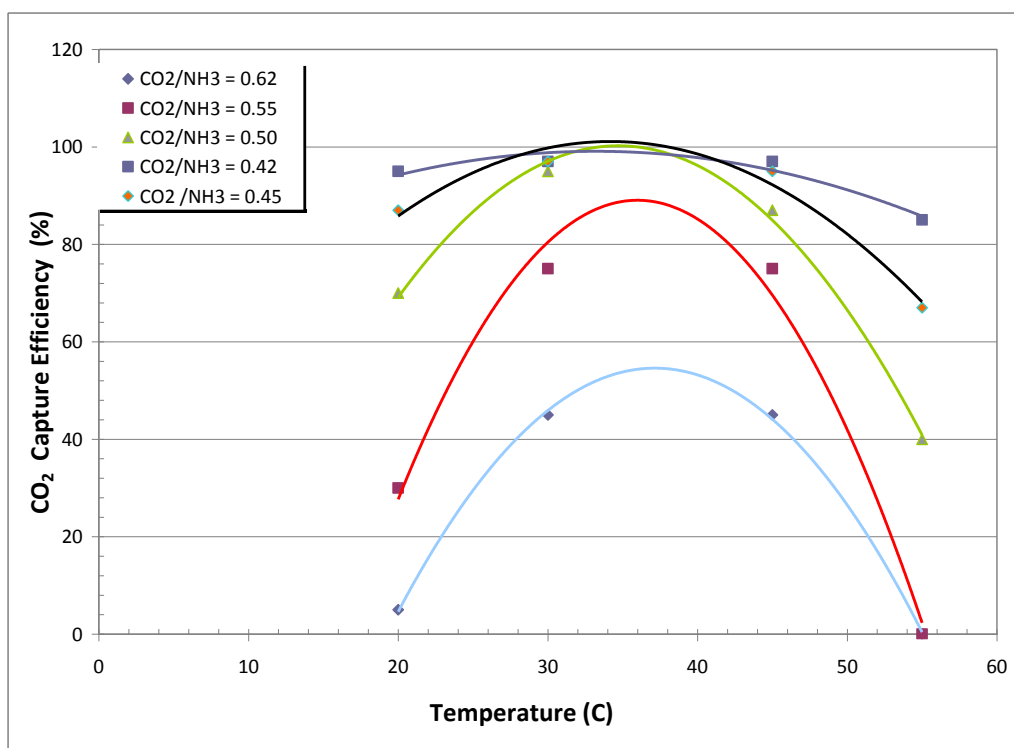


Figure 4. Variation of CO_2 capture efficiency with temperature for 4 M ammonia solution at 165 psi at varying CO_2 loadings.

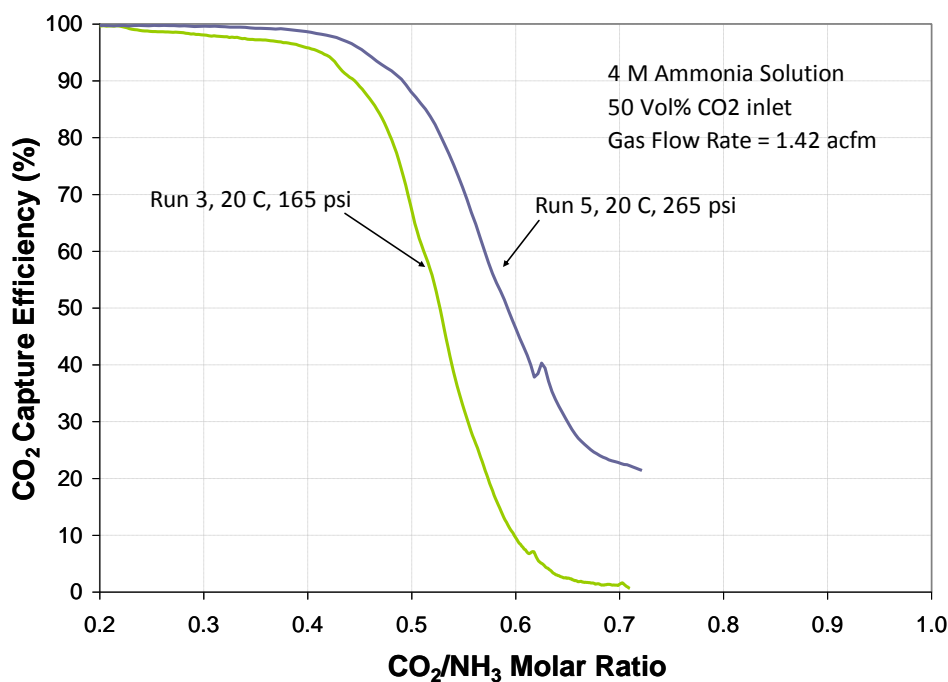


Figure 5. CO₂ capture efficiency of a 4 M ammonia solution at 165 and 265 psig at 20°C.

In another series of tests (Test Series B), we used a higher ammonia concentration to achieve a > 10 wt% CO₂ loading at a CO₂/NH₃ solution ratio less than 0.6. Figure 6 shows the calculated CO₂ loading in the solution as a function of the solution composition for 4-, 6-, and 10-M ammonia solutions. With a 6 M ammonia solution, 10 wt% CO₂ loading can be achieved even at a CO₂/NH₃ ratio of 0.4.

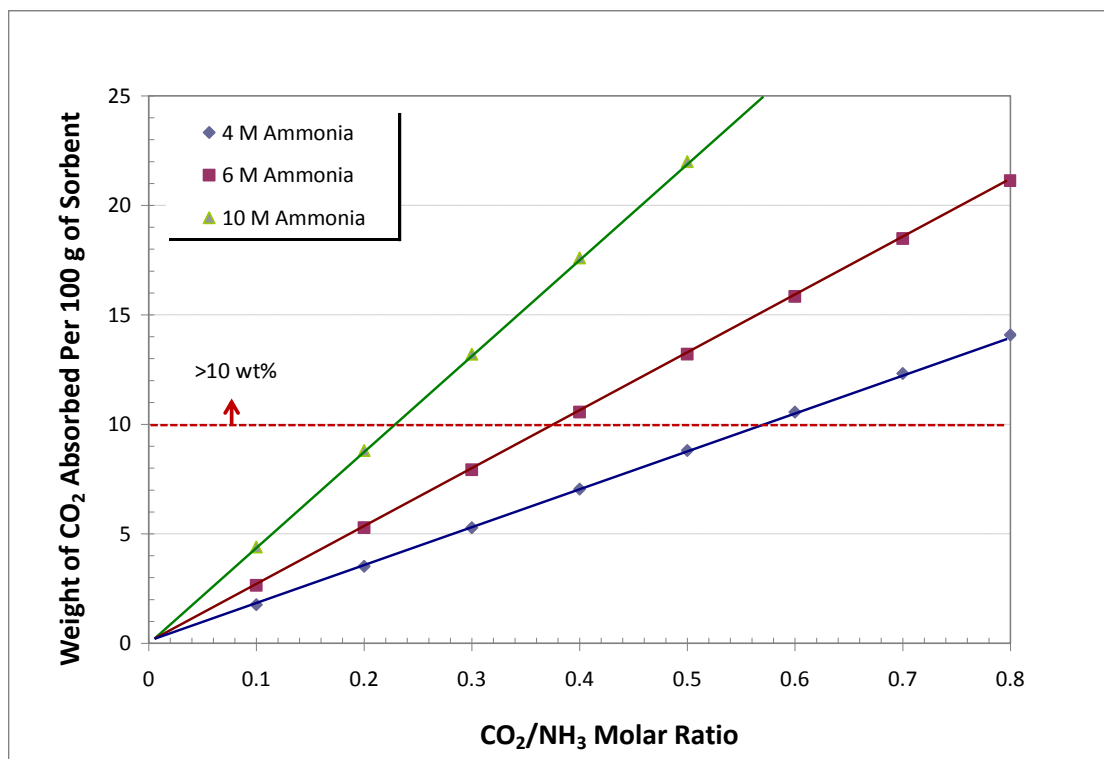


Figure 6. Calculated CO₂ loading at varying CO₂/NH₃ ratios for 4, 6, and 10 M starting ammonia concentrations.

Test Series B was performed at a constant temperature (30°C) and pressure (265 psig) with varying CO₂ partial pressures. The rate of absorption of CO₂ was determined by measuring the CO₂ uptake with time. In this series of runs, the goal was to obtain the CO₂ absorption rate for a given ammonia concentration and a partial pressure of CO₂ as a function of the CO₂/NH₃ molar ratio in the solution. Table 2 shows the details of Runs #8, 9a, 9b, and 10, and the observed CO₂ absorption rate data is illustrated in Figure 7. Only the absorption rates that are comparable to the first series of runs (< 14 SLPM) and that can be measured with a reliable accuracy (the rate of change in the absorption rate is very fast in solution with low CO₂/NH₃ ratios) are reported here. Data from Figure 7 indicate that at high CO₂ partial pressures, it is possible to achieve high CO₂ absorption rates even at high CO₂ loadings. The CO₂ absorption rate is 14 standard liters/min at 30°C and 265 psi (25 %v/v CO₂) for a 6 M ammonia solution and a CO₂/NH₃ ratio of 0.65. This rate is reasonable for the size of the absorber (0.0045 m³) used in this work. A comparison of CO₂ loadings (wt %) and the CO₂ partial pressure at the gas inlet corresponds to the 8 and 14 SLPM CO₂ absorption rate shown in Figure 8. This shows that the CO₂ loading of the solution at a given temperature increases with increasing partial pressure of CO₂.

Table 2. Details of the absorber test conditions at 30°C.

Run Number	NH ₃ Concentration	Starting CO ₂ Loading	CO ₂ Partial Pressure		Total Pressure
	(M)	(CO ₂ /NH ₃ molar ratio)	(vol. %)	(psi)	(psia)
Run 8	6	0.12	6	15.9	265
Run 9a	6	0.17	9	23.8	265
Run 9b	6	0.17	9	23.8	265
Run 9c	6	0.17	9	23.9	265
Run 10	6	0.17	25	66.2	265

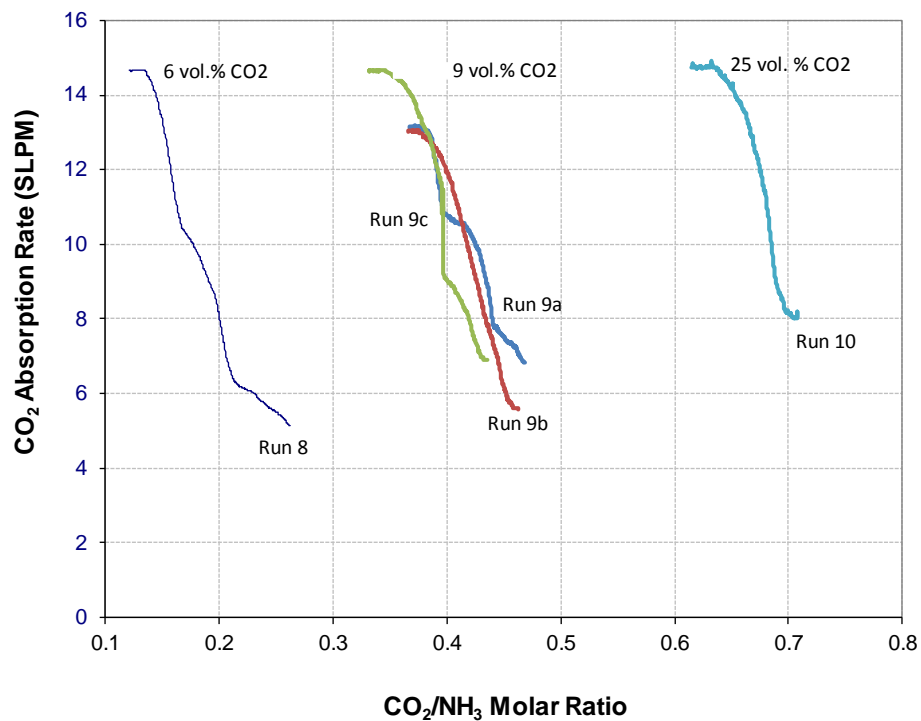


Figure 7. Observed CO₂ capture as a function of the CO₂/NH₃ ratio and the CO₂ partial pressure at 30°C and 265 psia.

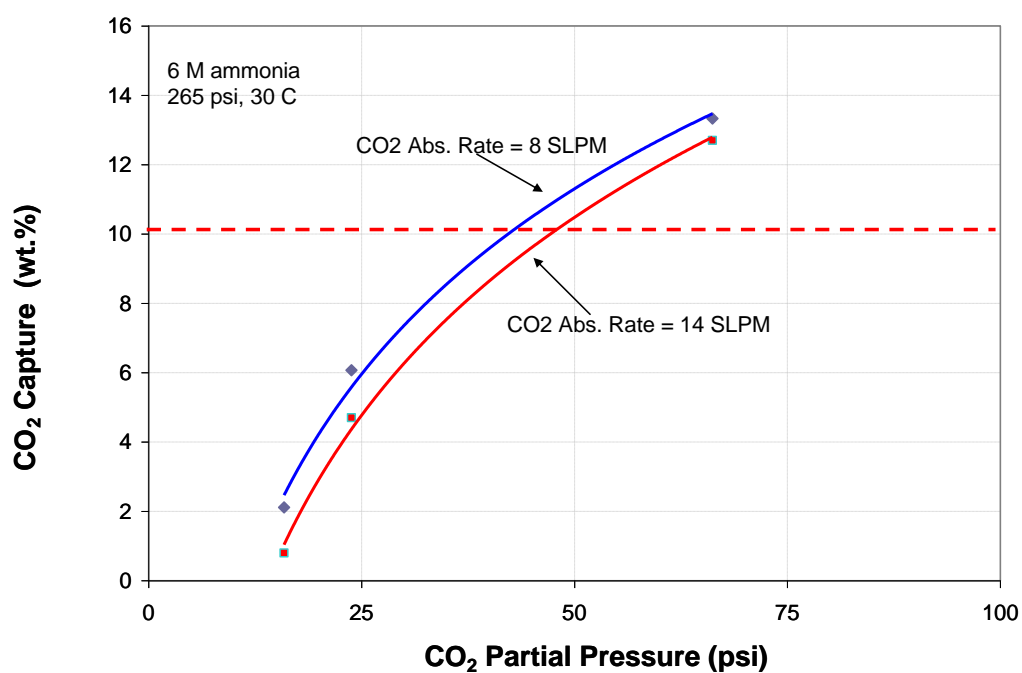


Figure 8. Observed CO₂ loading for a 6 M ammonia solution as a function of CO₂ partial pressure at 30°C and 265 psig.

Another series of tests (Test Series C) was conducted to determine the CO₂ capture efficiency as a function of temperature and pressure with the absorber operating under a continuous flow mode. We used feed solutions containing 4 or 8 M ammonia with varying [CO₂]/[NH₃] molar ratios (defined as R'), ranging from 0.45 to 0.7. Two different pressures (165 and 265 psi) and varying temperatures (33° to 55°C) were used. A constant feed gas flow rate of 100 SLPM was used in these tests.

Table 3 shows the test conditions for this series of tests. When conducting these tests, the reactor was filled initially with a predetermined volume of the feed solution with known NH₃ and CO₂ loadings. The solution was circulated through the packing, and the heat exchanger was kept at the set pressure so the solution was equilibrated. A gas mixture containing 25 % v/v CO₂ in N₂ was introduced through the bottom of the absorber, and the CO₂ concentration outlet gas was measured using a Horiba infrared CO₂ analyzer. The percentage CO₂ capture efficiency of the ammonia solution was calculated from the difference between the CO₂ concentrations in the feed and the outlet gas streams. To maintain a constant CO₂ loading during each run, a small stream of make-up ammonia solution was metered into the absorber. The liquid level in the absorber was held constant by bleeding the solvent solution to match the make-up addition.

Table 3. Absorber test conditions to determine the CO₂ capture efficiency.

Run #	[NH ₃] (mol/L)	Bulk CO ₂ loading (CO ₂ /NH ₃)	Liquid Recirculation (L/min)	Liquid Flow (L/min)	Gas Flow (L/min)	CO ₂ - Feed (% v/v)	Total P (psia)	T (°C)
11	4	0.63	3.1	0.36	100	25	165	43
13a	4	0.63	3.1	0.36	100	25	225	44
13b	4	0.71	3.1	0.36	100	25	295	45
14	4	0.63	3.1	0.36	100	25	215	39
15	4	0.50	3.1	0.36	100	25	90	32
16a	4	0.60	3.1	0.36	100	25	280	33
16b	4	0.65	3.1	0.25	100	25	280	33
17a	4	0.62	3.1	0.36	100	25	275	50
17b	4	0.66	3.1	0.25	100	25	280	50
18	4	0.62	3.1	0.36	100	25	270	43
19a	4	0.65	3.1	0.36	100	25	265	60
19b	4	0.61	3.1	0.40	100	25	250	60
20a	4	0.61	3.1	0.32	100	25	265	42
20b	4	0.67	3.1	0.25	100	25	265	42
20c	4	0.56	3.1	0.40	100	25	265	40
21a	8	0.46	3.1	0.21	100	25	255	54
21b	8	0.52	3.1	0.19	100	25	255	54
22a	8	0.54	3.1	0.18	100	25	275	64
22b	8	0.56	3.1	0.15	100	25	275	64
23	8	0.60	3.1	0.15	100	25	275	61

Figure 9 compares the effect of CO₂ loading in the solution (R') on the CO₂ capture efficiency; the data (Runs #16, 17, 18, 19, and 20) was normalized to a CO₂ partial pressure of 450 kPa (66.25 psi). The data shows that the capture efficiency (moles of CO₂ absorbed/moles of NH₃ in feed) is ~ 100% at R' values less than 0.4, indicating that the absorption of CO₂ into the solution is rapid. As more CO₂ is absorbed into the solution, the CO₂ capture rate decreases due to increased CO₂ loading in the solution. The capture efficiency decreases at high temperatures due to the increasing equilibrium partial pressure of CO₂ with increasing temperatures.

The corresponding CO₂ absorption rates (mole/min) are shown in Figure 10. This data shows that even at high CO₂ loadings ($R'=0.6$) and a temperature of 50°C, CO₂ can be captured at 70% efficiency (CO₂ capture rate = 7×10^{-1} mole/min rate) in a 0.0045 m³ absorber. We limited our test to $R' < 0.6$ because operating an absorber with less than 70% CO₂ capture efficiency is not desirable. The data shows that the temperature dependency on the CO₂ capture efficiency is not high at efficiencies approaching 100% (1 mole/min CO₂ capture rate). Even at higher CO₂ loadings, there is only a minimal temperature effect on the CO₂ capture rate at 265 psi.

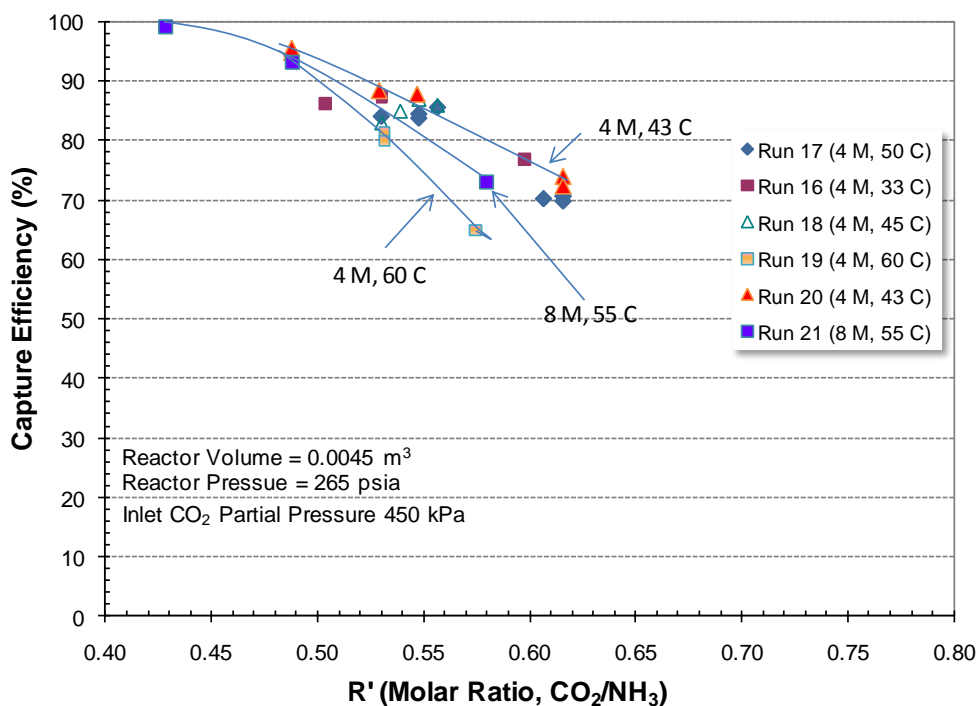


Figure 9. CO₂ capture efficiency of 4 and 8 M ammonia solutions at 265 psia at 30° to 60°C.

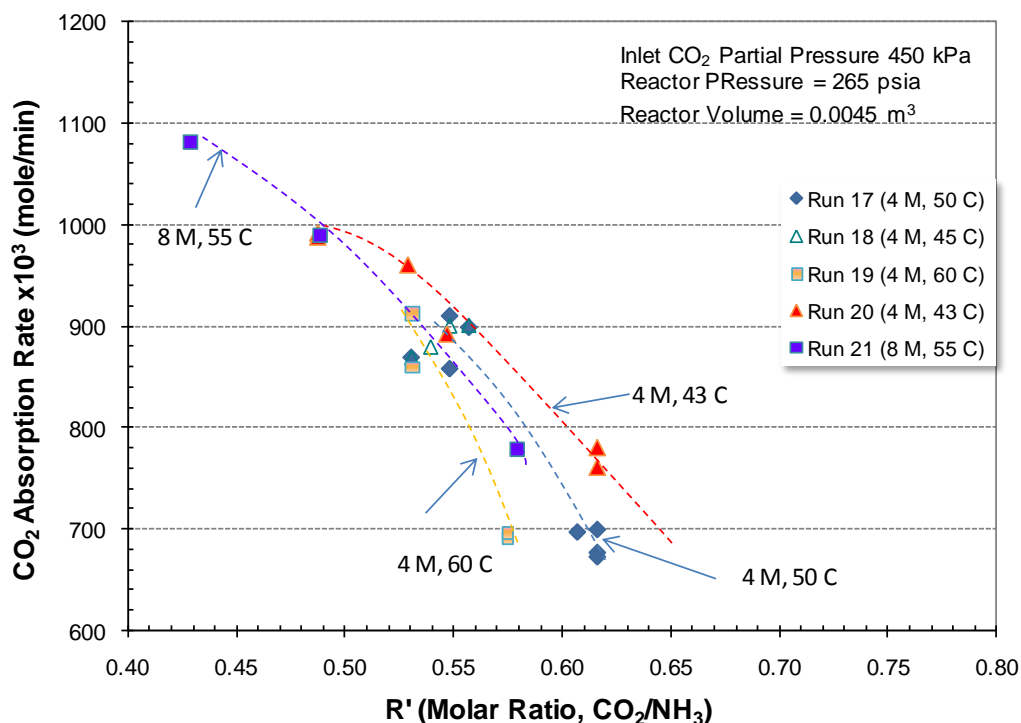


Figure 10. CO₂ capture rates of 4 and 8 M ammonia solutions at 265 psia at 43° to 60°C.

Figure 11 illustrates the temperature dependence at R' values at two higher CO₂ loading values ($R' = 0.55$ and 0.6). Our preliminary data on temperature effect on CO₂ capture indicated that at a reactor pressure of 265 psi, the capture efficiency increased with increasing temperature from 20° to 45°C due to increased reaction kinetics, but may decrease at higher temperatures due to thermodynamic limitations (see Figure 4). In this series, we investigated the absorption temperature up to 60°C to study the temperature effect under steady-state conditions. The new data suggests the absorber can be operated up to 60°C with only a slight decrease in the capture rate.

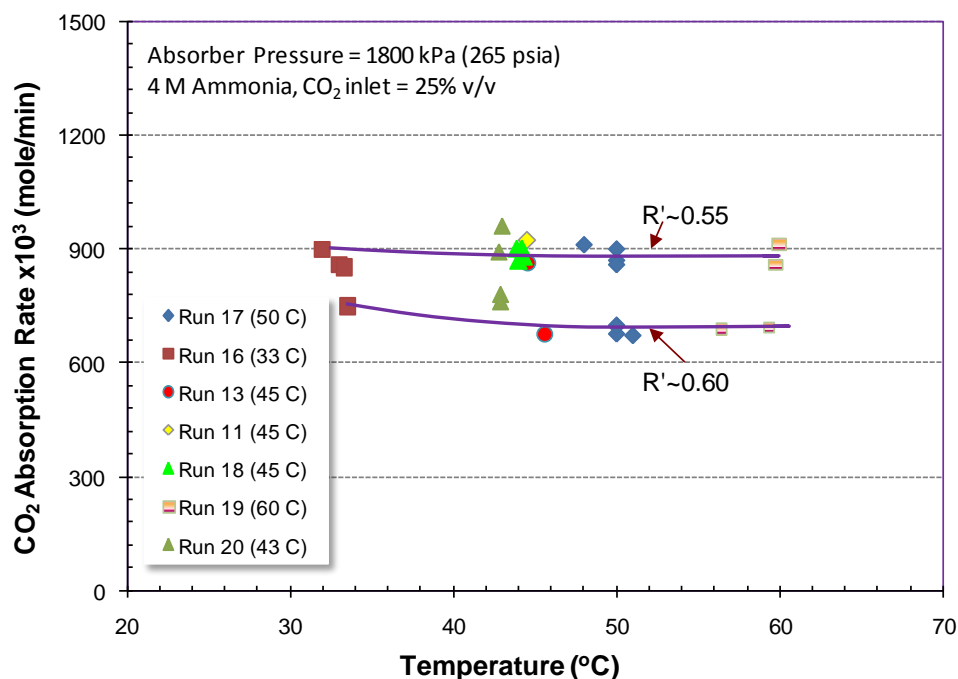


Figure 11. CO₂ capture rate of 4 and 8 M ammonia solutions at 265 psia at 33° to 60°C.

Residual NH₃ and CO₂ Levels in the Absorption Step: As the absorption temperature increased at a given absorber total pressure, both the equilibrium partial pressures of NH₃ and CO₂ increased. The increased partial pressure of NH₃ led to the loss of NH₃ from the solution. The residual NH₃ vapor in the absorber exit gas can be scrubbed, recovered, and reabsorbed in the absorber feed solution. However, process conditions that minimize NH₃ loss from the absorber are preferred. The residual ammonia partial pressure is function of temperature, the solution ammonia concentration, and CO₂ loading. Table 4 shows the measured absorber residual ammonia levels in the gas. The measured ammonia partial pressures were less than 500 ppmv at 60°C and 265 psia.

Table 4. Residual NH₃ partial pressures at varying temperature and CO₂ loadings.

Run #	T (°C)	Bulk CO ₂ loading (CO ₂ /NH ₃)	Total P (psia)	NH ₃ Partial Pressure (ppmv)
14	39	0.63	215	150
16a	33	0.60	280	280
18	43	0.62	270	250
19a	60	0.65	265	300
19b	60	0.61	250	200
20a	42	0.61	265	225
20b	42	0.67	265	100
20c	40	0.56	265	325

At a higher temperature, the partial pressure of CO₂ in equilibrium with the solution also increases, providing a backpressure for absorption and the rate of CO₂ capture decreases. The partial pressure of CO₂ (back pressure) is a function of temperature, solution molarity, and CO₂ loading (R' value). Figure 12 shows the correlation between calculated CO₂ back pressure and measured CO₂ absorption rates at different R' values in the range 0.46 to 0.67 at 265 psia and temperatures in the range 40° to 60°C. As expected, as the solution is loaded with CO₂, the partial pressure of CO₂ in equilibrium with the solution increases and the rate of absorption decreases.

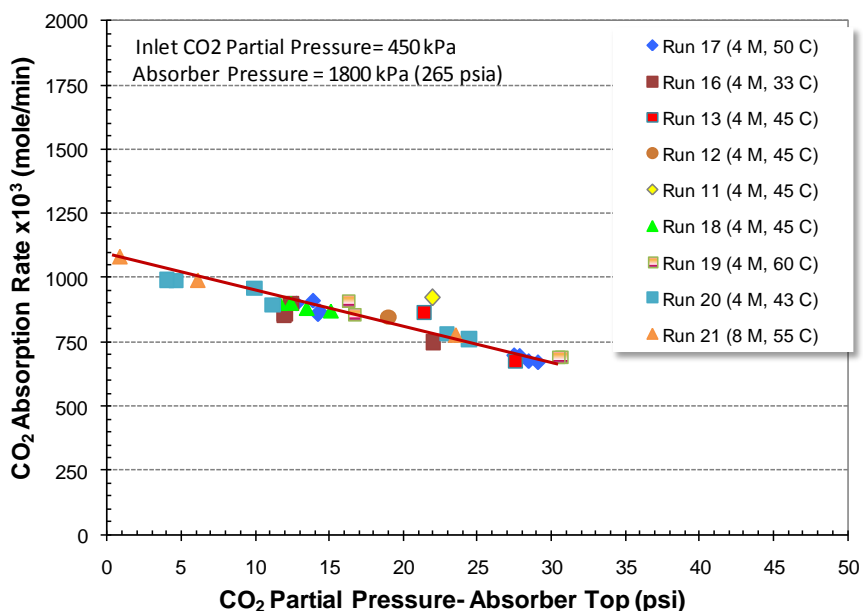


Figure 12. The relationship between calculated CO₂ back pressure and the measured CO₂ capture rate.

Absorption of H₂S in Ammonia Solutions with Varying CO₂ Loadings: The IGCC gas stream downstream of the water-gas shift reaction contains mainly H₂, CO₂, and small quantities of H₂S. H₂S will react with the ammoniated solution, forming sulfide or bisulfides.

A series of tests (Test Series D) was performed to determine the efficiency of the test solutions to capture H₂S at varying CO₂ loadings. In these tests, we used solutions containing 2.3 and 7.6 M ammonia with a CO₂/NH₃ molar ratio (R' value) ranging from 0.25 to 0.5. The feed gas is a mixture of N₂ containing 1 to 2 % v/v H₂S flowing at a rate varying from 20 to 50 SLPM. We used N₂ instead of H₂ as the major gas because the solubility of H₂ in the ammonium carbonate solution is extremely low, and the gas substitution will not influence the results. Three different pressures (135, 205, and 215 psia) and two temperatures (20° and 50°C) were used. In these tests, no make-up liquid was introduced so that the capture efficiency at different H₂S loading in the solution could be determined.

Table 5 shows the test conditions for test series D. When conducting these tests, the reactor was filled initially with a predetermined volume (4 to 6 liter) of 2.3 or 7.6 M ammonia solution with known CO₂ loading. After the temperature and pressure in the column were stabilized, a gas mixture containing 1-2 % v/v H₂S in N₂ was introduced through the bottom of the absorber. No make-up ammonia solution was added during these tests to allow the H₂S loading in the solution to change with time. The H₂S capture efficiency of the solution for capturing H₂S from the test gas stream was evaluated by measuring the inlet and outlet H₂S concentration using an online gas chromatograph.

Table 5. Absorber test conditions to determine the H₂S capture efficiency.

Run #	[NH ₃] (mol/L)	Bulk CO ₂ loading (CO ₂ /NH ₃)	Liquid Recirculation (L/min)	Gas Flow (L/min)	H ₂ S. Feed (% v/v)	Total P (psia)	T (°C)
25	2.3	0.48	3.1	50	2	135	25
26	7.7	0.27	3.1	20	1	215	50
27	7.5	0.34	3.1	20	1.7	215	50
28	7.6	0.26	3.1	20	1.7	250	50

The measured H₂S capture efficiency is shown in Figure 13 for 8 M ammonia solutions with R' values in the range 0.26 to 0.34. In these tests, the feed gas was 1% (v/v) H₂S in N₂ and the absorber pressure was ~ 210 psia. Under these conditions, the H₂S capture efficiency exceeded 90%.

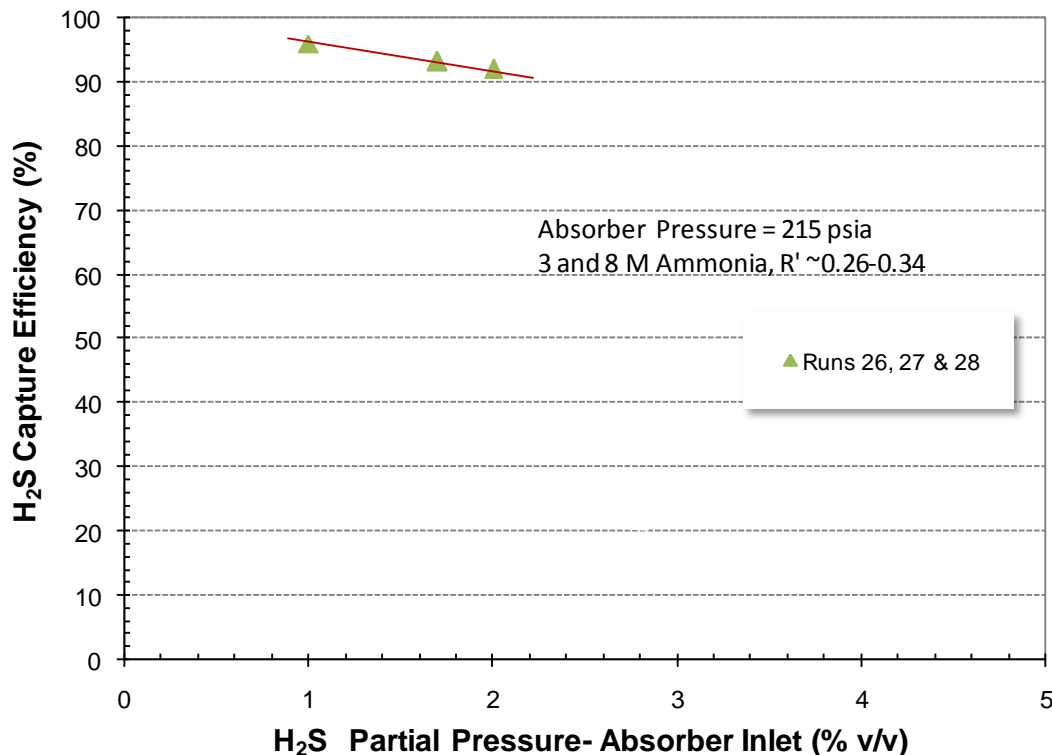


Figure 13. Measured H₂S capture efficiency for 7.5 to 8 M ammonia solutions at 50°C.

Solubility of H₂, N₂, and CH₄ in Aqueous Solutions: The IGCC gas stream downstream of the water-gas shift reaction contains mainly H₂, CO₂, and small quantities of N₂, CO, CH₄, and H₂S. Both CO₂ and H₂S will react with the ammoniated solution forming carbonates, bicarbonates, sulfides, or hydrogen sulfides. Other gaseous components will not react with the solution but will dissolve in the liquid. The solubilities of these gases in water increase with pressure but decrease with temperature according to the well-known Henry's law. Gases such as H₂, CO, and CH₄ dissolved in the absorber solution will desorb during regeneration and result in a loss of the fuel gases from the CO₂-free fuel gas stream that will be used in a gas turbine or fuel cell. The dissolution of N₂ in the absorber and released in the regenerator will represent a dilution of the CO₂ gas stream. Hence, the solubility of these gases in the ammoniated solution must be known.

The Henry's law constant, K , for the solubilities of H₂, CO, CH₄, and N₂ in water has been reported in the literature (Perry, 1973). The solubility is related to the partial pressure by the relation:

$$P_g = K_g \cdot X_g \quad (5)$$

Where P_g is the partial pressure, K_g is the Henry's law constant, and X_g is the mole fraction of the gas in the liquid. The K values for H₂, CO, CH₄, and N₂ are 6.8×10^4 , 4.9×10^4 ,

3.8×10^4 , and 8×10^4 , respectively. The constant is a weak function of pressure in the range of interest.

The solubility of these gases in aqueous solution decreases when salts are dissolved in water. This salting effect is known for several electrolytes and is described as the activity coefficient, γ_g , modifying equation 5 as follows:

$$P_g = K_g \cdot \gamma_g \cdot X_g \quad (6)$$

The activity coefficient increases with the salt content of the solution. For a solution of 10 M KOH (40 wt%) aqueous solution at 25°C, the coefficient is 20 (Shoor, 1966). The solubility of H₂, CO, and CH₄ in a 2.5 M K₂CO₃ aqueous solution is decreased by a factor of 5 (Field, 1960). Table 6 lists the calculated solubility of these gases in water at 1 and 40 atm and in a concentrated solution at 40 atm assuming that the activity coefficient is 5. These results indicate that in the concentrated aqueous solution of ammonium carbonate-bicarbonate, the solubility of the H₂, CO, CH₄, and N₂ will be negligibly small. The solution will contain less than 0.002 wt% of these gases if they were present as pure gases at a pressure of 40 atm. H₂ is the major component of the IGCC gas stream at less than 50% v/v; the loss of H₂ will be negligibly small, and the loss of other gases will be even smaller.

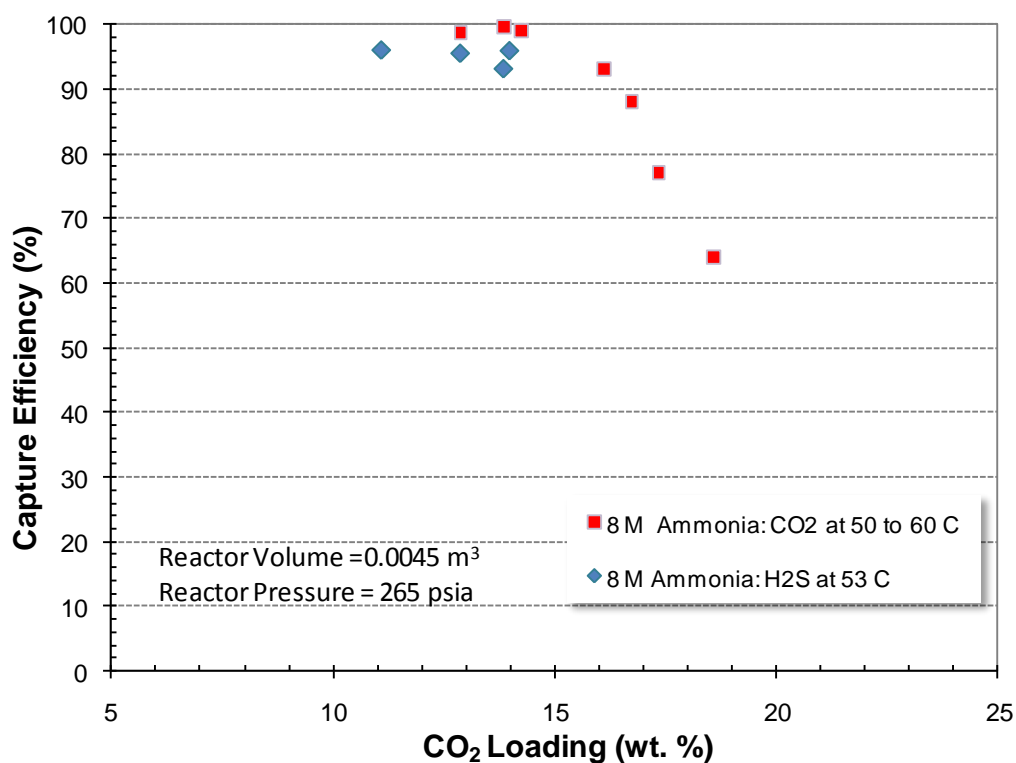
Table 6. Solubility of gases in aqueous solutions at 20°C.

Gas	K	Mole Fraction in Water		g Gas/kg Solution at 40 atm pressure	Gas Component Concentration (%v/v)	g Gas/kg Solution at 40 atm total pressure
		X (1atm)	X (40 atm)			
H ₂	6.80E+04	1.47E-05	5.88E-04	0.013	50.0	0.0065
CO	4.90E+04	2.04E-05	8.16E-04	0.018	2.0	0.0004
CH ₄	3.80E+04	2.63E-05	1.05E-03	0.023	2.0	0.0005
N ₂	8.00E+04	1.25E-05	5.00E-04	0.011	1.0	0.0001

Bench-scale Absorber Tests: Mixed Gas Experiments: In addition to operating the absorber for preparing CO₂ and H₂S-rich solutions for regenerator operation, additional tests (Test Series E and F) were also conducted to complete the analysis of data from data generated in Test Series C and D. Table 7 provides the data for H₂S loading at ~ 50°C and pressures near 215 to 250 psia for ~ 8 M ammonia solutions with varying CO₂ loadings (Test Series E). The CO₂ and H₂S capture efficiencies observed in this study clearly show that both CO₂ and H₂S can be captured at efficiencies higher than 90% even at high loadings of CO₂ (see Figure 14). The data shown in Figure 14 are for individual H₂S and CO₂ absorption.

Table 7. Absorber test conditions to determine the H₂S capture efficiency in gas mixtures.

Run No.	[NH ₃] (mol/l)	Bulk CO ₂ Loading (CO ₂ /NH ₃)	H ₂ S Loading mol/l	Liquid Recirculation (l/min)	Gas Flow (l/min)	H ₂ S Feed (vol%)	Total Pressure (psia)	T (°C)
26	7.7	0.27	NM	3.1	20	1	215	50
27	7.5	0.34	NM	3.1	20	1.7	215	50
28	7.6	0.26	NM	3.1	20	1.7	250	50
29	8.5	0.4	0.51	3.1	95	0.8	210	53
29	8.4	0.32	0.42	3.1	95	0.8	210	53
30	8.2	0.37	0.49	3.1	95	1	215	52
30	8.2	0.4	0.49	3.1	95	1	215	52
NM: Not Measured								

**Figure 14.** CO₂ and H₂S capture efficiencies of ammonia solutions at varying CO₂ loadings.

Mixed gas experiments were also conducted to determine the H₂S capture rates (Test Series F). The 8 M ammoniated solutions were tested at three different CO₂/NH₃ molar ratios (R' values) varying from 0.33 to 0.45 and at two different liquid circulation rates and gas flow rates. These tests were conducted under ambient conditions to determine the effect of gas flow rate and liquid recirculation rate on the H₂S capture efficiency and the sulfide loading in the absorber solution. The absorber was operated under continuous flow mode. In this testing,

1% v/v H₂S in N₂ or 1% v/v H₂S, or 20% CO₂ in N₂ were used to test the efficiency of H₂S capture. In each run, both the remaining H₂S in the gas stream exiting the absorber and the H₂S loading in the recirculating liquid were measured. Table 8 shows the test conditions and the measured data for H₂S exiting the absorber and the measured H₂S concentration in the recirculating liquid at the end of each run.

Table 8. Bench-scale absorber data for H₂S absorption under varying conditions.

NH ₃ Concentration, M	8	8	8	8	8	8				
CO ₂ /NH ₃ , R'	0.33	0.33	0.33	0.33	0.33	0.33				
L/G, gpm/Kacfm	7574	4545	2525	5050	3030	1683				
Liquid Recycle, LPM	3	3	3	2	2	2				
Gas Flow Rate, SLPM	3	5	9	3	5	9				
Inlet H ₂ S Cocentration (v/v%)	1	1	1	1	1	1				
Outlet H ₂ S Concentration (gas stream), ppmv	200	300	200	300	500	200				
H ₂ S Concentration (liquid), ppm	54		214	286	243	286				
NH ₃ Concentration, M	8	8	8	8	8	8				
NH ₃ /CO ₂ , R	0.25	0.25	0.25	0.25	0.25	0.25				
L/G, gpm/Kacfm	7574	4545	2525	5050	3030	1683				
Liquid Recycle, LPM	3	3	3	2	2	2				
Gas Flow Rate, SLPM	3	5	9	3	5	9				
Inlet H ₂ S Cocentration (v/v%)	1	1	1	1	1	1				
Outlet H ₂ S Concentration (gas stream), ppmv	250	500	120	500	800	150				
H ₂ S Concentration (liquid), ppm	83	25	273	417	359	490				
NH ₃ Concentration, M	8	8	8	8	8	8	8	8	8	8
NH ₃ /CO ₂ , R	0.2	0.2	0.2	0.2	0.2	0.2	0.2	0.2	0.2	0.2
L/G, gpm/Kacfm	7574	4545	3246	2525	1515	5050	3030	2164	1683	1010
Liquid Recycle, LPM	3	3	3	3	3	2	2	2	2	2
Gas Flow Rate, SLPM	3	5	7	9	15	3	5	7	9	15
Inlet H ₂ S Cocentration (v/v%)	1	1	1	1	1	1	1	1	1	1
Outlet H ₂ S Concentration (gas stream), ppmv	100	150	90	40	34	100	100	100	200	200
H ₂ S Concentration (liquid), ppm	185	243	408	432	437	345	417	319	446	348

In the tests shown above, we observed the rate of H₂S capture increased with decreasing R' (CO₂/NH₃ ratio) in the solution as expected. Even at an R' value of 0.33, a greater than 98% H₂S absorption efficiency can be achieved at a gas flow rate of 9 SLPM with a 3 liter/min liquid recirculation rate at 25°C. Figures 15, 16, and 17 illustrate the effects of gas flow rate, R', liquid circulation rate, and the ratio of the liquid circulation rate to the gas flow rate (L/G ratio) on the H₂S concentration in the exit gas. The data in Figure 15 clearly shows that the effect of R' is significant at lower gas flow rates. In general, with increasing gas flow rate, the gas residence time will decrease, thereby reducing the amount of H₂S absorbed. However, at higher gas flow

rates, the enhanced mass transfer will take precedence over the reduced gas residence time. In our tests at sufficiently high liquid flow rates (e.g., 3 liters/min), when gas flow rate was increased from 3 to 15 SLPM, H₂S in the exit gas stream increased steadily and then was reduced after reaching a maximum value at around 5 SLPM. This is due to increased liquid hold-up. The minimum H₂S level observed in these tests was 34 ppm. The decreased extent of H₂S absorption on the high gas flow rate during the low liquid circulation rate could be due to gas bypass in the absorber.

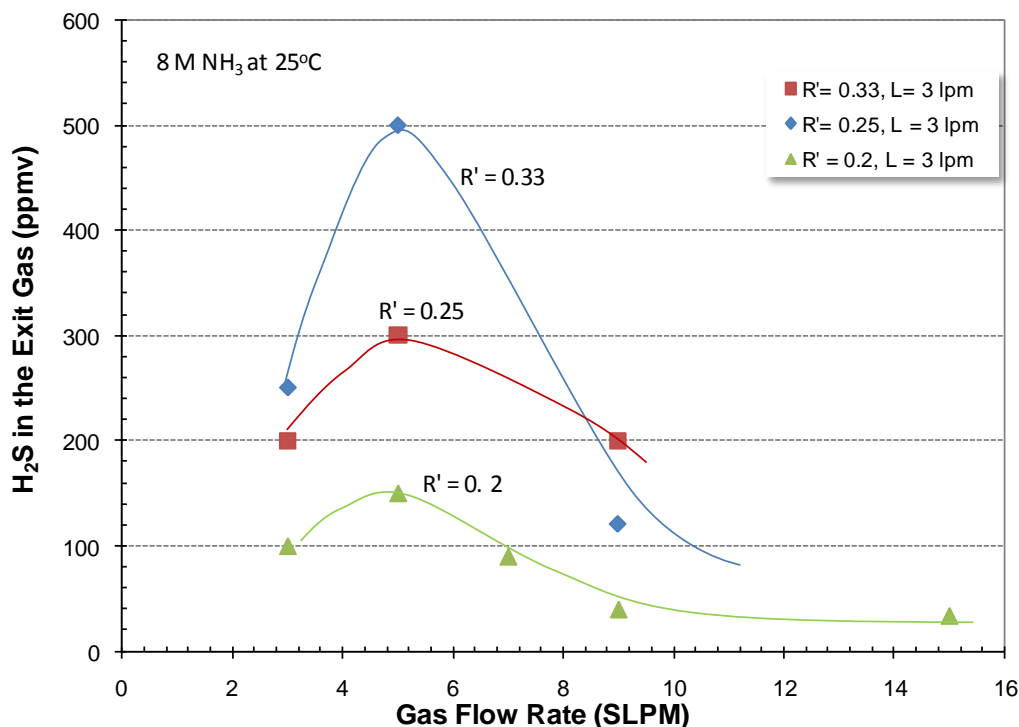


Figure 15. Effect of gas flow rate and the scrubbing solution CO₂/NH₃ ratio on H₂S absorption at 25°C.

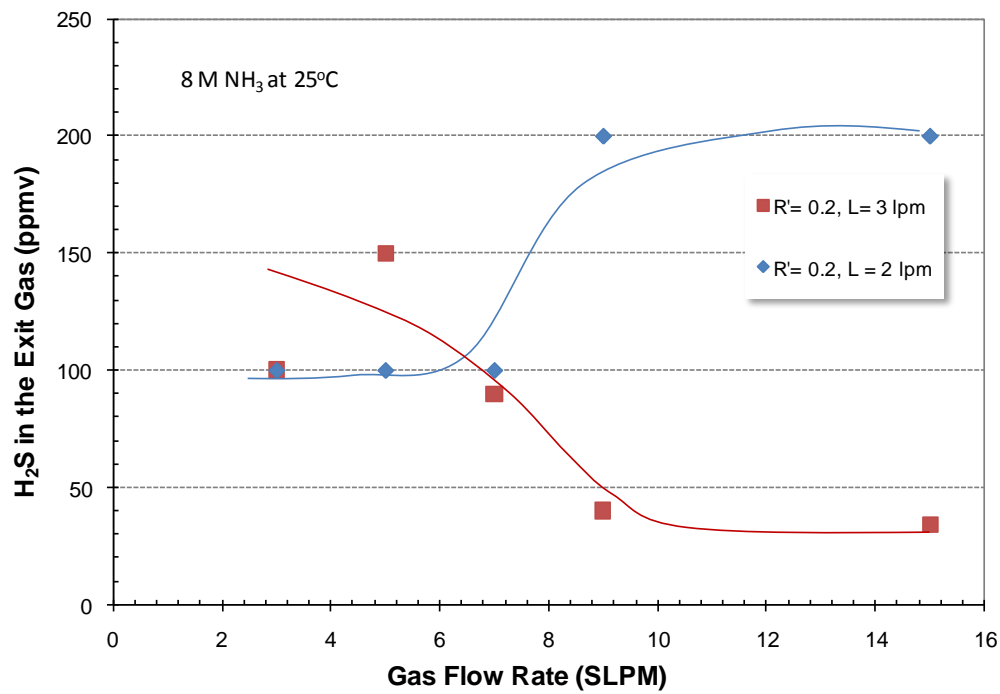


Figure 16. Effect of gas flow rate and the liquid recirculation rate on H₂S absorption

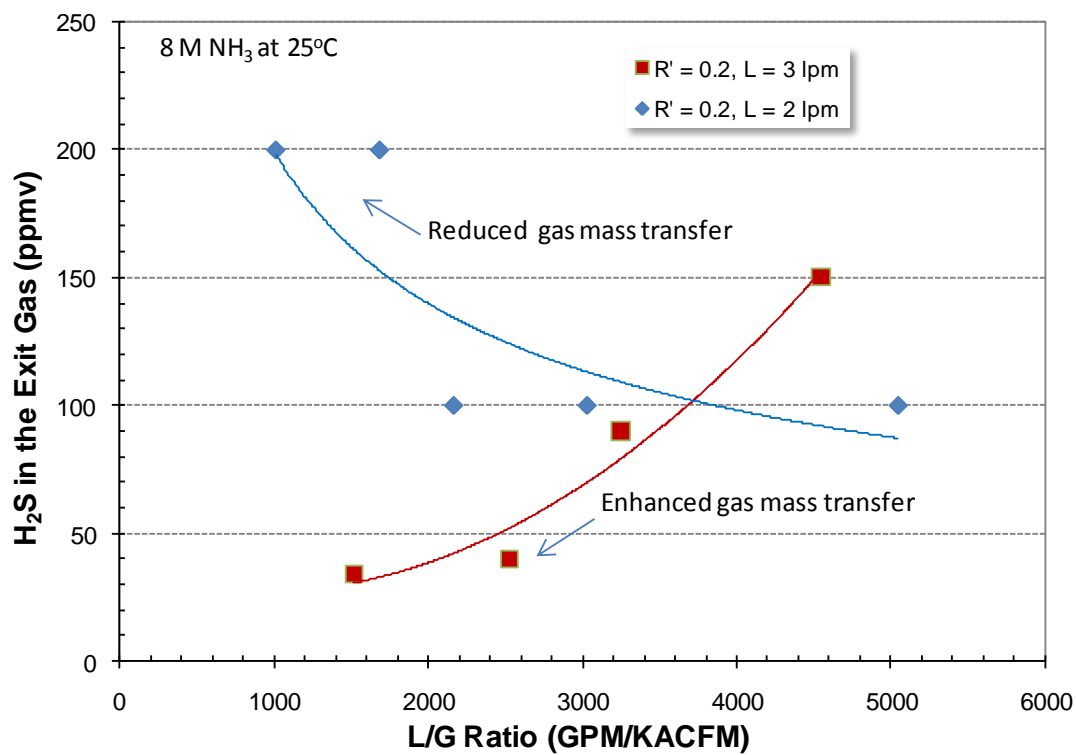


Figure 17. Effect of liquid circulation to gas flow rate ratio on H₂S absorption.

Bench-scale Regenerator Testing

Figure 18 is the schematic diagram of the bench-scale regenerator system. In the regenerator, the CO_2 and H_2S -rich solutions are heated to liberate CO_2 and H_2S , leaving behind a CO_2 and H_2S -lean solution that is suitable for subsequent use in the absorber. The main component of the regenerator system is the high-pressure reactor (with an ID of 4 in and a length of 48 in) that is constructed of stainless steel and capable of operating up to 600 psi and 200°C . The feed ammonium carbonate solution with high CO_2 and H_2S loading was injected at the top of the column using a high-pressure metering pump. The feed solution reservoir was maintained at $\sim 40^\circ\text{C}$ to avoid precipitation of ammonium bicarbonate from the highly CO_2 -loaded solution. The solution was further heated to a temperature of 60°C using a heat exchanger before it entered the regenerator column. The solution flowed down the reactor and was heated to the regeneration temperature by an immersion heater (reboiler) located at the bottom of the reactor releasing CO_2 and H_2S . A stainless steel structural packing was placed above the reboiler to facilitate the contact between up-flowing vapor and down-flowing liquid. This arrangement minimizes the escape of NH_3 and H_2O vapors from the reactor as they equilibrate rapidly with the incoming solution. Figure 19 is a photograph of the regenerator.

In a typical test, the regenerator reboiler section of the column is filled with sufficient starting solution to cover the heating coil. Once the desired temperature and pressure are achieved, feed solution (rich solution) is continuously added at the top of the column, while the lean solution is removed at the same rate from the bottom of the column to maintain a constant liquid level in the system. The process variables such as pressure, temperature, and flow rates of liquid and gas streams are monitored and recorded. The regenerated lean solution is collected and analyzed to determine the rate of regeneration and the residual CO_2 and H_2S levels in the regenerated liquid. The gas mixture exits from the top of the column through a series of pressure control valves that maintain the regenerator column pressure to a set value. The evolved gas consisting of CO_2 , NH_3 , H_2O , and H_2S is scrubbed to remove H_2S and NH_3 and vented. A slip stream of the gas is analyzed for its composition by gas chromatography.

The temperature and pressure conditions were varied to determine the extent of regeneration as a function of these variables. In the first series of regenerator testing (Test Series G), temperature was varied between 110 to 175°C , and the pressure was varied from 150 to 300 psig.

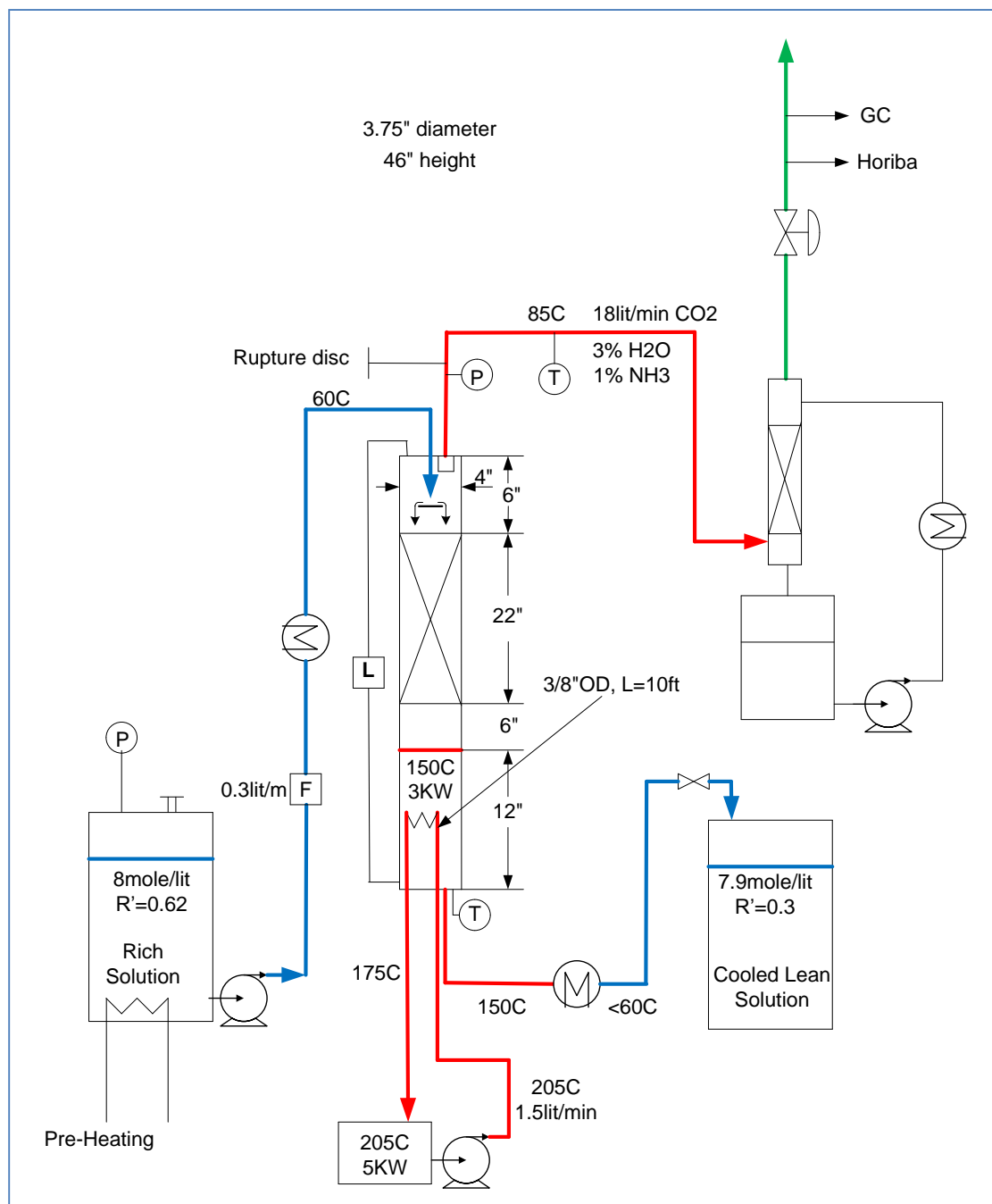


Figure 18. Schematic diagram of the bench-scale regenerator unit.

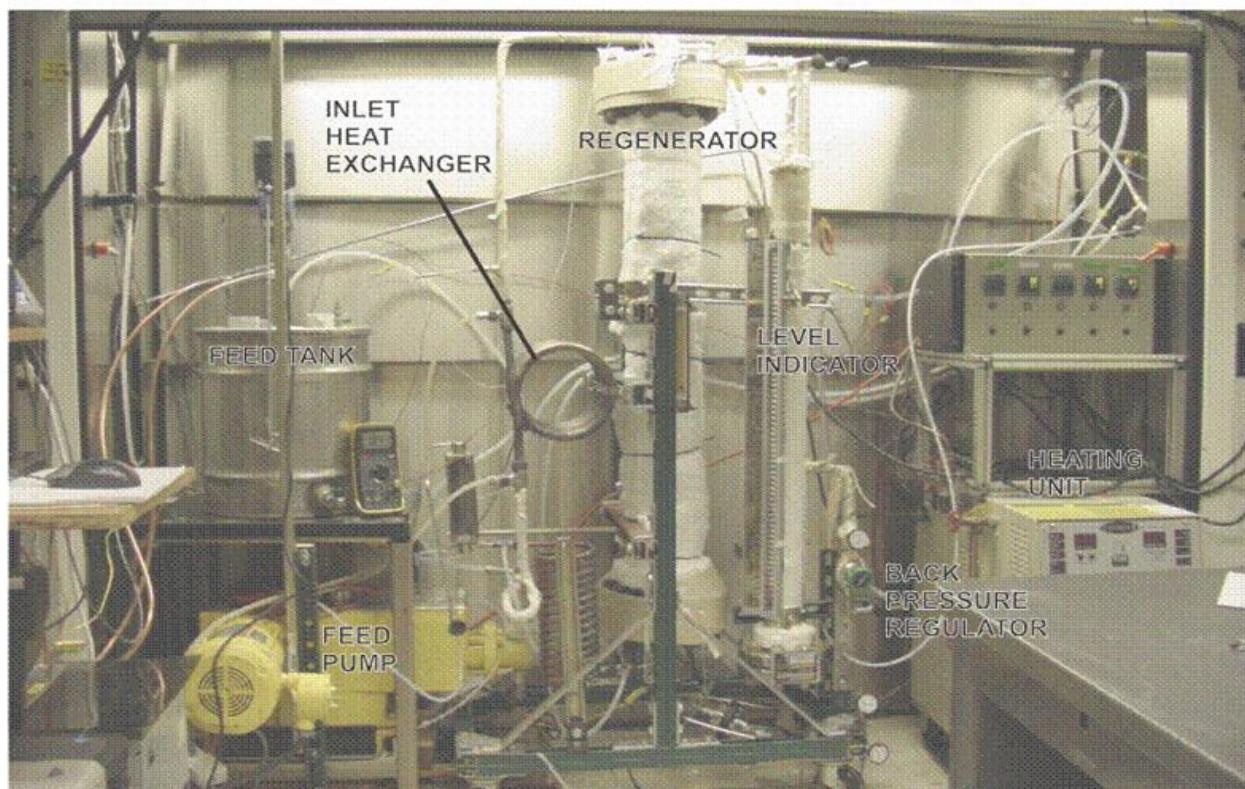


Figure 19. Photograph of the regenerator.

CO₂ is released at high pressure as the CO₂-rich ammoniated solution is heated to the elevated temperature (Figure 20). In these tests, the ammonium bicarbonate solution is heated at various temperatures to determine the pressure increase due to CO₂ release. Note that the equilibrium pressure of steam at various temperatures is a small fraction of the observed pressure, indicating that the increase in the pressure is mainly due to release of CO₂ from the solution. The total pressure observed at 135° C is 800 psi, whereas the steam pressure is only 40 psi.

In solutions containing both carbonates and sulfides, the evolved gases will contain both CO₂ and H₂S. The pressure of these gases will depend on the concentration of carbonate and sulfide species in the solution. Figure 21 illustrates the variation in the total pressure for two solutions of 8 M ammonia containing 1 M sulfide (as H₂S), but with two different CO₂ loadings (CO₂/NH₃ ratio of 0.6 and 0.7). The data shows that the total pressure increases rapidly with increasing temperature. At high CO₂ loadings ($R' = 0.7$), the evolved gases are expected to be mainly CO₂. As the CO₂ loadings in the regenerator solution decrease due to the release of CO₂ gas, increasingly more H₂S gas evolved from the liquid.

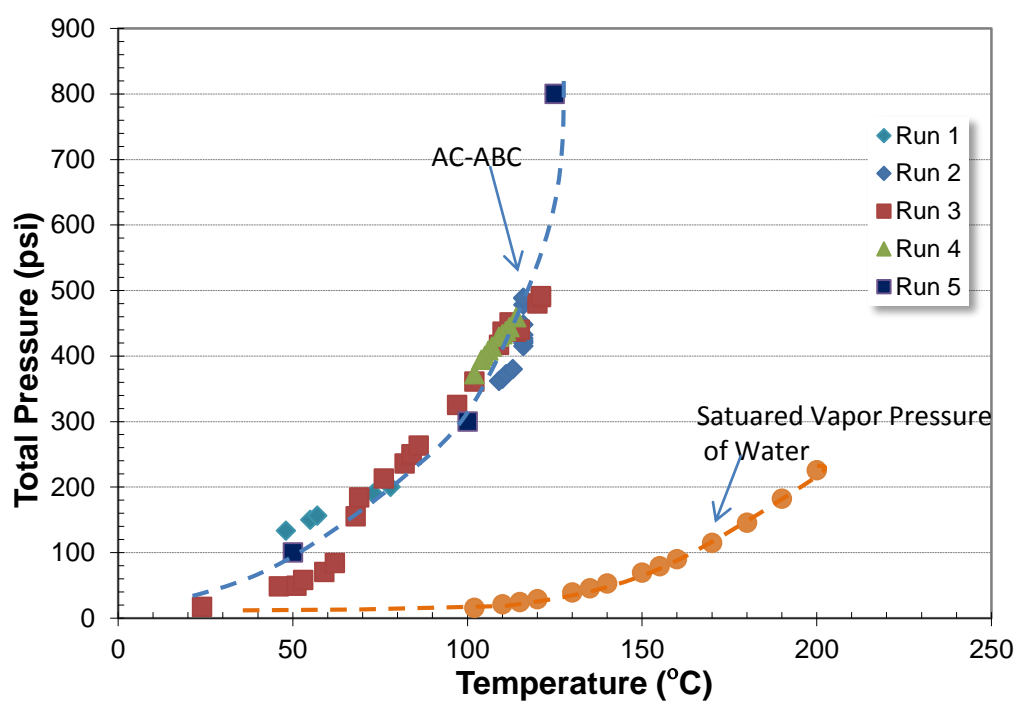


Figure 20. Evolution of CO₂ from the ammonium bicarbonate solution as a function of temperature.

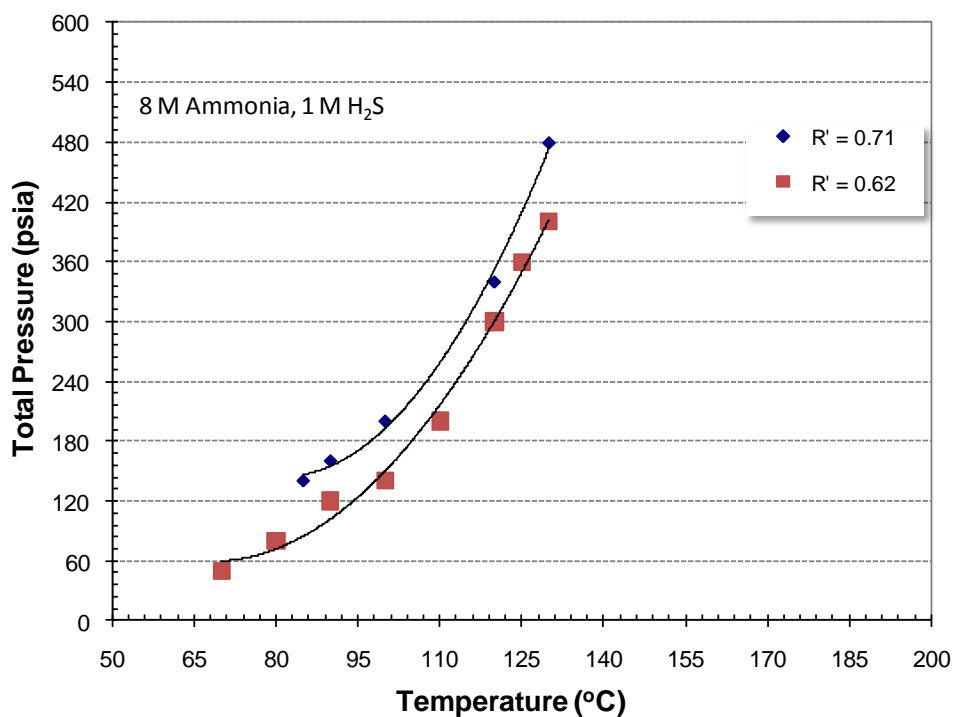


Figure 21. Measured P-T curves for H₂S-H₂O-CO₂-NH₃ from static experiments.

We used a thermodynamic equilibrium calculation of the $\text{NH}_3\text{-CO}_2\text{-H}_2\text{S-H}_2\text{O}$ system to determine the maximum equilibrium loading of H_2S at varying CO_2 loadings at 20 and 40 bar (Figure 22). Based on this data, the maximum solubility of H_2S at 50°C at 20 bar with 1 vol% of H_2S in the gas phase is 0.45 M while that at 40 bar is 0.75 M. Therefore, we elected to determine the regeneration of the CO_2 -loaded ammonia solution with H_2S concentrations closer to 0.4 M for regeneration tests at 20 bar. The data from modeling was confirmed by the measured H_2S absorption data as well.

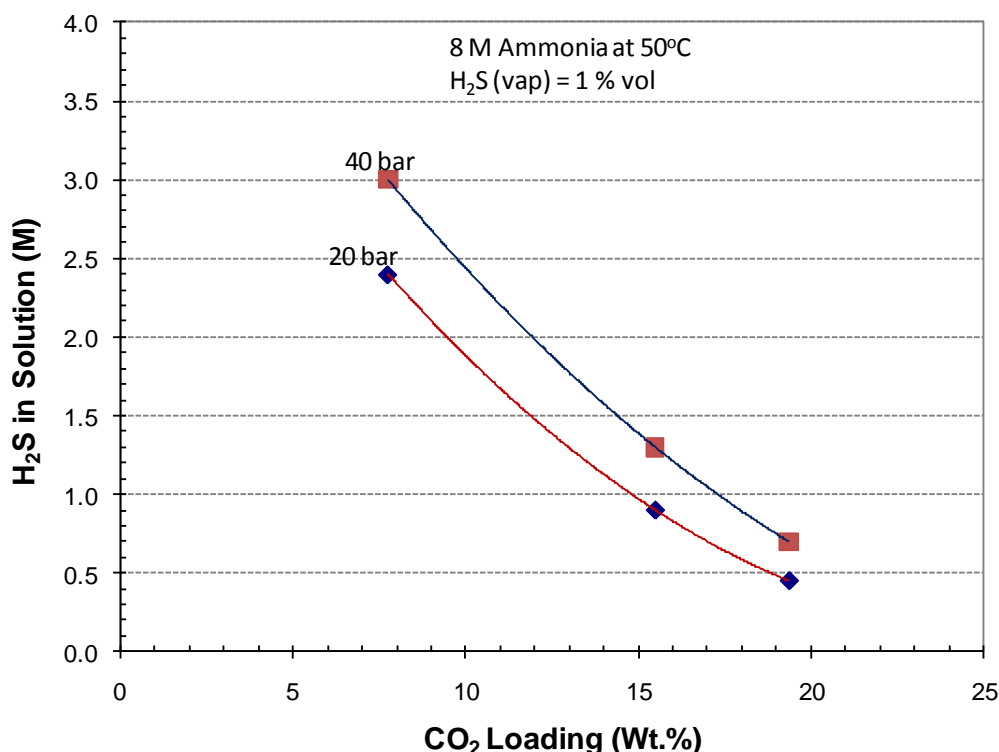


Figure 22. Equilibrium solubilities of H_2S in $\text{H}_2\text{S-H}_2\text{O-CO}_2\text{-NH}_3$ system at a temperature of 50°C and pressures of 20 and 40 bar.

Experiments (Test Series H) were performed in the bench-scale regenerator to determine the effect of temperature on the regenerability of the CO_2 and H_2S rich solutions. Table 9 describes the results and test conditions from selected regenerator runs: (1) regeneration of saturated solution containing CO_2 only, and (2) regeneration of saturated solutions containing both H_2S and CO_2 .

Table 9. Test conditions and results from regenerator runs.

Run		P/psig psig	T reboiler °C	T top °C	T feed °C	Liq Feed Rate lpm	[S2]aq M	[CO2]aq M	[NH3]aq M	H2Sg vol %	CO2g vol %
No H2S											
33		298	145	75	60	0.1	0	NM	NM	0	5*
33		300	150	85	60	0.2	0	NM	NM	0	11*
33		304	157	98	56	0.2	0	NM	NM	0	12*
33		310	158	80	52	0.2	0	NM	NM	0	13*
33	feed						0	5	8		
With H2S											
34		250	135	58	58	0.1	0.25	NM	NM	5.2	NM
34		300	150	62	58	0.1	0.22	NM	NM	4.9	NM
34		300	156	79	58	0.1	0.20	NM	NM	5.0	NM
34		300	163	90	58	0.1	NM	NM	NM	5.0	NM
34		300	165	101	58	0.1	NM	NM	NM	5.3	NM
34		275	165	108	58	0.1	NM	NM	NM	6.9	NM
34		185	165	116	58	0.1	NM	NM	NM	13.9	NM
34		172	162	120	58	0.1	0.095	NM	NM	19.7	NM
34	feed						0.4	4.4	8		
With H2S											
36		250	100	53	60	0.2	0.18	2.9	7.3	NM	NM
36		250	110	53	60	0.2	0.19	3.0	7.4	3.3	83
36		250	118	54	60	0.2	0.18	1.9	7.3	3.5	90
36		300	118	60	53	0.2	0.13	2.1	7.3	3.3	92
36		200	118	65	53	0.2	0.13	1.4	7.2	3.6	93
36		200	118	65	53	0.2	0.12	1.4	7.1	3.6	93
36		150	118	65	53	0.2	NM	NM	NM	3.5	94
36	feed						0.4	3.9	7.5		
* Gas flow rate in lpm, NM: Not Measured											

Figure 23 shows the change in the NH_3/CO_2 molar ratio (defined as R values) of regenerated CO_2 rich absorber solution with regenerator temperature. As an example, in Run #33, an 8 M ammonia solution with a 22 wt% CO_2 loading was regenerated in the temperature range of 140° to 165°C at 300 psig pressure. Based on this data, lean solutions with only 1 wt% CO_2 ($R = 4.5$ or $R' = 0.22$) can be achieved at 165°C while releasing CO_2 at 20 bar. This translates into removal of 95% of absorbed CO_2 from the CO_2 rich solution from the absorber. This level of CO_2 removal is more than sufficient because the absorber tests have shown that 90% CO_2 capture can be achieved using solutions containing less than 15 wt% CO_2 .

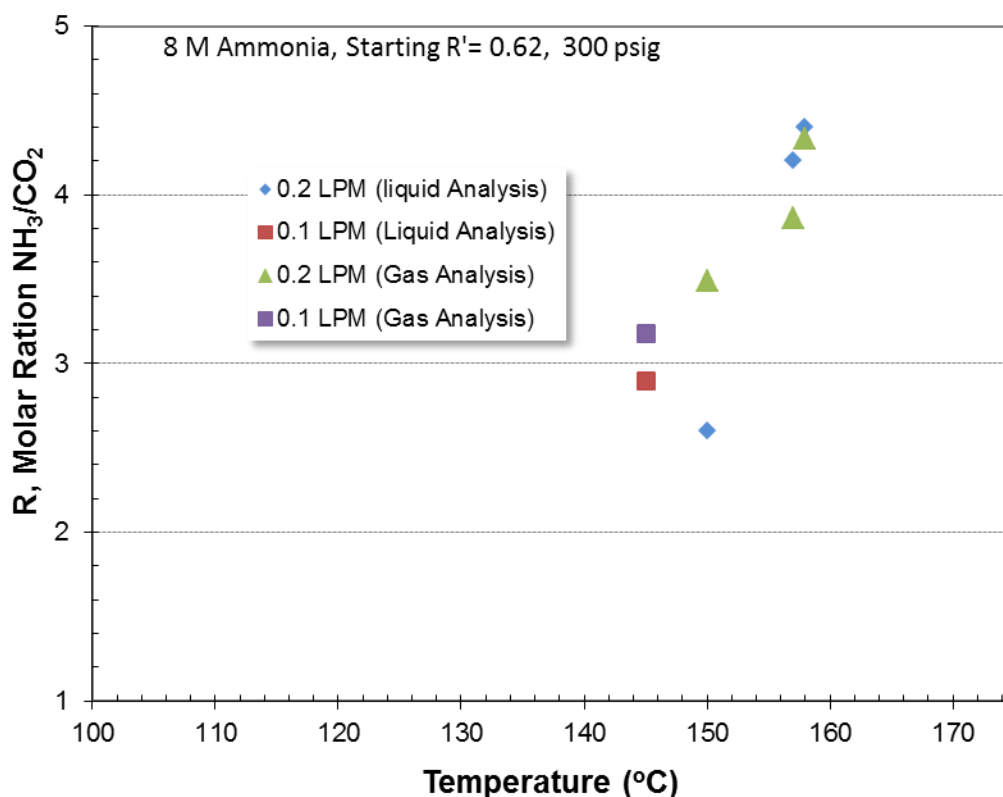


Figure 23. Variation of the R value (molar NH_3/CO_2 ratio) in the regenerated solution as a function of regenerator temperature at 300 psig.

The regeneration of 8 M ammonia solution loaded with 19 wt% of CO_2 and 1.4 wt% of H_2S is shown in Figure 24, which shows the volume percentage of H_2S in the exit gas from the regenerator at varying regenerator temperatures. This data indicates that the effect of temperature on the H_2S gas composition is very minimal in the tested temperature range of 110° to 165°C while the effect of pressure is more pronounced. Figure 25 shows the H_2S composition in the regenerator exit at 125 and 165°C. This data indicates the pressure effect for H_2S removal only becomes important at high temperature. This behavior is expected, as the H_2S removal step requires a higher temperature than that of CO_2 .

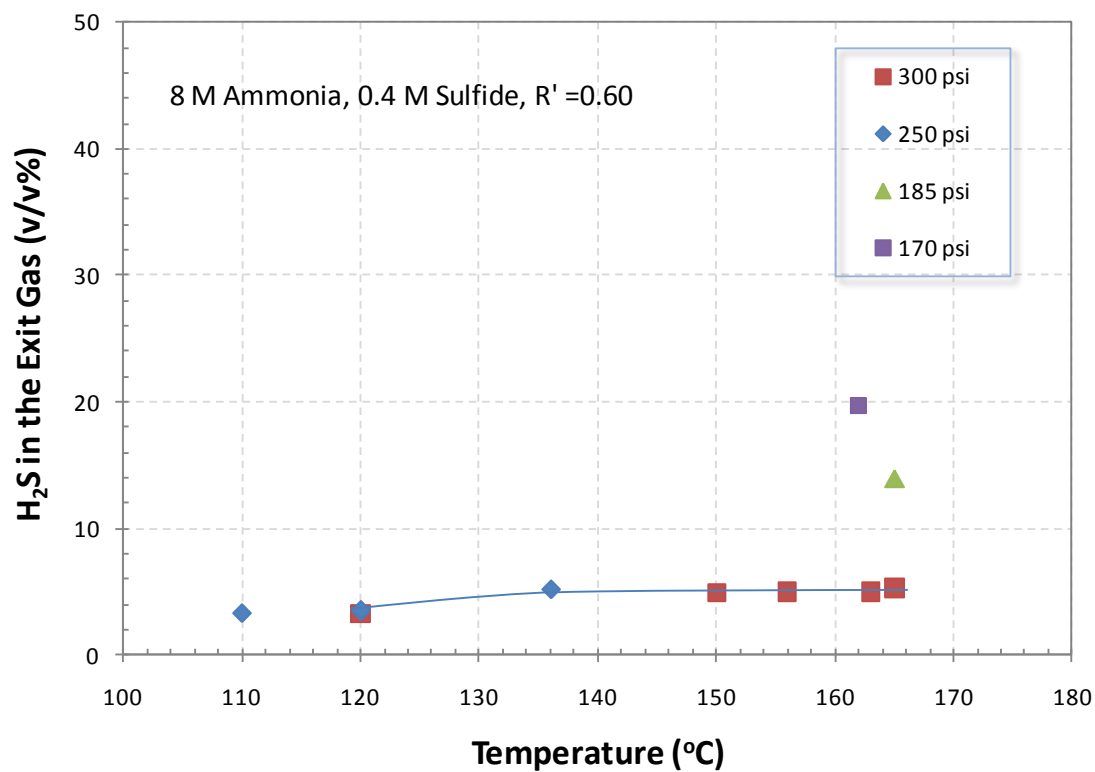


Figure 24. Effect of temperature and pressure on H_2S composition in the regenerator exit gas.

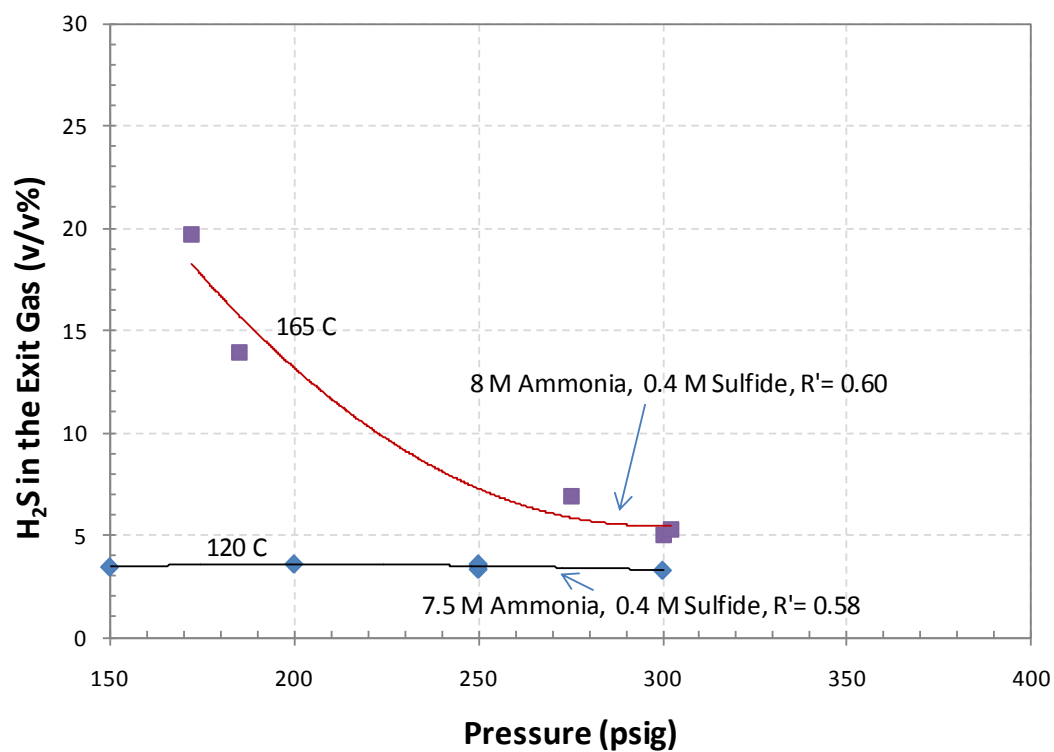


Figure 25. Effect of pressure on H_2S composition in the regenerator exit gas at 120° and 165°C.

Figure 26 shows the variation of the CO₂ to H₂S ratio in the regenerator exit gas as a function of pressure at 125°C and 165°C. The concentration of H₂S in the regenerator exit gas is an indication of its suitability to produce elemental sulfur from the gas mixture by the Claus process. At 125°C (and throughout the tested pressure range), the ratio of CO₂/H₂S remains very high (25 to 28 vol%). At 165°C, the ratio of CO₂/H₂S was 5 at 175 psig and about 18 at 300 psig. These results show that the regeneration process produces a H₂S-rich stream suitable for the Claus process.

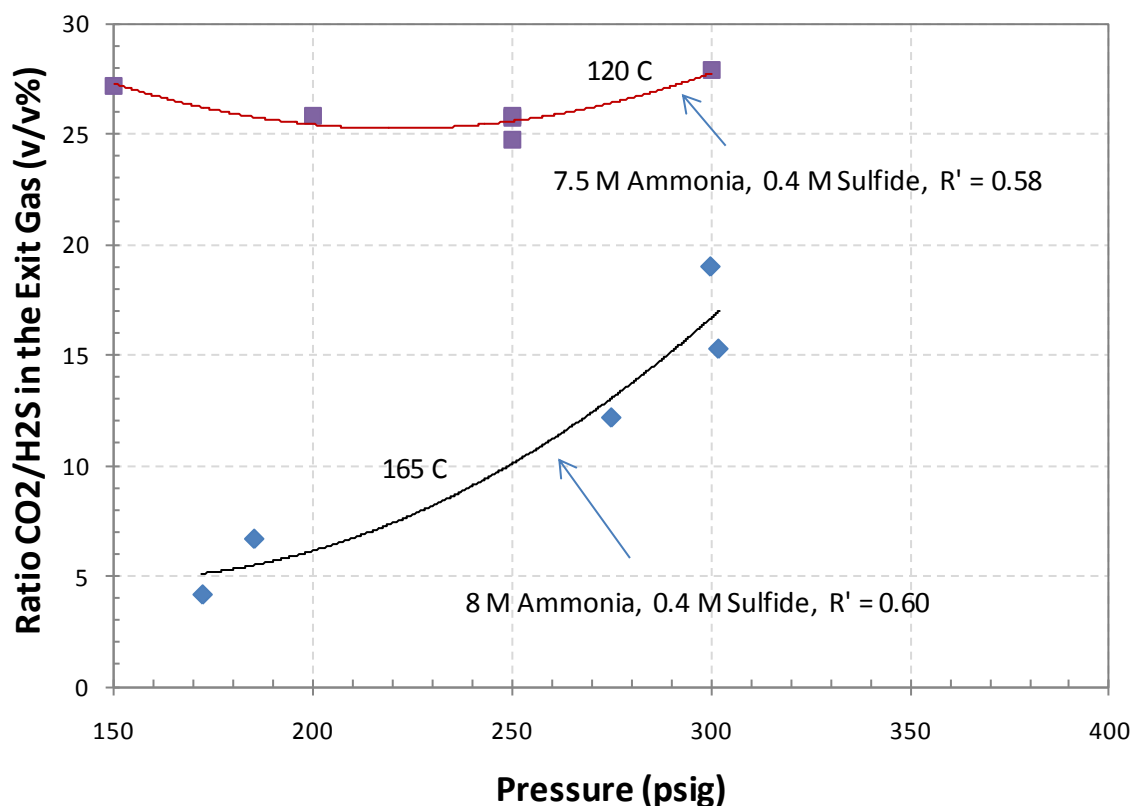


Figure 26. Variation of CO₂/H₂S ratio in the regenerator exit gas with pressure at 120° and 165°C.

Polishing of Fuel Gas for Fuel Cell and Chemical Production Applications: Although electricity generation using the IGCC does not require a fuel gas that is free of H₂S, electricity generation using fuel cells will require H₂S concentrations of 1 ppm or less. The ability of the AC-ABC process to attain a fuel gas stream containing such trace levels of H₂S is shown experimentally in Figure 27. The data clearly shows that sub-ppm levels of H₂S can be achieved by the AC-ABC process.

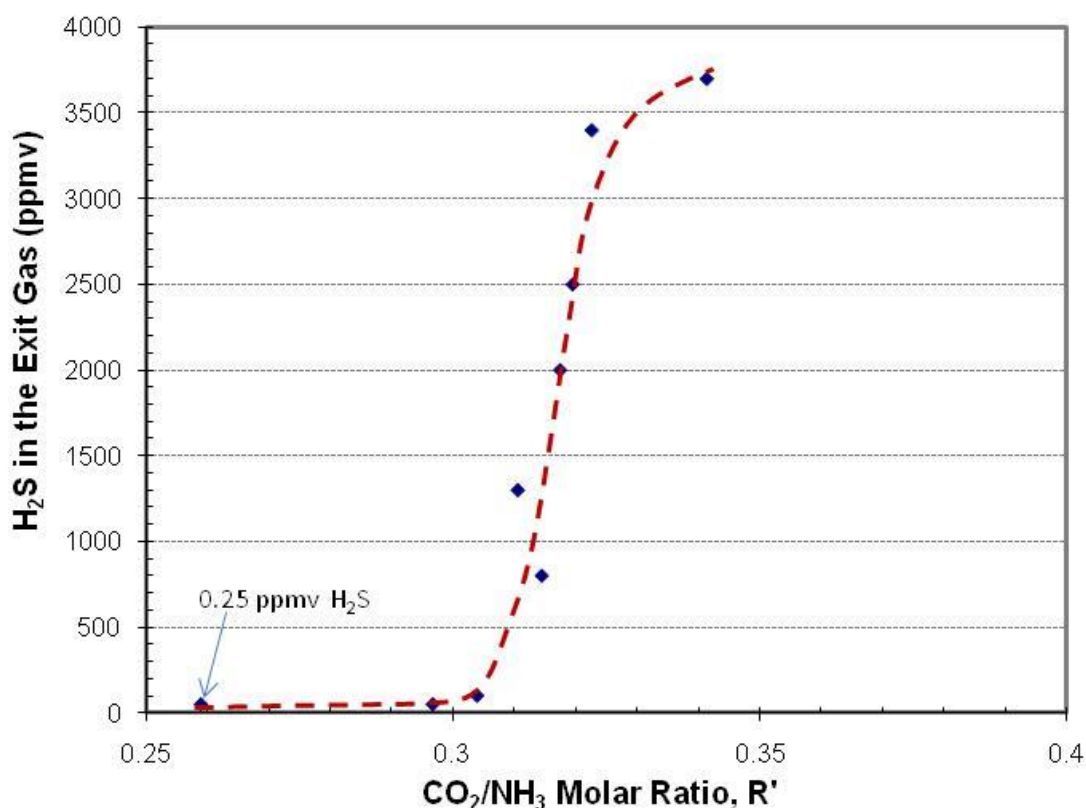


Figure 27. Trace removal of hydrogen sulfide from the absorber exit gas.

Bench-scale Test Data Analysis

In our experience, the high-temperature regeneration of the CO₂-rich solution and the evolution of CO₂ are very rapid and the rates are controlled by heat transfer. However, the absorption step is performed at a relatively low temperature and the chemical reactions cannot be assumed to reach equilibrium. Hence, we analyzed the results from the absorption reaction in terms of its ability to reach equilibrium.

Figure 28 depicts the data from runs with 4 and 8 M ammonia at 265 psia with 25 v/v% CO₂ in the inlet gas stream. This figure shows the concentration of CO₂ (in the gas stream at the top of the absorber column) as a function of CO₂/NH₃ ratio (R' value) in the solution. Also shown is the expected equilibrium CO₂ partial pressure for a 10 M ammonia solution at 55°C and 265 psi pressure. It is clear from this data that the system can be operated very close to the equilibrium line when R' values are closer to 0.4 (~ 12 wt% CO₂ loading). This data allow us to design multistage CO₂ absorbers for capturing 90% CO₂.

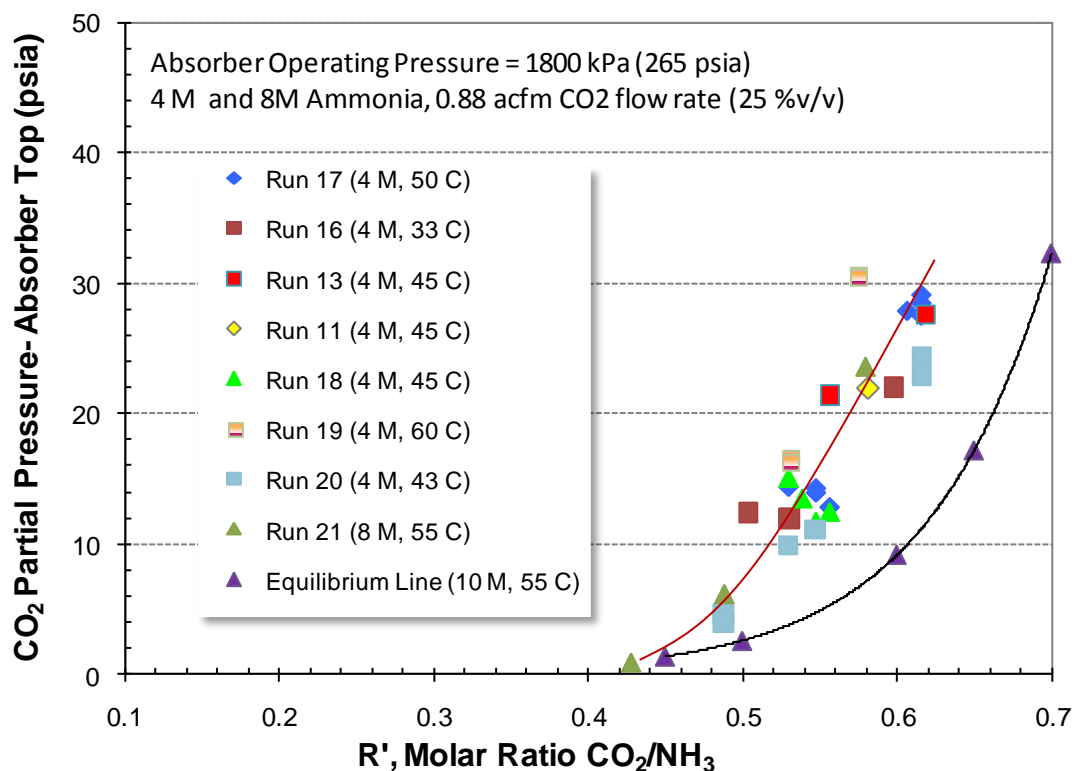


Figure 28. Partial pressure of CO₂ at the top of the absorber column as a function of the scrubbing solution CO₂/NH₃ ratio.

We calculated the heat of reaction for CO₂ absorption based on the measured data. Figure 29 shows the measured temperature rise (temperature difference across the absorber packing) with the change in the CO₂ absorption rate. The heat of reaction is a function of the CO₂/NH₃ ratio in the scrubbing solution at a given temperature. We calculate the heat of the CO₂ absorption reaction to be 57 kJ/mole based on an observed temperature increase of 4°C for an 8 M ammonia solution with a CO₂/NH₃ ratio of 0.43. Although the data was obtained in a small bench-scale reactor with relatively poor thermal management, it provides the information necessary for estimating the heat requirements of the CO₂ stripper.

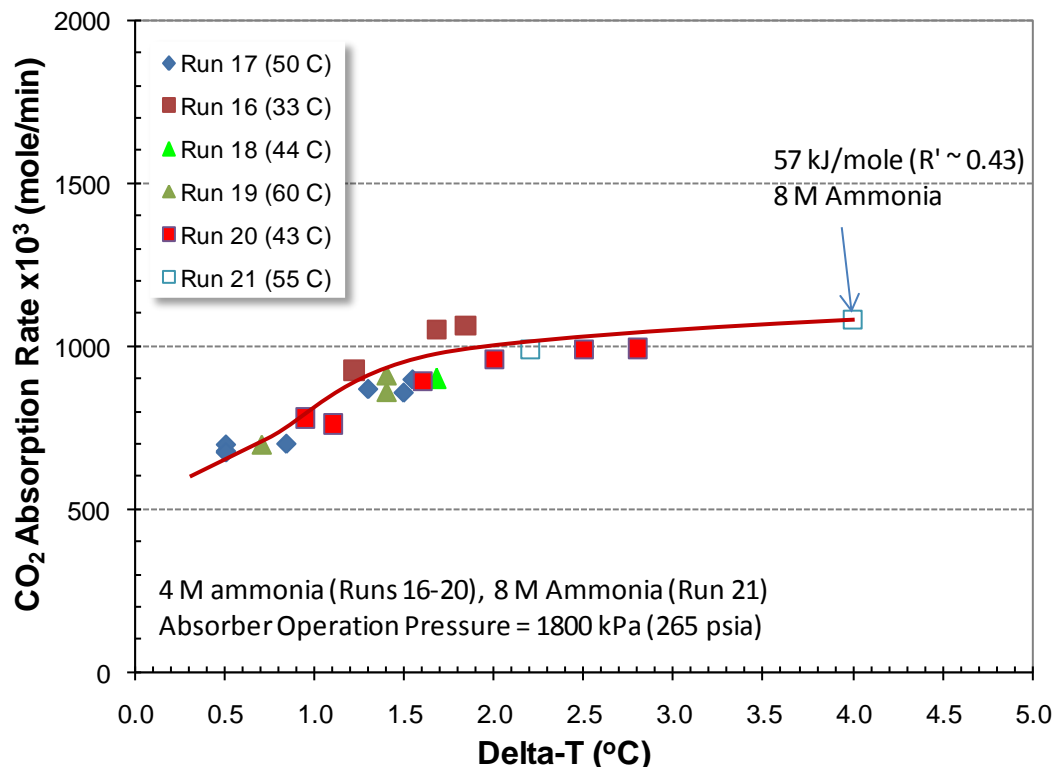


Figure 29. Estimated heat of reaction for CO₂ absorption into an 8 M NH₃ solution.

Below, we discuss the estimation of the required column heights for 90% CO₂ capture using a pilot-scale absorber for a given stream containing 40-50 v/v% CO₂.

In this estimation, we apply the concept of absorption coefficient, which is the most convenient approach for a packed-column design. Volumetric-based calculations are generally used in order to determine the total absorber volume. We estimated the volumetric CO₂ absorption rates from our 4-in packed column test data. We applied the well-established relationships between the gas absorption rate and the gas mass transfer driving forces to estimate the required absorber volumes for a given volumetric flow rate.

The theoretical height required to provide a product with a specified concentration in a separation process (absorption and distillation) is governed by the following relationship:

$$Z_t = \text{HTU} \cdot \text{NTU} \quad (1)$$

Where Z_t is the tower height, HTU is the height of a transfer unit, and NTU is the number of transfer units. From our absorber test data, we have calculated the height of the mass transfer unit to correspond to different CO₂-loaded ammonia solutions. This estimation is specific to the packing type used (SRI bench-scale absorber packing density: 425 m²/m³) at 50-55°C and at 20 bar of operating pressure. The value of HTU is inversely proportional to the overall gas transfer mass coefficient, K_G (mol/h/m³), based on the gas-phase driving force.

$$HTU = (V/S)/ K_G \quad (2)$$

Where V is the volumetric gas flow rate and S is the absorber cross section.

In estimating HTU values that correspond to the tests conducted using 4-in diameter absorber, we used the expanded version of the mass transfer equation for the packed tower

$$Zt = \left(\frac{V}{K_G S} \right) \int \frac{dy}{y-y^*} \quad (3)$$

The expanded version of Eqn (3) can be expressed as

$$NTU = \int dy/(y-y^*) = (y_a - y_b)/\Delta y_L \quad (4)$$

Δy_L = logarithmic mean driving force $(y_b - y_b^*)$ and $(y_a - y_a^*)$

y_a = mole percent CO₂ in the gas phase at column bottom

y_b = mole percent CO₂ in the gas phase at column top

Figure 30 illustrates the values of gas mass-transfer coefficient for CO₂ absorption at 55 C and 20 bar. The rate of absorption (mole/hr) relates to the NTU and K_G (m³/hr/m³) as given in Eq (5), where V_t is the gross tower volume

$$R = K_G (V_t) \Delta y_L \quad (5)$$

By using the HTU values calculated from the test data at various CO₂ loadings, we were able to estimate the required column height, achieving a desired efficiency at fixed-solution R' values (CO₂/NH₃ values).

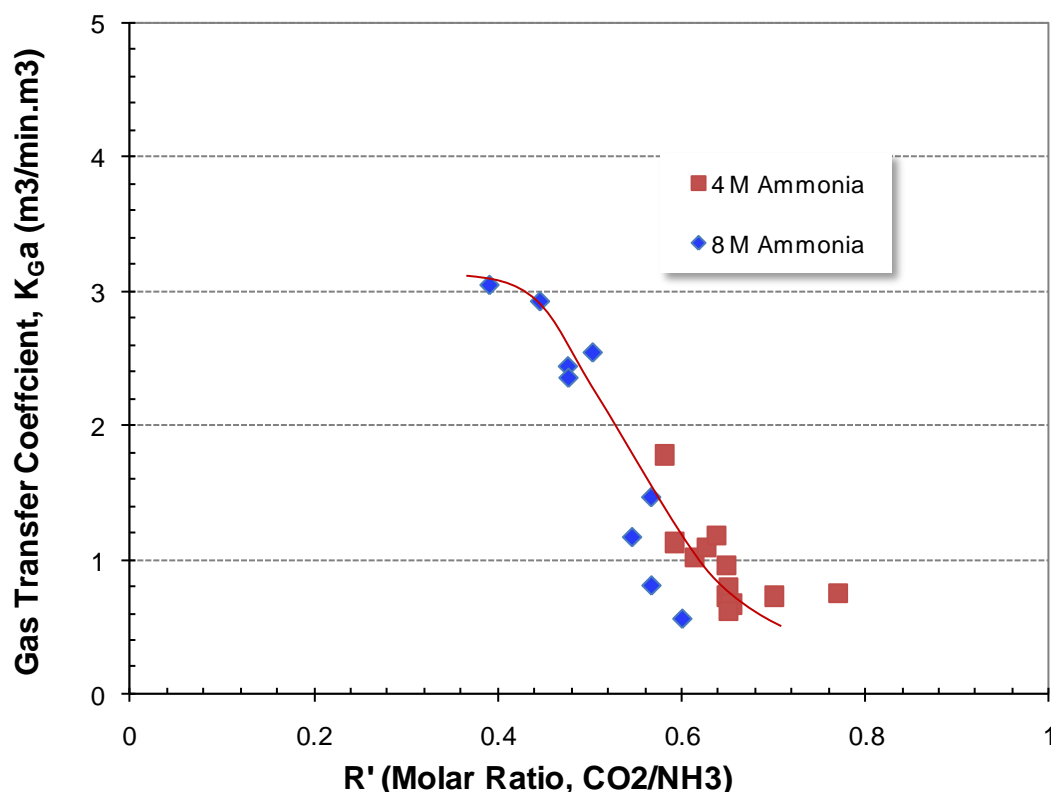


Figure 30. Gas mass-transfer coefficient for CO₂ capture at 55°C and 20 bar.

The corresponding HTU values for CO₂ scrubbing solutions with varying CO₂ loadings are shown in Figure 31. This data shows that the absorber system is very efficient even at 18 wt% CO₂ loadings (e.g., HTU is < 14 inch). In the current lab scale absorber, only 5 wt% solvent loading in the absorber packing is used due to the pump limitations in small-scale operations. For scale-up operations, the absorber solvent loading can easily be increased to 10%, thereby further reducing the HTU values. The result will be an enhancement in absorber efficiency.

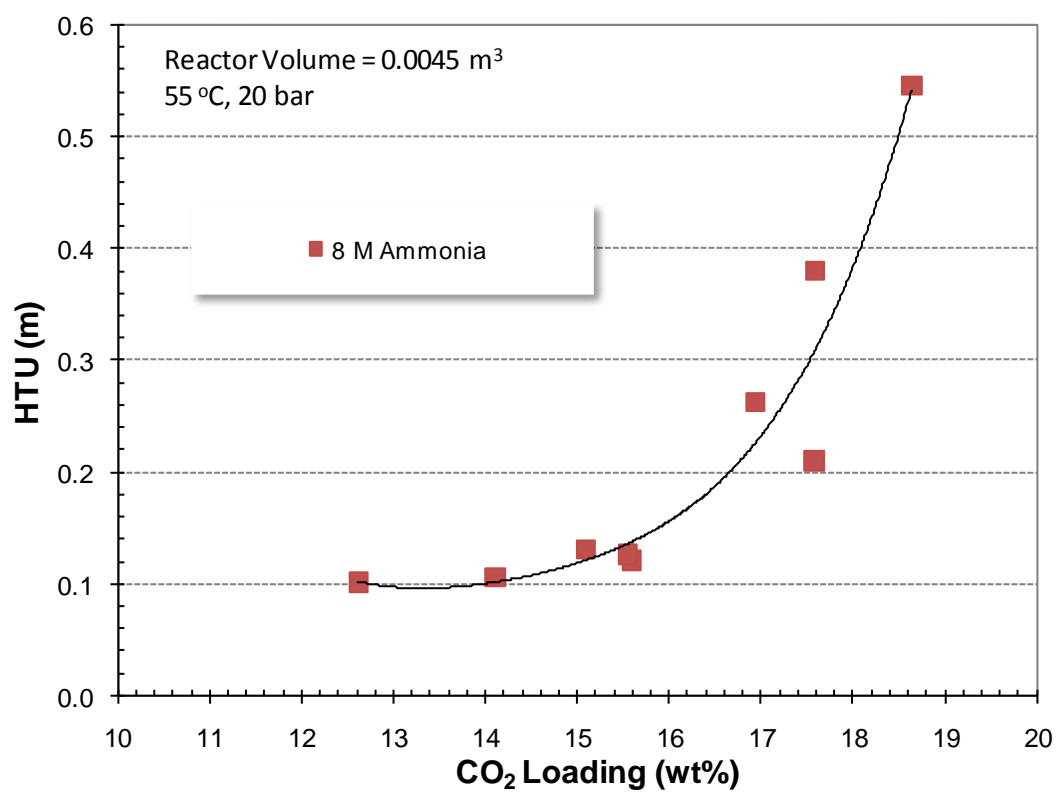


Figure 31. Height of mass-transfer unit for CO₂ absorption as a function of CO₂ loading of the ammonia capture at 55°C and 20 bar.

Preliminary Process Modeling and Cost Economics

Preliminary process modelling and cost economic analysis were performed using ASPEN Plus and GT Pro, and the analyses were updated based on test data from the pilot plant. The topical report of process modelling and the techno-economic analysis was submitted to NETL, and a summary is included in this document.

BUDGET PERIOD 2

Small Pilot-Scale Design

Based on the data obtained from bench-scale batch testing, a small pilot plant, 0.15 MWe, was designed to process 500 lb/hr syngas from the syngas cleanup unit (SCU) at the NCCC. Construction of small-scale pilot plant was completed at the NCCC during spring/summer 2015. An integrated system was designed (see Figure 32) and installed with a single absorber column for simultaneous capture of CO₂ and H₂S from syngas and a single regenerator for simultaneous stripping of CO₂ and H₂S at moderate temperature and elevated pressure. A compressor was used to increase the syngas pressure supplied from the air blown gasifier at the NCCC. The syngas compressor was equipped with a variable frequency drive to enable syngas mass flow control to the absorber.

The absorber was comprised of an 8-in ID, 40-foot tall stainless steel column with three absorption stages. Commercially available stainless steel structural packing was used in the first and second absorption stages for gas-liquid contacting. The third stage used bubble cap trays, also fabricated out of stainless steel. The purpose of the third absorption stage was to control ammonia emission from the system. A Horiba CO₂ analyzer based on infrared (IR) technology was used to monitor CO₂ concentration in the incoming syngas.

Two positive displacement pumps were used to circulate the solvent in each of the first and second stages of absorption. A third positive displacement pump was used to deliver fresh lean solution to the top of the third absorption stage. The bottom of the absorber column was maintained at 120°F using heat tracing to prevent precipitation.

An 8-in ID and 40-foot tall water-wash column was installed downstream of the absorber to capture ammonia from the clean syngas using deionized (DI) water. The water-wash column was equipped with one stage of structural packing and a second stage of bubble cap trays to minimize ammonia emissions. An automated back-pressure control valve was used to maintain desired pressure in the absorber and water-wash columns. A positive displacement pump delivered DI water to the top of the water-wash column, while another positive displacement

pump was used to circulate the water through the first absorption stage. A Horiba CO₂ analyzer was used to monitor CO₂ concentration in the clean syngas. A Fourier transform infrared (FTIR) spectrometer was installed to monitor ammonia loss in clean syngas.

A slip stream of rich solution was taken out of the first absorption stage at the bottom of the absorber column recirculation loop using a level controller and an automatic control valve. The level controller maintained the rich solution inventory in the bottom of the absorber column, and the slip stream was delivered to the regenerator for stripping CO₂ and H₂S. The rich solution delivery lines were heat-traced to prevent precipitation.

The regenerator column was equipped with a reboiler to use moderate pressure steam and strip CO₂ and H₂S from the rich solution. The regenerator column was designed with 8-in ID and 40-foot tall stainless steel column. The top stage of the regenerator contained the water wash for the stripped gas stream to reduce ammonia emission. An automated back-pressure control valve maintained the stripping gas pressure in the regenerator column.

The rich solvent was transferred from the absorber to the regenerator using a small pressure differential between the two columns, while lean solution from the regenerator bottom was transferred to a lean solution surge tank and pumped to the top of the absorber using a positive displacement pump.

The waste water streams from the absorber water-wash and regenerator water-wash columns were collected into a spent water tank for disposal. In a larger system, the waste water will be sent to a sour-water stripper to recover ammonia. Chemical analysis of the samples from liquid waste streams and the lean solution demonstrated a low loss of ammonia during normal operation of the pilot plant.

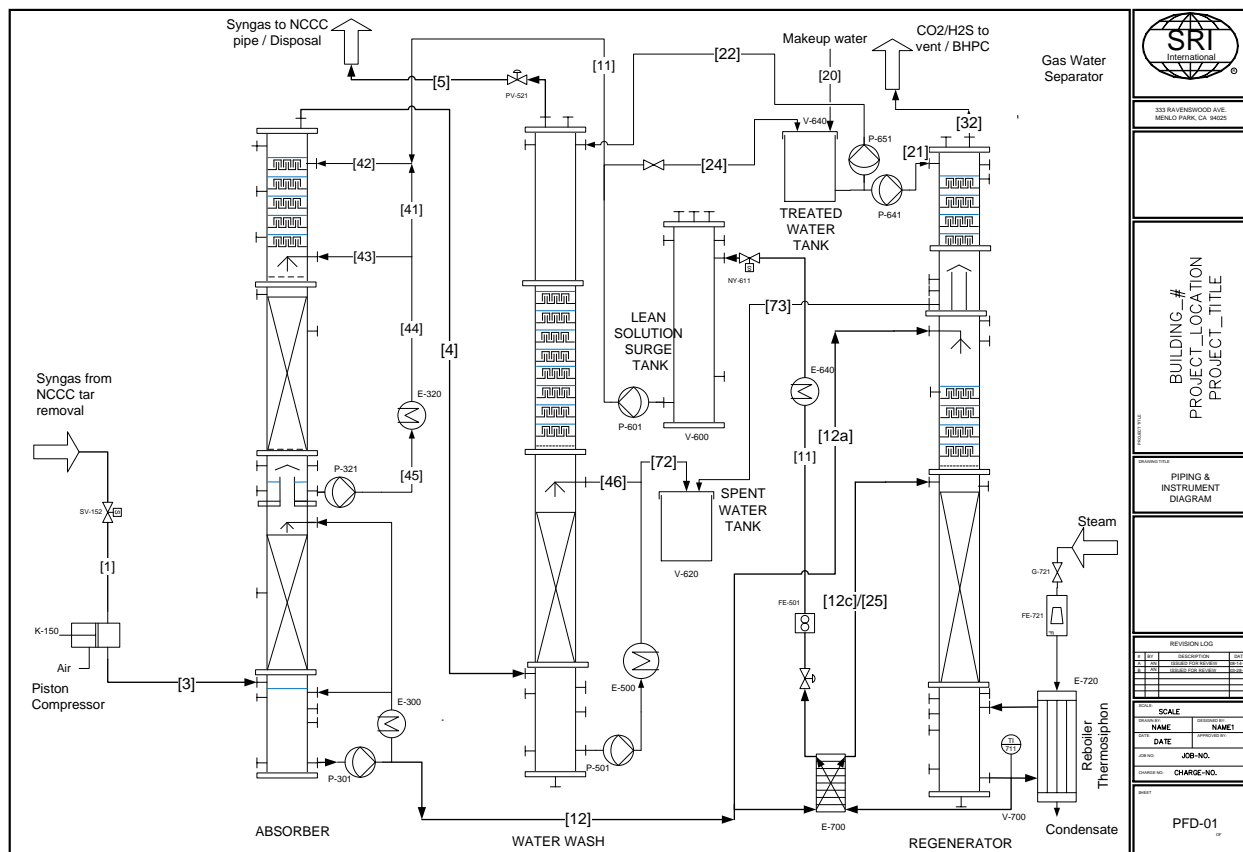


Figure 32. Process flow diagram of the AC-ABC system.

Integrated Plant Operation – First Test Campaign

The small-scale AC-ABC pilot plant was operated using a slipstream of up to 500 lb/hr syngas from air-blown gasifier at the NCCC, Wilsonville, AL in September / October 2015. Lignite coal with a high sulfur content was used by the NCCC in the gasifier, resulting in ~ 2000 ppmv hydrogen sulfide in the syngas slipstream. A shift reactor operated by the NCCC converted carbon monoxide to carbon dioxide using high-pressure steam. Syngas obtained after the shift reactor and quench typically had 14 – 16% CO₂, 0.2% H₂S, 1% CO, 12% H₂, 0.5% O₂, and 0.5% CH₄ with the balance as nitrogen. Syngas was supplied at 60°F, -70°F, and 180 psig. During upset conditions of the gasifier or syngas clean-up unit, the slipstream of syngas was replaced with nitrogen by the NCCC.

A syngas compressor, which was part of the AC-ABC pilot plant, was equipped with a variable frequency drive used to control the syngas mass flow through the AC-ABC absorber column. Syngas flow was varied between 300 – 450 lb/hr at 450 psig. An IR-based CO₂ analyzer was used to measure CO₂ in the syngas slip stream on a dry basis. In addition, the NCCC

monitored the composition of the syngas after the shift reactor and provided the syngas composition data. A high-pressure, positive displacement pump was used to feed lean solution at the top of the absorber column. The pump was equipped with a variable frequency drive to control the solvent flow through the system. The lean solvent flow was varied between 500 – 1000 lb/hr.

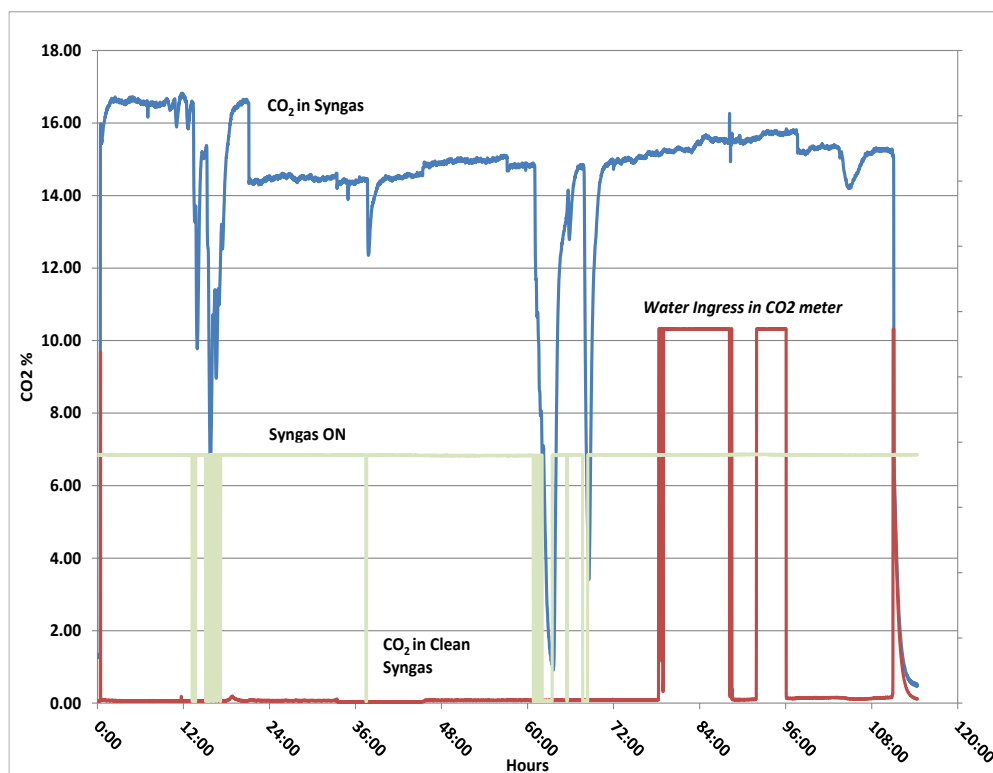


Figure 33. CO₂ concentration in syngas (Run #3).

Figure 33 shows CO₂ concentration in the incoming syngas at the inlet of the absorber and in the clean syngas at the outlet of the absorber water wash. It also shows availability of syngas flow. During the interruption at the syngas cleanup unit (SCU) syngas stream was replaced with nitrogen by the NCCC staff. Between ~ 75 hr to 95 hr, the outlet CO₂ analyzer experienced water ingress and showed erroneous readings. The objective of this run was to demonstrate high CO₂ capture efficiency, shown in Figure 34, under a steady-state, 100-hour operation of the pilot plant. Figure 35 shows H₂S concentration in incoming syngas and in the clean syngas at the outlet of absorber water wash. H₂S was measured by NCCC staff using a gas chromatograph (GC). The data shows high capture efficiency for H₂S.

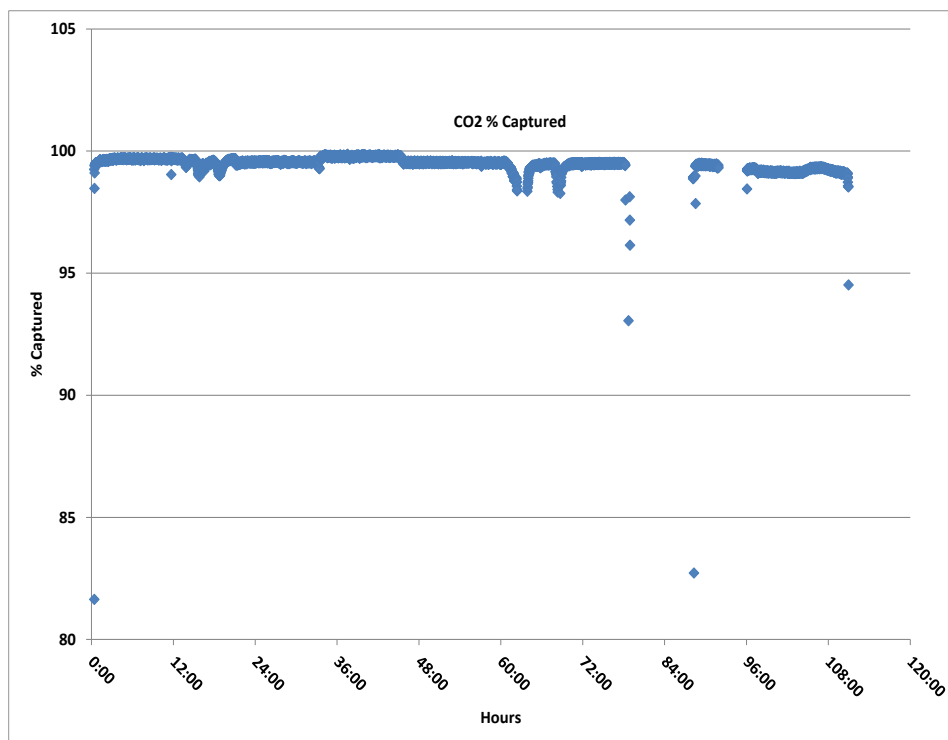


Figure 34. CO₂ capture efficiency (Run #3).

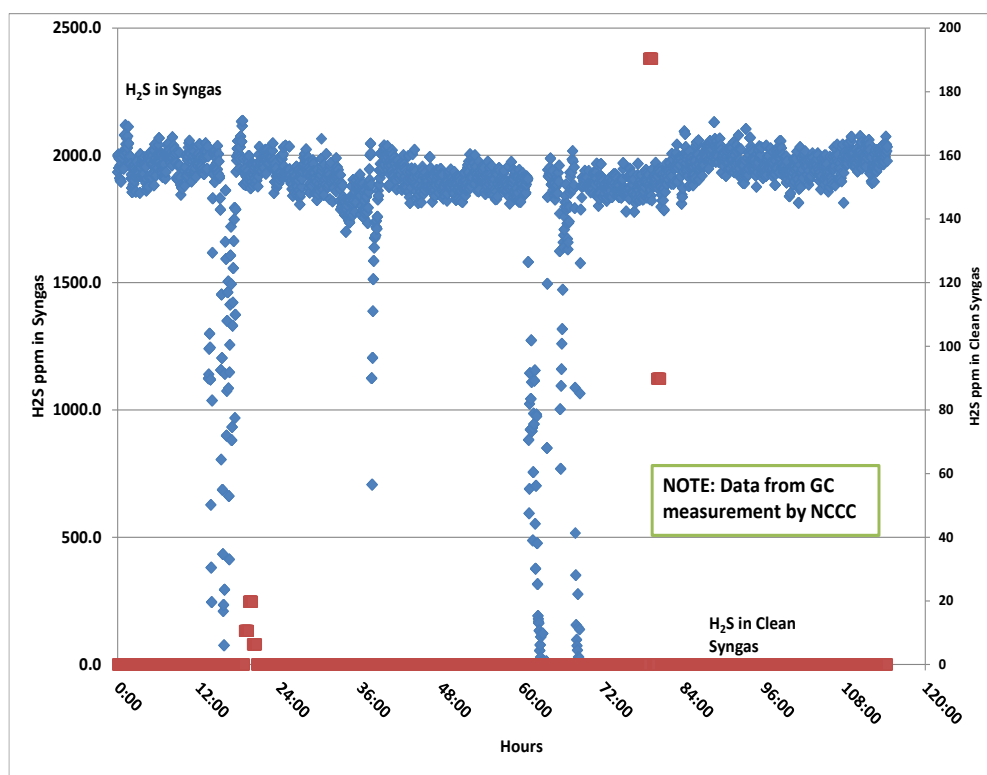


Figure 35. H₂S concentration in syngas (Run #3).

The bottom section of the absorber column was used as a reservoir for rich solution. A positive displacement pump circulated the rich solution through the first absorption stage of the absorber. The reservoir and first stage of the absorber were heat-traced, and the temperature was maintained at 120°F to prevent precipitation of solids from the CO₂-rich solution. A positive displacement pump was used to circulate the solvent through a water-cooled heat exchanger with a bypass control to maintain the temperature and maximize CO₂ capture in the second stage of absorber. Both the first- and second-stage absorbers were comprised of stainless steel structural packing.

The third stage of the absorber was equipped with bubble cap trays. The purpose of the trays was to minimize ammonia loss by controlling the lean solution and semi-rich solution flow rates.

Clean syngas was obtained after the capture of CO₂ and H₂S and was passed through a water-wash column to remove ammonia. An automated back-pressure control valve at the exit of water-wash column was used to control the absorption pressure in the absorber.

Demineralized water was added to the top of the water-wash column using a positive displacement pump to reduce the ammonia emission. An IR-based CO₂ analyzer was used to monitor CO₂ in the clean syngas to determine efficacy of CO₂ absorption process. In addition, an FTIR spectrometer was installed to monitor ammonia content in the clean syngas stream. The clean syngas composition was monitored by the NCCC staff using a GC on a continuous basis.

As the lean solution was added to the top of the absorber, an automated level control valve sent a side stream of rich solution to the regenerator column. All rich-solution lines, instrumentation, and control valves were heat-traced to prevent precipitation of solids.

Liquid samples were collected from the water-wash waste stream to monitor ammonia loss.

Figure 36 shows the syngas pressure at the absorber inlet, near the first absorber stage, and near the top of the absorber column. The pressure at the absorber water wash was controlled using a backpressure control valve.

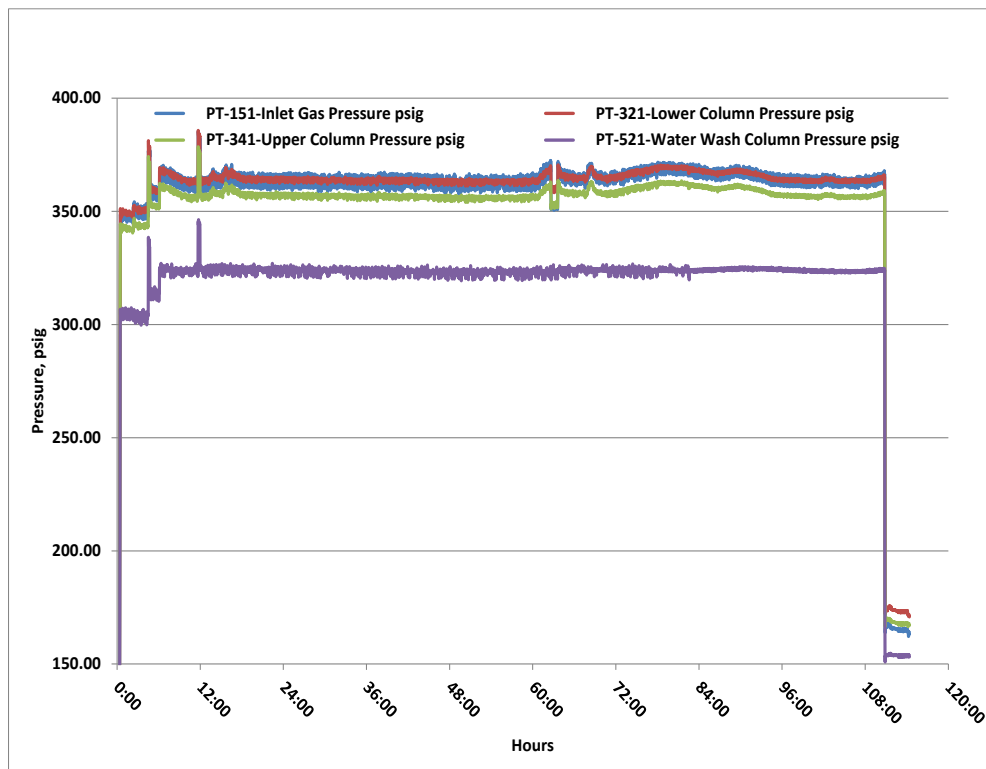


Figure 36. Absorber pressure (Run #3).

The rich-solution side stream to the regenerator was passed through a heat-recovery exchanger to recover heat from the lean solution. Low-pressure steam was supplied to the reboiler attached to the regenerator. Steam flow was controlled using a manual control valve. As expected, a thermal siphon developed between the regenerator and reboiler. Part of the rich-solution stream was split from the main stream and fed to the middle stage of regenerator to reduce ammonia loss from the regeneration process. A water-wash stage using demineralized water was added to the top of the regenerator column to remove ammonia from the regenerated gas stream. Liquid samples were collected from the water-wash waste stream and monitored for ammonia content.

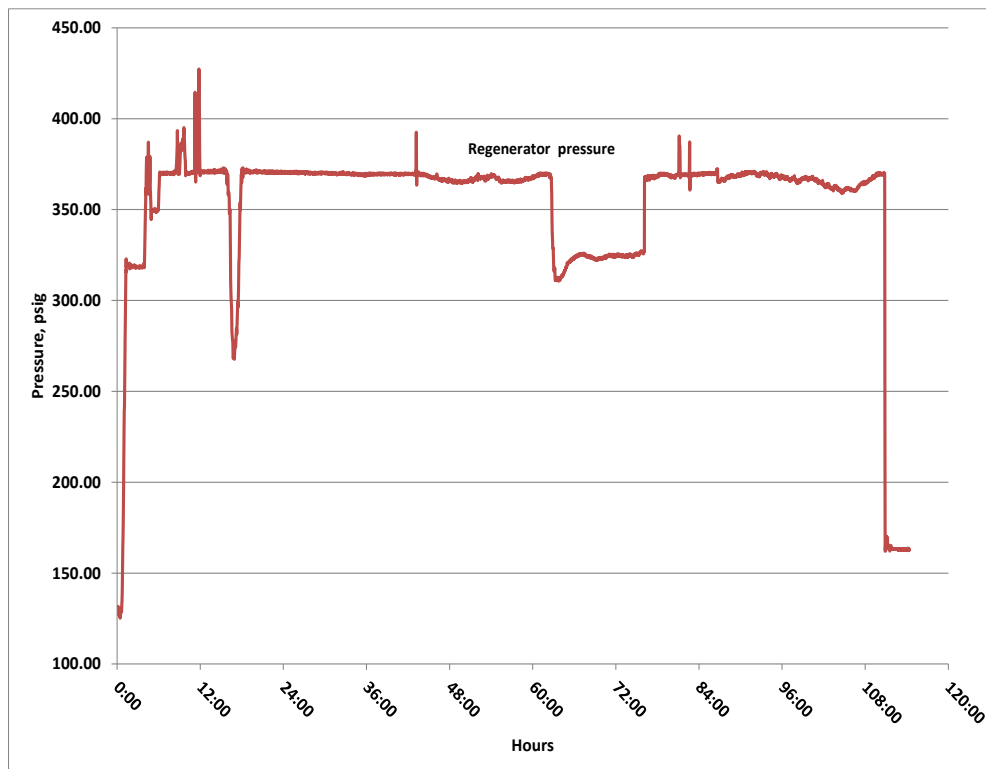


Figure 37. Regenerator pressure (Run #3).

An automated back-pressure control valve was used to maintain the regenerator pressure, and the regenerated stream was sent to the BPSC skid to convert H_2S to elemental sulfur. Figure 37 shows that CO_2 can be regenerated at high pressure under steady-state operation. Operating the regenerator at near the absorber pressure required less pump power for circulating solvent through the system. This also reduced the number of compression stages for the CO_2 compressor used for CO_2 transportation. The level controller maintained the liquid level in the regenerator bottom section, and the lean solution was returned to lean solution surge tank through a heat recovery heat exchanger.

The reboiler was operated at 290°F – 310°F by controlling the steam input and maintaining a back pressure of 300-350 psig.

Analytical Testing

Liquid samples were collected periodically from the lean solution stream and analyzed for ammonia and CO_2 loading. A target CO_2/NH_3 loading ratio for the lean solution was set at 0.4 – 0.45. A CO_2 loading of $\sim 100\text{g/liter}$ of solvent was demonstrated under one operating condition [Figure 40: CO_2 loading (Run #2)] during the first test campaign.

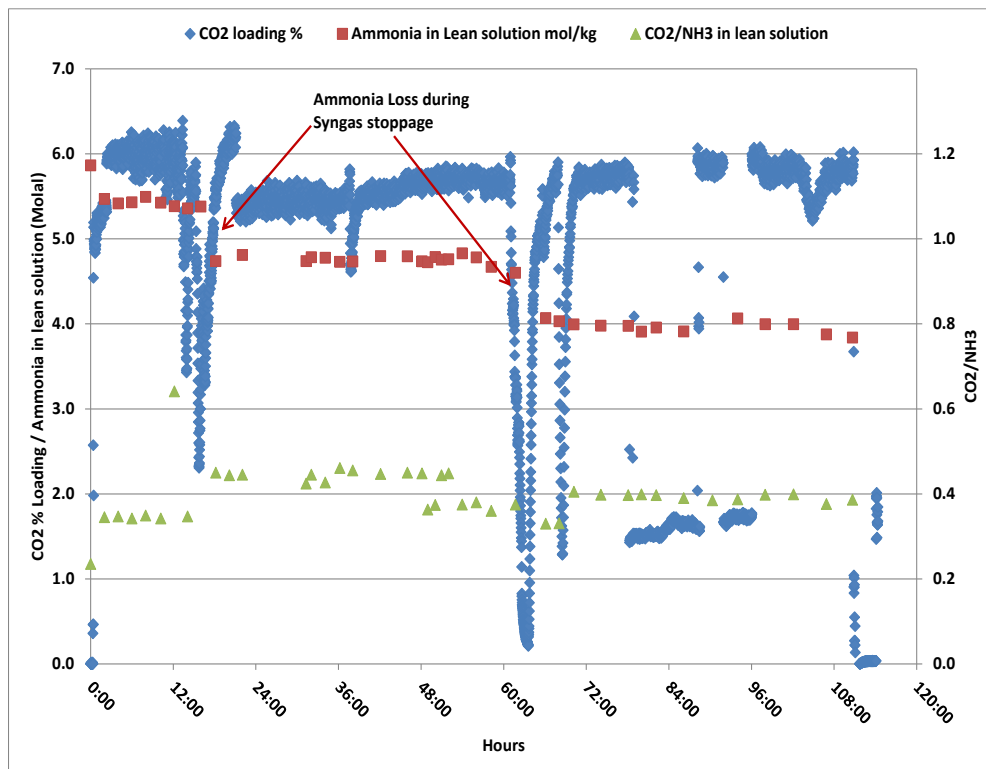
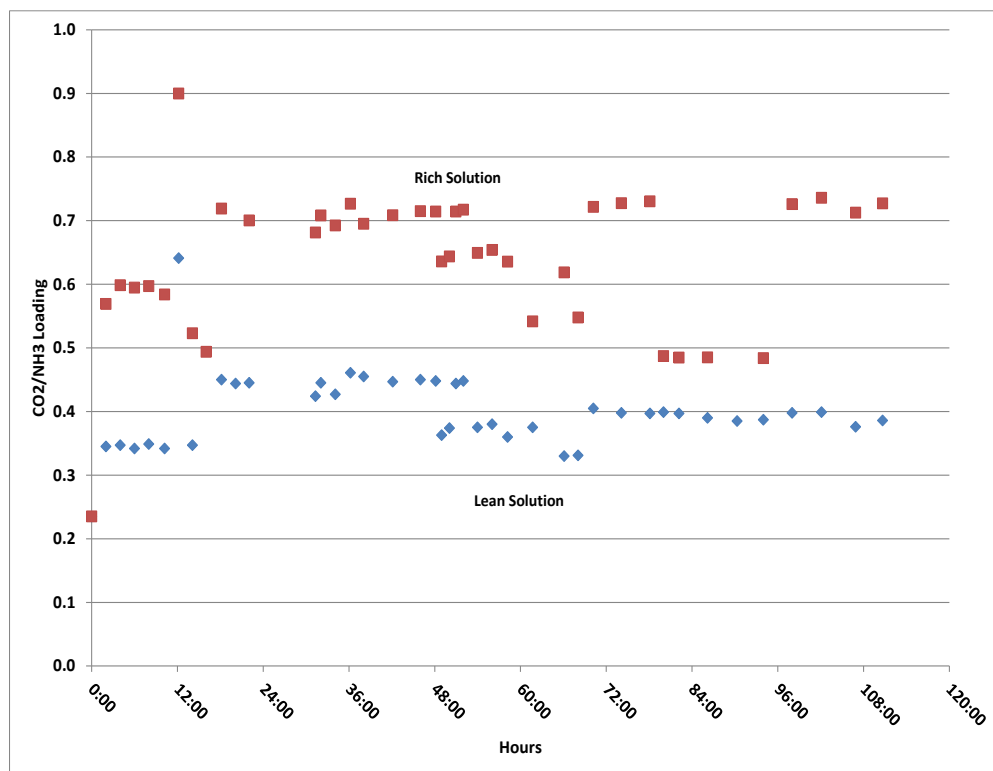
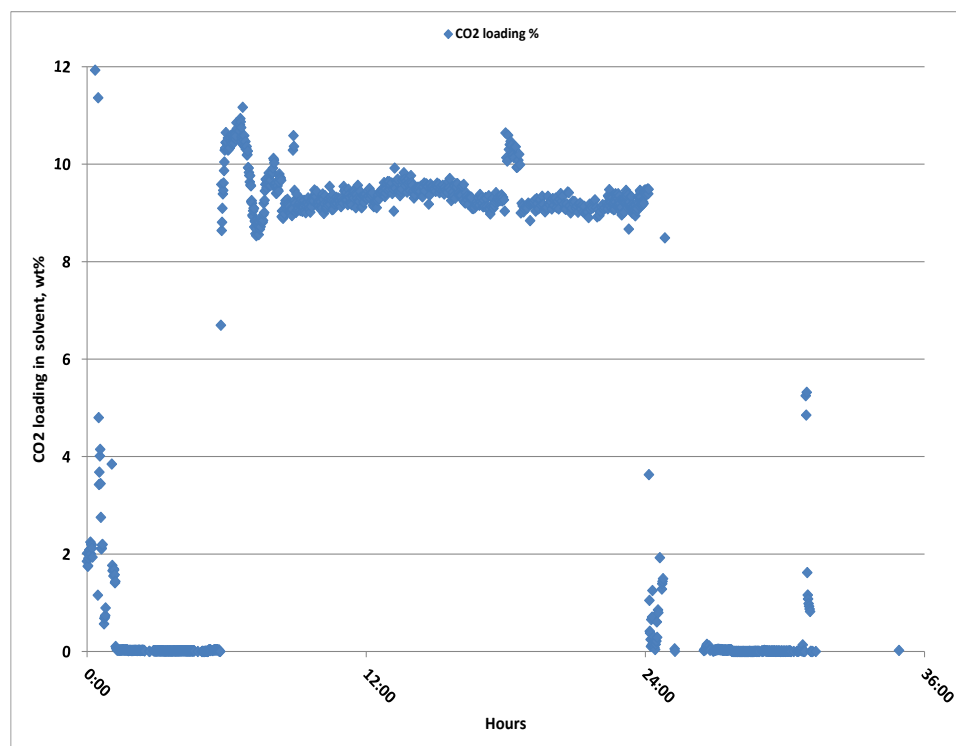


Figure 38. CO₂ loading (Run #3).

As mentioned earlier, syngas was replaced by nitrogen during the upset conditions of the gasifier and/or SCU at the NCCC. This caused a system upset in AC-ABC pilot plant and a loss of ammonia from the solvent [Figure 38. CO₂ loading (Run #3)]. A modified operating procedure was implemented to minimize ammonia loss in the second test campaign.

Based on lean solution analysis, the CO₂/NH₃ ratio was determined to be at 0.4 – 0.45. Rich-solution loading was calculated as 0.7 [Figure 39. CO₂ / NH₃ loading (Run #3)]. With heat tracing in place, there was no appreciable solids precipitation in the rich-solution path. A higher CO₂ loading in the rich solution (0.8) and a lower loading (0.35) in the lean solution were targeted for the second test campaign to improve CO₂ loading in the water up to 150 g/liter or higher.

**Figure 39.** CO₂ / NH₃ loading (Run #3).**Figure 40.** CO₂ loading (Run #2).

The regenerated gas stream was analyzed for H₂S content using Draeger tubes. H₂S varied between 0.7 to 1.5% in the regenerated stream (Figure 41).

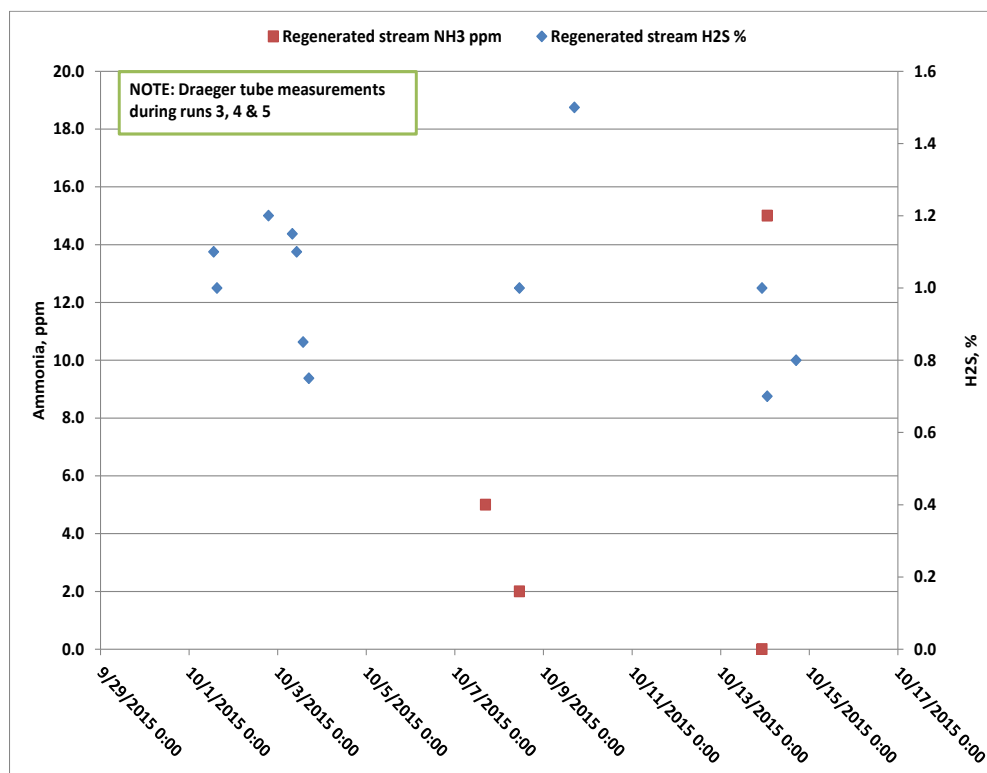


Figure 41. NH₃ & H₂S concentrations in regenerator gas.

A pressure-sampling vessel was used to collect gas samples from the regenerated gas stream, and it was analyzed at the NCCC using a GC. The gas analysis demonstrated a very low level of fuel gas species in the regenerated gas stream as shown in Figure 42 [Gas composition (dry basis) of regenerated gas stream]; thus, there was a negligible loss of fuel gas species from syngas, (Figure 43).

	10/13/2015	10/15/2015
Hydrogen (vol %)	0.07	0.08
Nitrogen (vol %)	1.56	0.45
Carbon monoxide (vol %)	0.02	0
Methane (vol %)	0	0
Argon (vol %)	0.26	0.01
Hydrogen sulfide (vol %)	1.42	1.56
Carbon dioxide (vol %)	96.67	97.9
Carbonyl sulfide (ppmv)	25	19

Figure 42. Gas composition (dry basis) of regenerated gas stream.

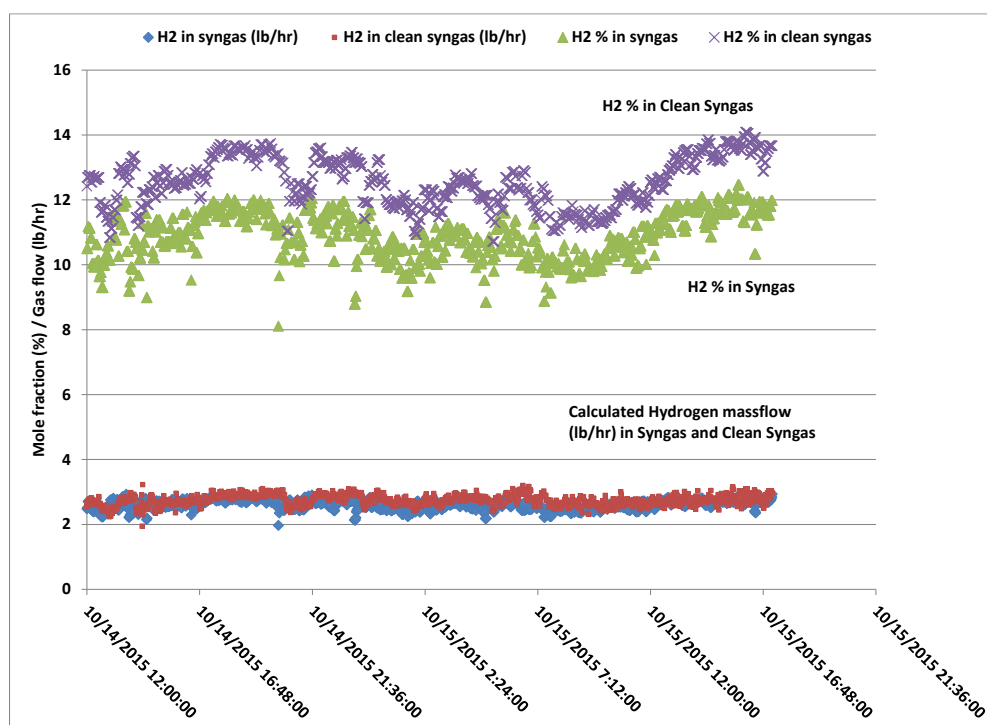


Figure 43. Mass balance of hydrogen.

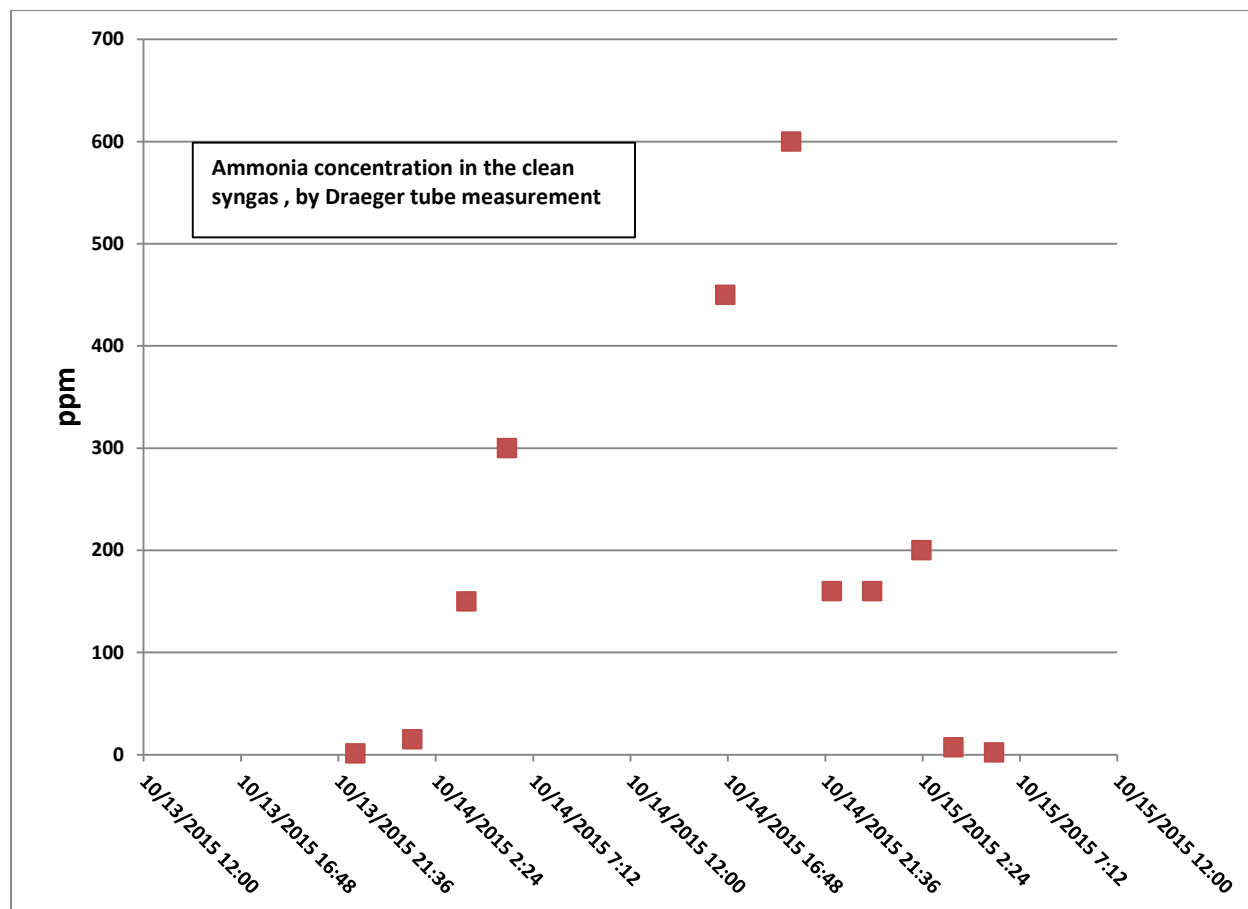


Figure 44. NH_3 concentration in clean syngas.

An FTIR was installed to monitor the ammonia concentration in the clean syngas stream. During the startup, the FTIR was damaged due to the presence of particles in the gas stream. Draeger tubes were used instead of FTIR to periodically monitor the ammonia concentration. The maximum ammonia concentration measured was 600 ppm in the clean syngas stream as shown in Figure 44. This level of ammonia was caused by failure of the bubble cap trays in the third stage of the absorption column.

System Modification and Maintenance

A high-pressure positive displacement pump for the lean solution failed during operation. The diaphragm was replaced, and the pilot plant was restarted. The probable cause of diaphragm failure was a pressure surge or the presence of syngas-entrained particles.

During upset conditions, particles were entrained with raw syngas. These particles were analyzed and found to be less than 100 micron in size and contained calcium, magnesium, iron, and chromium as main constituents. The syngas compressor was equipped with an inlet filter that

was sized to remove 100-micron or larger particles from the gas stream. The particles clogged several control valves, and the pilot plant had to be shut down. After removing the solvent, the system was rinsed several times to clean the control valves, lines, and columns, and the system was restarted. The source of particles is undetermined. The particles were recovered from the liquid stream and tested for size and composition (Figures 45-47).

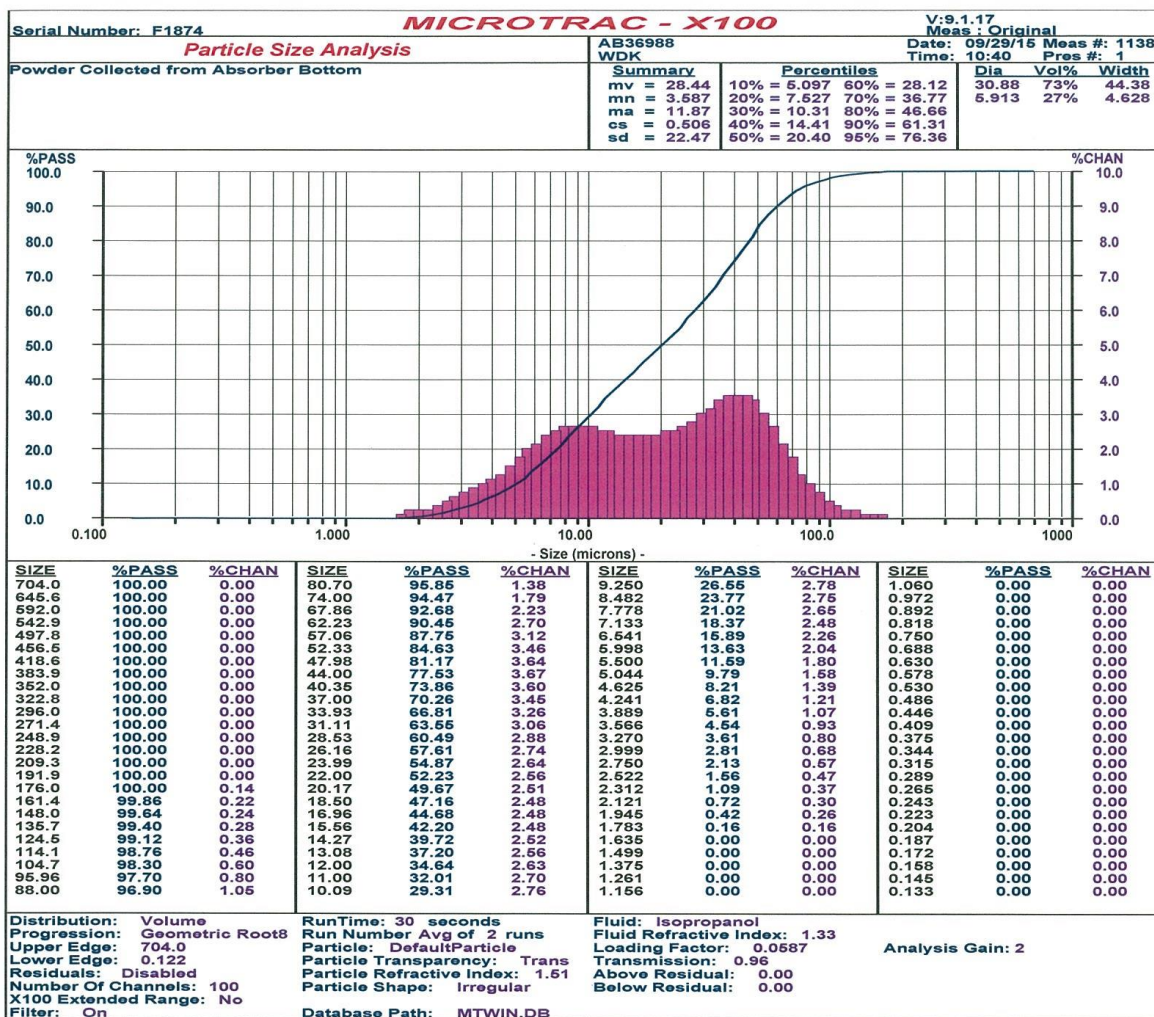


Figure 45. Entrained particles – size distribution.

Alabama Power
General Test Laboratory
P.O. Box 2641
Birmingham, Alabama 35291
(205) 664 - 6032 or 6171
FAX (205) 257-1654



CERTIFICATE OF ANALYSIS

To: Ms. Wynema Kimbrough
PSDF P.O. Box 1069
Wilsonville, AL 35186

Customer Account: DTNCCCC
Sample Date: 9/29/2015
Customer ID Number: PSDF
Delivery Date: 9/30/2015

Description: PSDF # AB36988
Powder from Absorber Bottom

Laboratory ID Number: AV22912

Name	Reference	Results	Units
Comment			
Aluminum Oxide	XRF (E. Scan)	0.18	percent
Arsenic Oxide	XRF (E. Scan)	Not Detected	percent
Calcium Oxide	XRF (E. Scan)	57.60	percent
Cobalt Oxide	XRF (E. Scan)	0.02	percent
Chromium Oxide	XRF (E. Scan)	3.11	percent
Copper Oxide	XRF (E. Scan)	0.07	percent
Iron Oxide	XRF (E. Scan)	4.84	percent
Magnesium Oxide	XRF (E. Scan)	27.66	percent
Manganese Oxide	XRF (E. Scan)	0.37	percent
Molybdenum Oxide	XRF (E. Scan)	0.06	percent
Sodium Oxide	XRF (E. Scan)	0.03	percent
Niobium Oxide	XRF (E. Scan)	0.01	percent
Nickel Oxide	XRF (E. Scan)	0.43	percent
Phosphorus Pentoxide	XRF (E. Scan)	0.18	percent
Silicon Oxide	XRF (E. Scan)	1.09	percent
Strontium Oxide	XRF (E. Scan)	0.04	percent
Sulfur Oxide	XRF (E. Scan)	4.19	percent
Titanium Oxide	XRF (E. Scan)	0.07	percent
Zinc Oxide	XRF (E. Scan)	0.02	percent
Zirconium Oxide	XRF (E. Scan)	0.02	percent

This Certificate states the physical and/or chemical characteristics of the sample as submitted. This document shall not be reproduced, except in full, without written consent from Alabama Power's General Test Laboratory.

Comments:

cc:

Quality Control _____ Supervision _____

Reported: 10/1/2015

Version: 1.0

Figure 46. X-ray fluorescence analysis of the syngas-entrained particles.

Alabama Power
General Test Laboratory
P.O. Box 2641
Birmingham, Alabama 35291
(205) 664 - 6032 or 6171
FAX (205) 257-1654



CERTIFICATE OF ANALYSIS

To: Ms. Wynema Kimbrough
PSDF P.O. Box 1069
Wilsonville, AL 35186

Customer Account: DTNCCCC

Sample Date: 9/29/2015

Customer ID Number: PSDF

Delivery Date: 9/30/2015

Description: PSDF # AB36988

Powder from Absorber Bottom

Laboratory ID Number: AV22912

Name	Reference	Results	Units
Aragonite - CaCO_3		56.7%	
Monetite - CaHPO_4		10.1%	
Sillimanite - Al_2SiO_5		7.9%	
Forsterite - Mg_2SiO_4		7.2%	
Olivine - $\text{Mg}_2\text{FeCaSiO}_4$		5.3%	
Diopside - $\text{CaMgSi}_2\text{O}_6$		5.1%	
Spinel - MgAl_2O_4		3.4%	
Iron Phosphide - FeP		2.9%	
Periclase - MgO		1.5%	

Results are semi-quantitative as determined by X-Ray Diffraction.

This Certificate states the physical and/or chemical characteristics of the sample as submitted. This document shall not be reproduced, except in full, without written consent from Alabama Power's General Test Laboratory.

Comments:

cc:

Quality Control _____ Supervision _____

Reported: 10/1/2015

Version: 1.0

Figure 47. Semi-quantitative analysis by X-ray diffraction of syngas-entrained particles.

CO₂ / H₂S Separation Process

A BPSC process was installed downstream of the AC-ABC system to separate H₂S from the CO₂ regenerated gas stream and convert the same to elemental sulfur using SO₂. There were several design, installation, and operational shortcomings in the BPSC system. A positive displacement pump was used to provide liquid SO₂ at a calculated rate based on H₂S concentration in the regenerated stream. Due to the small flows involved, it was difficult to control the pump output to match the desired demand. As shown in Figures 48 and 49, a significant amount of sulfur was recovered in elemental form from the regenerated gas stream, even after all the system problems. However, inadequate heat tracing prevented measurement of the flow and quantification of the sulfur produced.

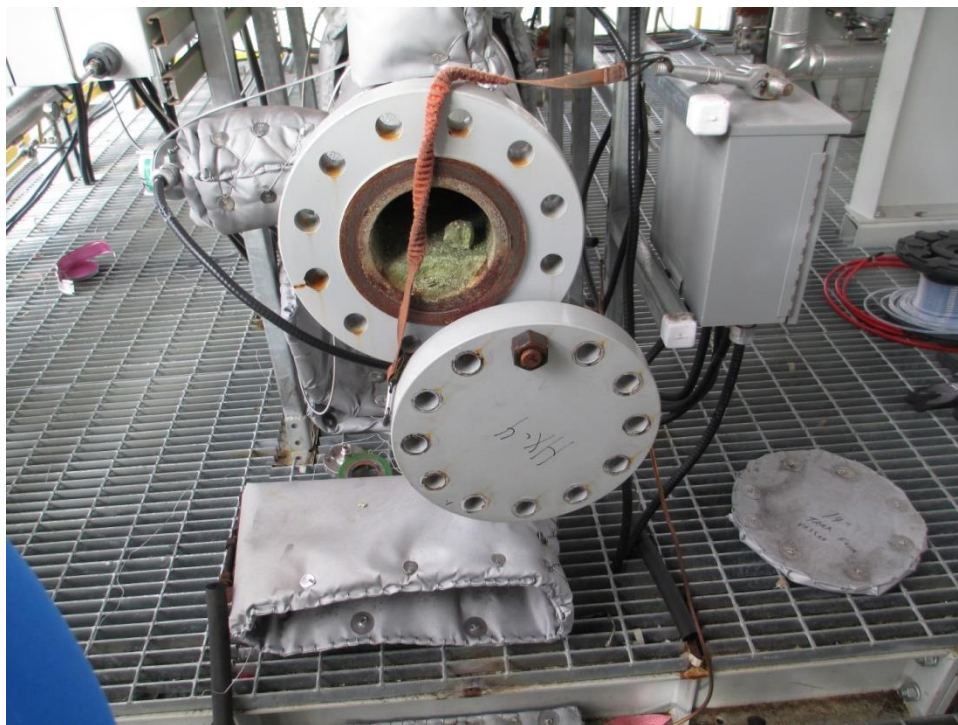


Figure 48. Sulfur in outlet plenum of reactor intercooler HX-04.



Figure 49. Close-up view of sulfur in outlet plenum of reactor intercooler HX-04.

Second Test Campaign

Based on the data from the first test campaign and operating experience, the following objectives were targeted for the second test campaign during April / May 2016:

1. **Objective:** Steady, continuous operation for 100 hours or more at 99+% CO₂ and H₂S capture efficiency; regeneration and sulfur production.

Results: A total of over 400 hr of operating data was collected from the second test campaign, including a 175-hr (7-day) continuous integrated run. The test results show that both CO₂ and H₂S can be captured in a single absorber operating at 350 psig, 120°F. A high capture efficiency for both CO₂ and H₂S (> 99+ %) was demonstrated during this test campaign. This test campaign had > 80% uptime for the pilot plant.

CO₂ in clean syngas was measured at 500 – 1000 ppm, compared to 14% CO₂ in the feed gas, when absorption was performed at 350 psig. Operation at higher pressure will further reduce this residual CO₂ emission. H₂S was reduced from 2000 ppm in the inlet gas stream to < 2 ppm (below the detection limit of GC) in the clean syngas stream.

A stream of > 98+ mol% CO₂ and 1.5 mol% H₂S was regenerated at 350 psig from a single regenerator. The downstream process demonstrated high conversion of H₂S to high-purity elemental sulfur. However, due to heat tracing problems on small-diameter interconnecting tubing, the liquid sulfur solidified and did not flow to the appropriate vessels; as such, sulfur production could not be quantified.

2. **Objective:** Achieve > 100 g CO₂ loading per 1000 g water using an 8-molal NH₃ solution.

Results: An effective loading of 120 gCO₂/1000 g water was demonstrated under steady-state operation during the test campaign with maximum loading, and 140 gCO₂/1000 g water was achieved.

3. **Objective:** Optimize operation of the top of absorber to minimize NH₃ flow to the water wash.

Results: Bubble cap trays in the top absorber section were replaced by structural packing for this test campaign, and later the top absorber section was bypassed due to ineffective liquid-to-gas contact. The absorber was operated with only two stages, and still the test results show high CO₂ capture efficiency. Ammonia emission from the absorber was measured at 500 – 1000 ppm under steady operating conditions. During operation at higher pressure and with the third-stage absorption, ammonia emissions can easily be reduced to a very low value (~ 20 ppm). In a commercial system, ammonia will be recovered in a sour-water stripper.

4. **Objective:** Optimize the water-wash operation to demonstrate low water use.

Results: Based on lab tests carried out at atmospheric pressure at SRI International, the bubble cap trays were modified to eliminate flooding experienced during the first test campaign. However, the modified bubble cap trays did not perform as expected, and low water use could not be demonstrated. ASPEN modeling shows it is possible to capture ammonia emissions from the absorber with minimal water use when properly designed bubble cap trays are used. Commercially designed bubble cap trays were not available for the small pilot-scale setup; however, the same will be included in a future test campaign to demonstrate low water use in the water-wash column at a larger scale.

5. **Objective:** Operate the regenerator steam in steady mode and operate the lean solution with CO_2 loading < 0.35 .

Results: The regenerator was operated with steady steam flow, and a low CO_2 loading in the lean solution ($< 0.35 \text{ CO}_2/\text{NH}_3$ ratio) was demonstrated. It is possible to automate steam flow control using a reboiler temperature feedback loop control. The same will be considered for a future test campaign.

6. **Objective:** Operate the BPSC skid with controlled SO_2 flow and quantify sulfur formation.

Results: The sulfur dioxide delivery system was modified to enable controlled flow of SO_2 to the process system. The test results show high conversion of H_2S to high-purity elemental sulfur. However, due to problems with heat tracing, liquid sulfur did not flow to the collection vessel and instead froze at cold spots in lines and/or valves and hence could not be quantified. A future test campaign could use higher-temperature heat tracing and better insulation.

Pilot-Plant Modification

Based on operational experience, data collected, and lessons learned from the first test campaign during September/October 2015, the following modifications were carried out prior to the second test campaign at the pilot plant.

1. During the first test campaign, some solid particles were entrained with raw syngas. An inlet syngas particle filter was installed upstream of the syngas compressor to remove any solids entrained in the raw syngas and prevent damage to the compressor.
2. Heat tracing and insulation on the system process piping and vessels were improved to prevent precipitation from the rich solution during the process upset conditions. The gas-sampling lines were heat-traced to prevent precipitation from the gas phase.

3. It was a challenge to commercially source the bubble cap trays for the small diameter of the pilot process vessels for the AC-ABC process. To demonstrate low water use for ammonia emission control, bubble cap trays are the most efficient gas-liquid contactors. For the first test campaign, in-house designed and fabricated bubble cap trays were installed. During the pilot plant operation, tray flooding was observed and the trays were bypassed during extended operation. Bubble cap trays were field-modified based on atmospheric pressure tests carried out at the SRI lab. The modified bubble cap trays did not perform as intended in the water-wash column and had to be bypassed again. For a future test campaign, we expect that commercial bubble cap trays will be used, and a potential source for them has been identified.
4. The absorber top stage also contained bubble cap trays to effectively control ammonia emissions from the absorber by adjusting the ratio of the lean solution feed rate to a recirculation flow rate. The first test campaign resulted in bubble cap trays flooding and solvent carryover to water-wash column. The top absorber stage bubble cap trays were replaced by structural packing. Due to low liquid loads, the structural packing was not effective. The third stage of absorber was bypassed, and the absorber was operated with two working stages. Test results show that capture efficiency was still very high for both CO₂ and H₂S even with only two operating stages. The recorded ammonia emissions were between 500 – 1000 ppmv.
5. Steam-cleaning valves were added to the piping where clogging was experienced due to process upset conditions during the first test campaign. This enabled faster turnaround between two test runs and resulted in > 80% uptime for the pilot plant during the second test campaign.
6. The solvent circulation pump's Viton diaphragms were replaced with EPDM material, which is more chemically compatible with sulfides in the solvent.
7. Thermal mass flow meters in the exit gas lines were replaced by a Coriolis meter for better data collection in the gas flows.
8. The particles entrained in raw syngas during the first test campaign damaged the FTIR mirrors. Hence, ammonia emissions could not be monitored during the first test campaign. The FTIR spectrometer was repaired and installed to monitor ammonia in the gas outlet from the absorber column.
9. A gas heater was added to provide heated nitrogen for regeneration of sulfur from the catalytic bed for the BPSC skid.

10. The SO₂ delivery system was modified, and a pulsation dampener was added to the SO₂ line to reduce flow fluctuations due to diaphragm pump. A new SO₂ vaporizer was installed to convert liquid sulfur dioxide to vapor. Under the modified arrangement for SO₂ delivery, a recirculation loop was added to the pump and a Coriolis-based flow control was designed to withdraw the desired amount of liquid from the loop. The performance of the SO₂ delivery system improved somewhat, but further improvements can be made by replacing the pump with one that has a larger flow rate such that the recirculation loop always has more than the desired quantity of liquid.
11. The sulfur product cooler/melter serves a dual purpose. As the gas product enters the cooler/melter before returning to the facility, this is the last opportunity to remove sulfur vapor and simultaneously provide a more dense vapor for compression. As a result, elemental sulfur vapor solidifies on the tubes. During the cycle, this exchanger moves from being a "cooler" to a "melter". Elemental sulfur is melted off of the tubes using steam on the opposite side of the heat exchanger. The sulfur is then collected with the other liquid sulfur from the normal process outlet. Steam tracing was added to the sulfur product cooler/melter to provide faster heating and cooling steps. Electric tracing was deemed not fast enough for the heat-up step. By using steam in the coil around the vessels, the desired temperature was achieved in a short time. During the cooling step, steam was replaced with cooling water to reduce the shell temperature of the vessel in a short period of time.

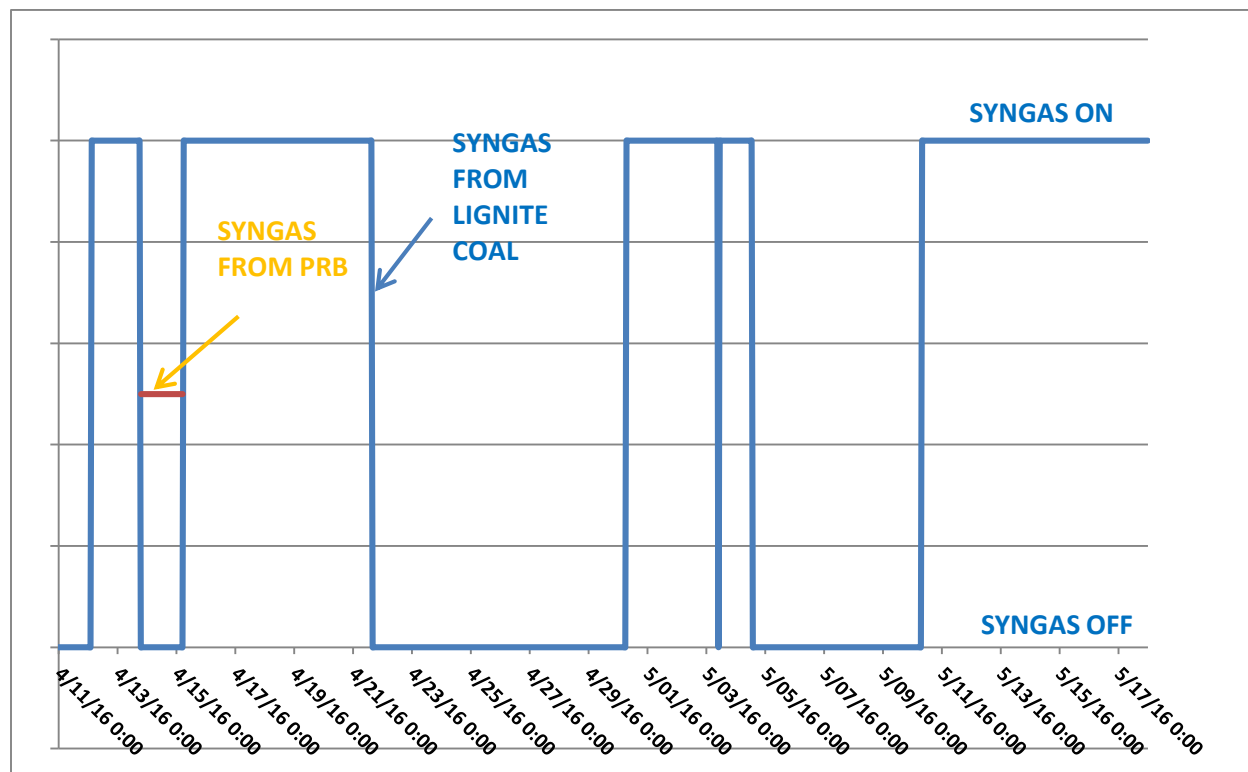
The above-mentioned modifications significantly improved the pilot operation during the second test campaign. During the April/May 2016 test campaign, five test runs were carried out with a total of 400 hr of data collected from 480 hr of syngas availability from the gasifier. This campaign included one continuous run of 175 hr (7 days).

Pilot-Plant Operation

The second test campaign of the AC-ABC / BPSC pilot plant was carried out at the NCCC in Alabama in April/May 2016. The NCCC operated the coal gasifier using PRB, a mix of PRB/lignite, and lignite coal. The SCU at the NCCC provided 500 lb/hr shifted syngas after tar removal at 170 psig and 50 – 60°F. Shifted syngas contained 12-15 mol% CO₂ and 1800 – 2000 ppmv H₂S. Availability of raw syngas from the NCCC gasifier was hampered by gasifier maintenance issues. The gasifier had to be shut down for maintenance a few times during the test campaign for multiple days at a time. The raw syngas with H₂S > 1000 ppmv was available for ~ 480 hours during the G4 test campaign.

Table 10. Typical raw syngas stream composition from the lignite coal gasifier at NCCC.

Syngas Temp	Syngas Pressure	Ar	N ₂	CO	CO ₂	CH ₄	H ₂	H ₂ S
TI9860	PI9863	AI2603A	AI2603B	AI2603C	AI2603D	AI2603E	AI2603G	AI2603J
°F	psig	%	%	%	%	%	%	ppm
67.4	170.2	0.6	74.4	0.03	13.4	0.6	10.1	2081.7

**Figure 50.** Raw syngas availability.

A syngas compressor was used to increase the pressure of raw syngas to 350 psig. The compressor is equipped with a variable speed drive to control the flow of syngas to the absorber. A particle filter was added to the compressor inlet, and a compressor bypass line was installed to vent any residual gases in the syngas supply line. IR-based CO₂ monitors were used to measure CO₂ concentration in the inlet raw syngas and clean syngas. In addition, the NCCC provided raw syngas composition and also measured clean syngas composition using a GC. A separate GC measured H₂S in the clean syngas. The repaired FTIR spectrometer was used to monitor ammonia concentration in the gas stream exiting the absorber. Coriolis meters were used to measure mass flow of raw and clean syngas and regenerated stream. Grab samples of regenerated gas stream were taken periodically and analyzed for composition by the NCCC.

using a GC. H₂S in the clean CO₂ gas after the sulfur recovery system was measured using Draeger tubes.

Discussion of Results

Detailed data and analysis are presented here for Run #10, when the pilot plant was operated for ~ 175 hr (7 days) on a 24-hr basis. During the run, some ammoniated solution was removed and fresh solution was added to the system. There was some interruption to syngas during this run; the pilot plant was put in a hot-standby mode and solvent circulation continued but the steam was cutback. The inlet and outlet syngas streams were closed. Another interruption was caused by back pressure in the syngas return line, probably due to clogging. The inlet syngas was temporarily stopped to clear the clog, and the pilot operation resumed.

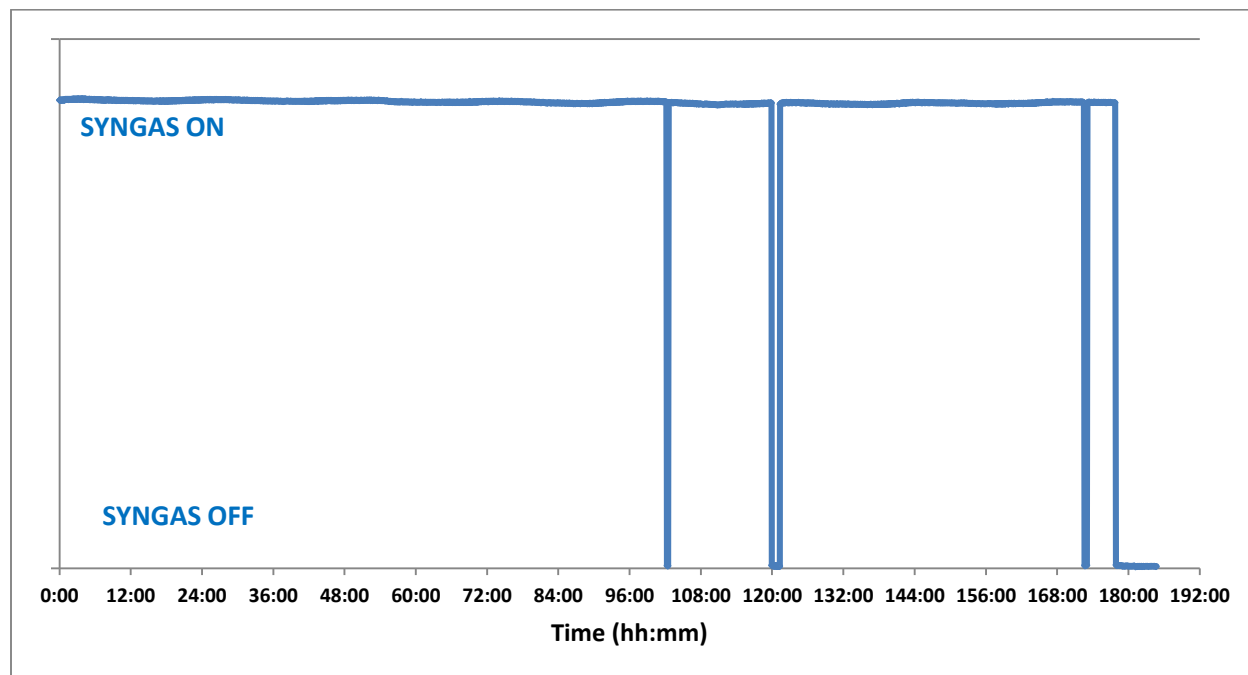


Figure 51. Syngas availability during Run #10.

During Run #10, raw syngas flow was maintained at 300 lb/hr with a back pressure regulated in the water-wash column at 350 psig. Near the very end of the run, the raw syngas flow rate was increased to 350 lb/hr to demonstrate high CO₂ loading. Figure 52 below shows mass flow rates of the three gas streams: raw syngas, clean syngas, and the regenerated gas stream. All gas flows were monitored using Coriolis flow meters.

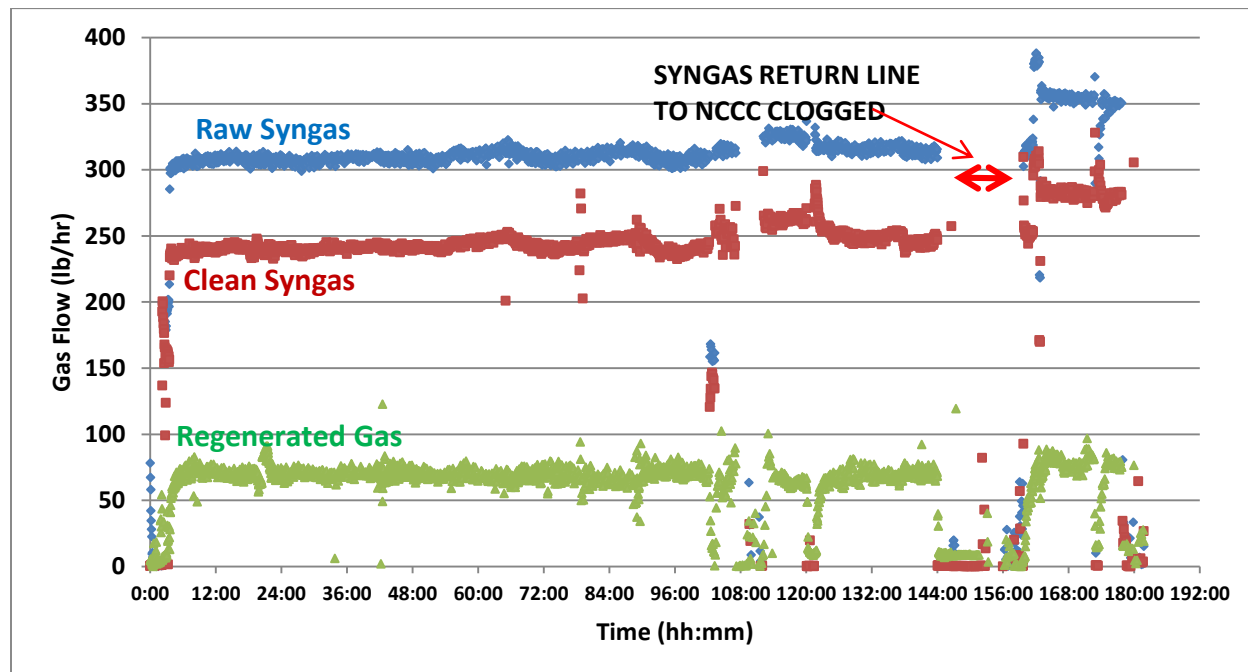


Figure 52. Raw syngas, clean syngas, and regenerated gas stream mass flow rate (Run #10).

Raw syngas contained 14 – 15 mol% CO₂ and ~ 2000 ppm H₂S. Figure 53 shows the concentration of CO₂ in raw and clean syngas, and Figure 54 shows H₂S concentration in raw and clean syngas.

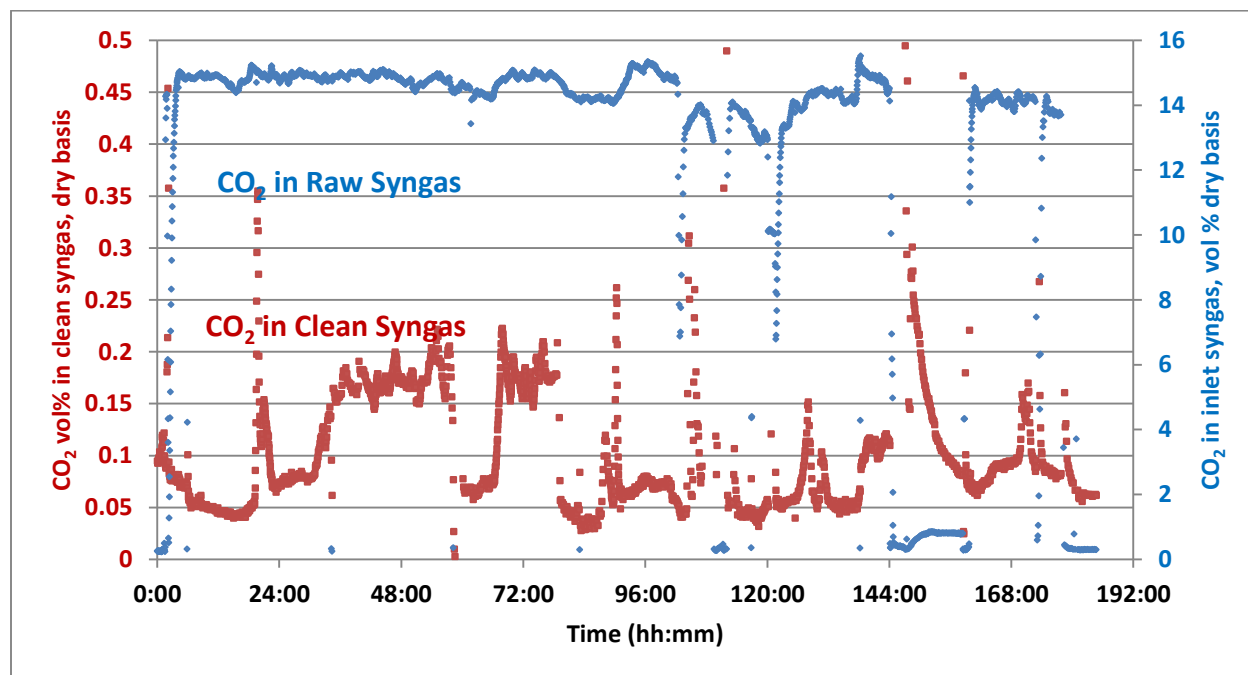


Figure 53. Concentration of CO₂ in raw and clean syngas (Run #10).

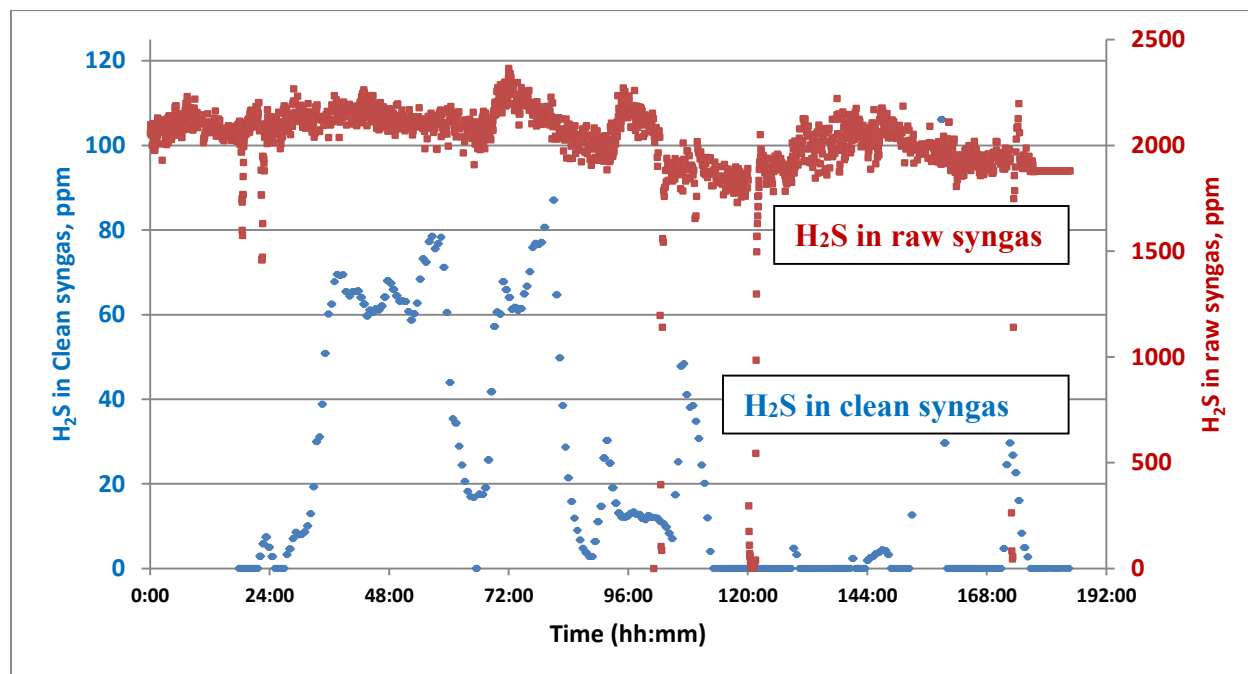


Figure 54. Concentration of H₂S in raw and clean syngas (Run #10).

Raw syngas was introduced in the absorber first stage. Semi-rich solvent was circulated at the bottom of the absorber with no external cooling. A PID controller and back-pressure regulating valve were used to maintain pressure in the absorber and water-wash column. After being scrubbed in the water-wash column, clean syngas was returned to the thermal oxidizer with a gas sampling line to a GC to monitor the gas composition. Solvent circulation was maintained using a level sensor in the absorber reservoir and a level control valve. Rich solution from the bottom of the absorber was sent to regenerator.

The regenerated gas stream was either returned to the thermal oxidizer or sent to the sulfur removal unit. Grab samples from the regenerated gas stream were tested by the NCCC to determine gas composition.

Bubble cap trays in the top stage of the absorber flooded during the first test campaign due to inadequate design. The trays were replaced by structural packing for the second test run. The packing did not perform well due to low liquid loads and was bypassed during the test runs. The absorber was operated with two stages and achieved > 99.5% CO₂ capture and > 99.5% H₂S capture in a single vessel as shown in Figure 55.

During a period from 30 to 84 hr, the capture efficiencies for both CO₂ and H₂S were marginally lower due to low ammonia concentration in the solvent. Fresh ammonia solution was added to the system resulting in high capture efficiency for both CO₂ and H₂S. Effective CO₂ loading was calculated based on the mass of CO₂ captured and the water content of the

circulating solution. The solvent circulation rate was varied to change the effective loading of CO₂ in solvent.

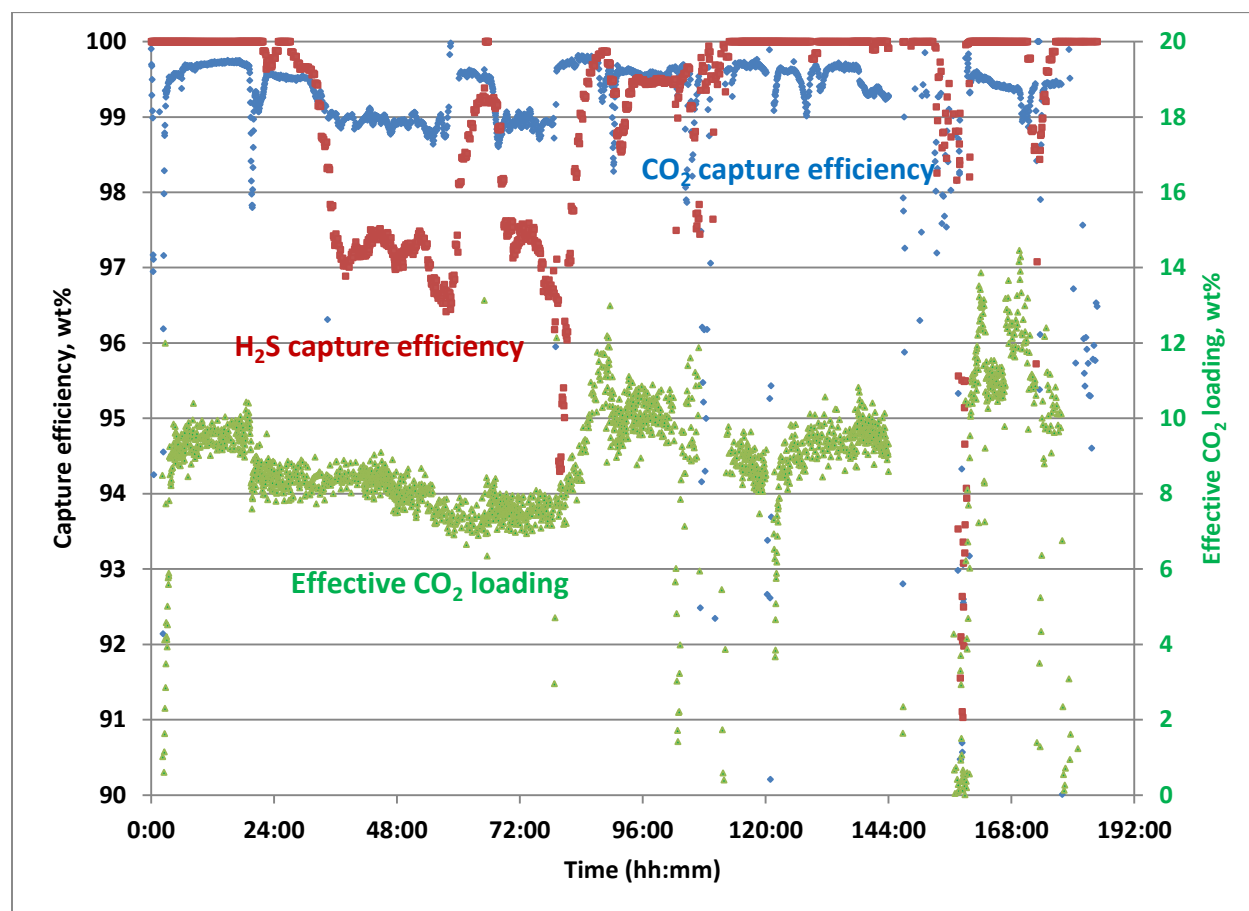


Figure 55. Capture efficiency and CO₂ loading in solvent (Run #10).

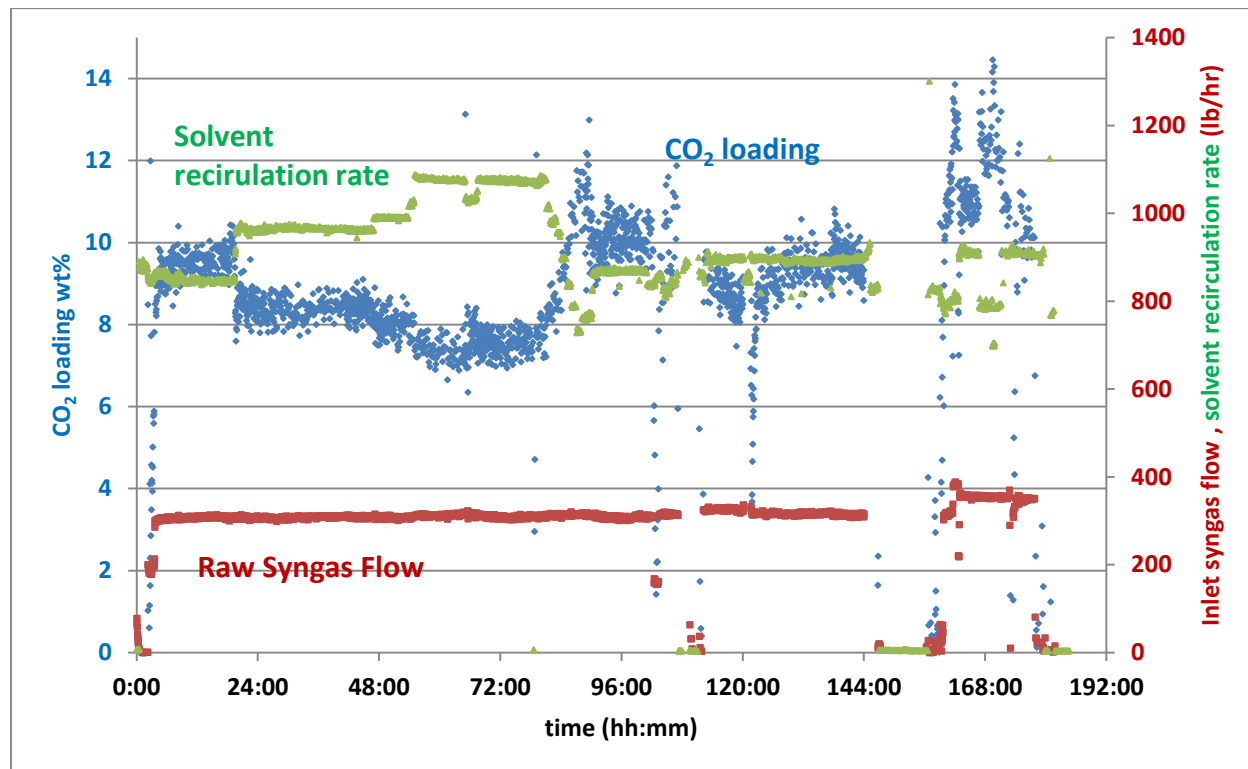


Figure 56. CO₂ loading varied by changing solvent recirculation rate (Run #10).

Ammonia concentration in the circulating solvent and CO₂ and sulfide loading were determined by wet analysis of liquid samples in the lab. Figure 57 shows ammonia concentration and sulfide concentration in lean solution, and Figure 58 shows the CO₂-to-ammonia concentration in lean solution. A titrator was used to determine ammonia and CO₂ loading in lean solution and the same was calculated for the rich solution. An ultraviolet visible (UV/Vis) spectrometer was used for sulfide concentration determination. Sulfides were stabilized in the liquid samples using a buffer, and color was developed using methylene blue. Sulfide was observed at a 665-nm wavelength.

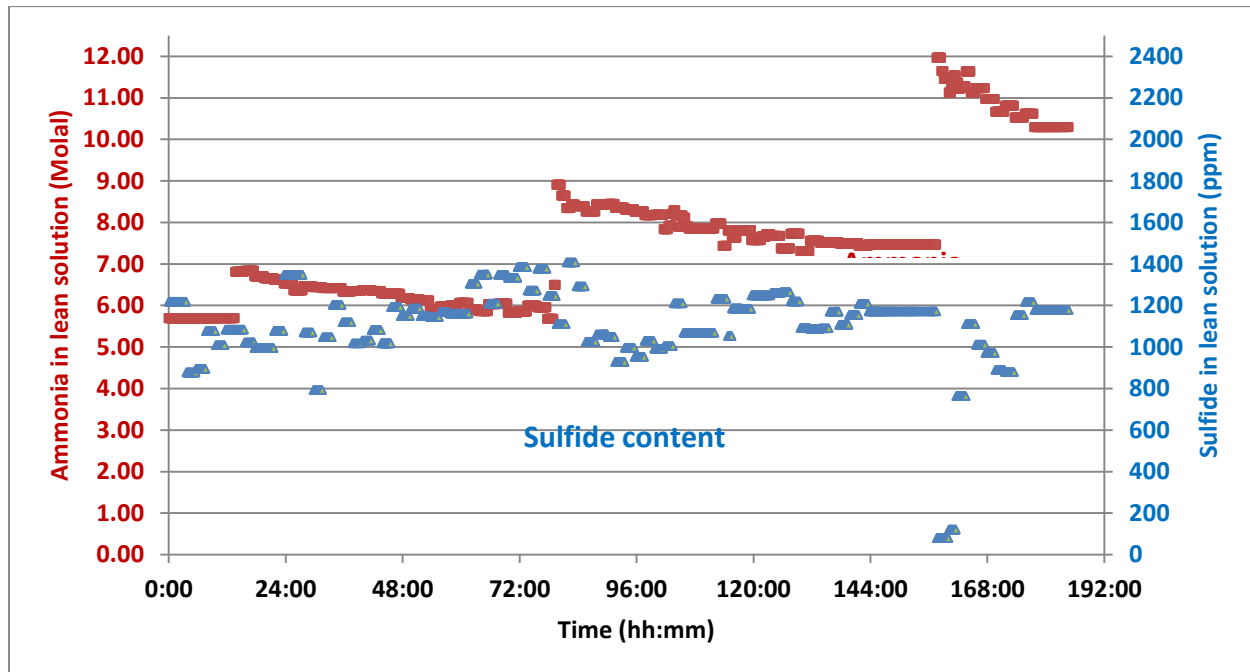


Figure 57. Ammonia and sulfide concentrations in lean solution (Run #10).

Relative CO₂ loading in the lean and rich solution determines the effectiveness of the CO₂ capture process. The titration method of liquid sampling to determine relative concentration can be replaced by an online concentration measurement system. Online measurement can guide the operation to improve effective CO₂ loading without precipitation and optimize steam use in the reboiler where CO₂ is regenerated.

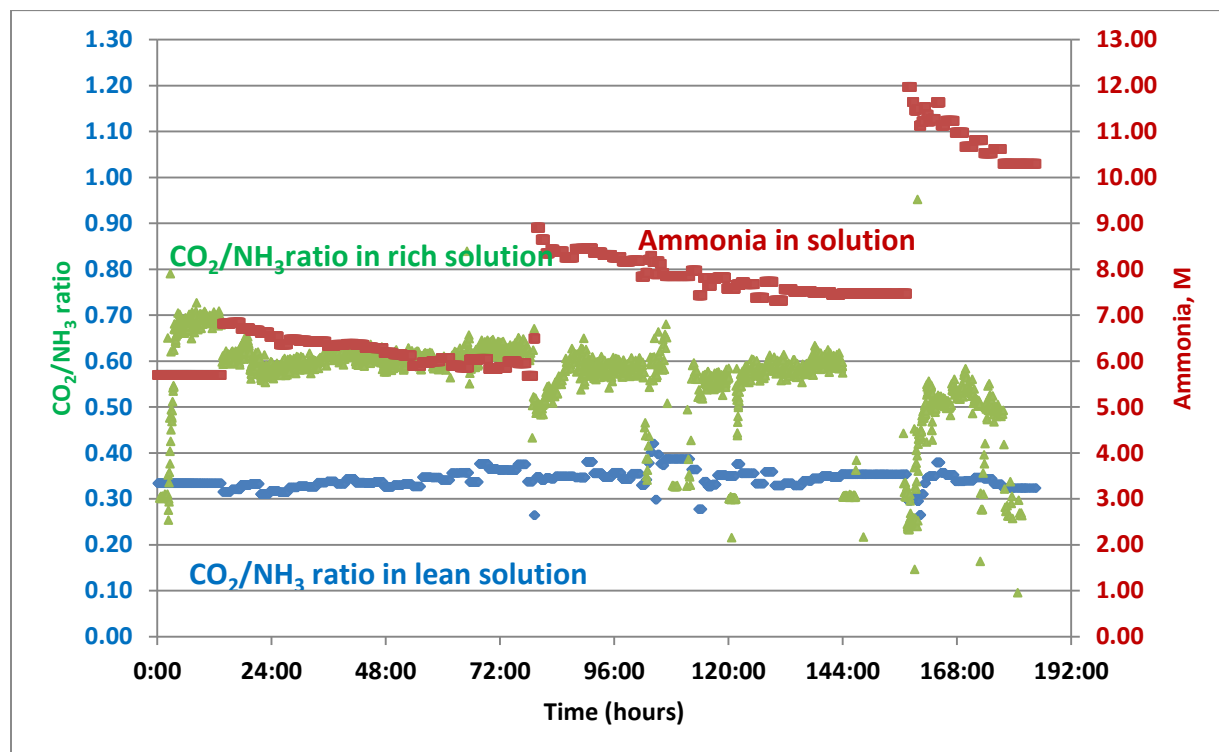


Figure 58. CO₂ loading in lean and rich solution (Run #10).

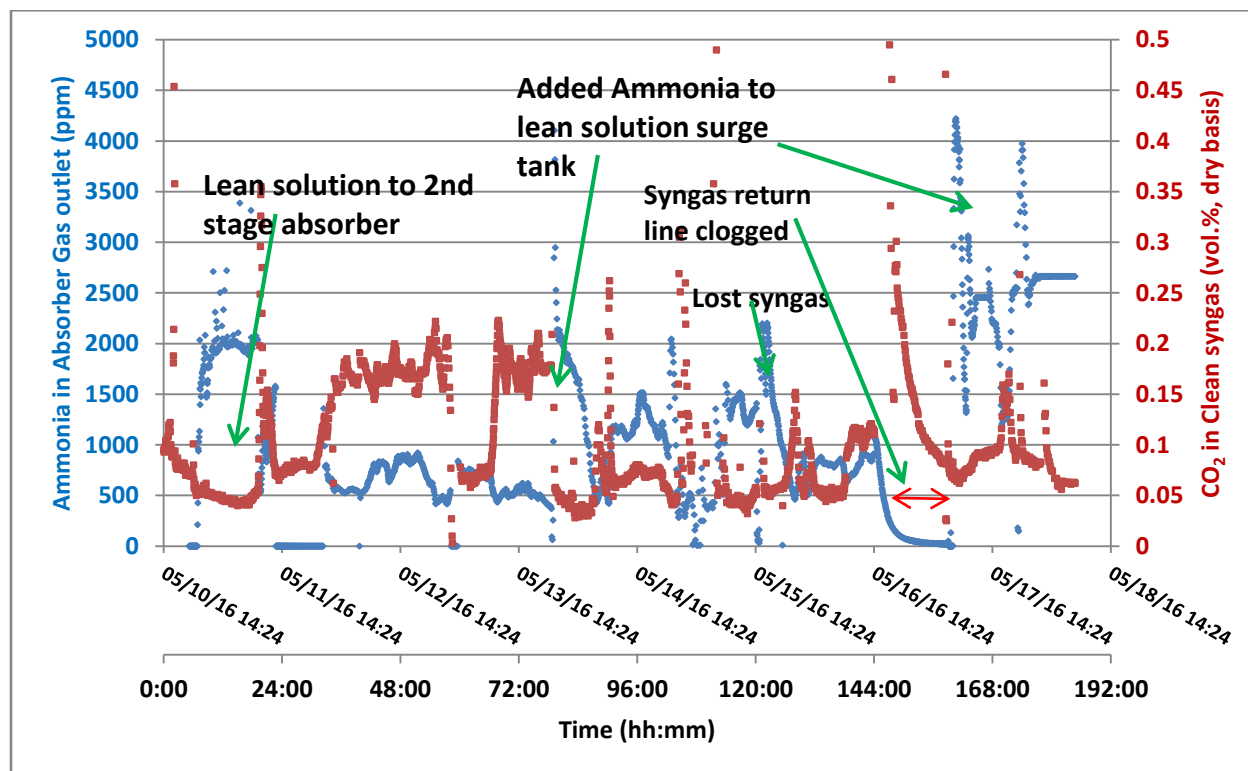


Figure 59. Ammonia in clean syngas from absorber (Run #10).

As explained earlier, bubble cap trays did not perform as designed. This resulted in operating the absorber with only two stages. Ammonia emissions from the absorber were recorded using an FTIR spectrometer. Figure 59 shows ammonia in the clean syngas stream from the absorber. This gas stream was subsequently passed through a water-wash column. Ammonia in the clean syngas from the water-wash column was monitored using Draeger tubes, and it was found to be present at 250 ppm or less.

Process modeling using ASPEN shows that it is possible to reduce ammonia emissions to < 50 ppm using a water wash with well-designed bubble cap trays. In a future test campaign, we expect to install commercially designed bubble cap trays and show efficacy of ammonia capture in the water-wash column. Ammonia from the water-wash waste stream will be recovered in a sour-water stripper in a commercial plant.

Electric heat tracing was used to maintain the 120°F temperature in the bottom of the absorber to prevent precipitation from the rich solution. All rich-solution transfer lines from the absorber to the regenerator were heat-traced. The second stage of the absorber had a recirculation loop to cool the semi-rich solution. Fresh lean solution was added to the second absorber stage to reduce ammonia emission.

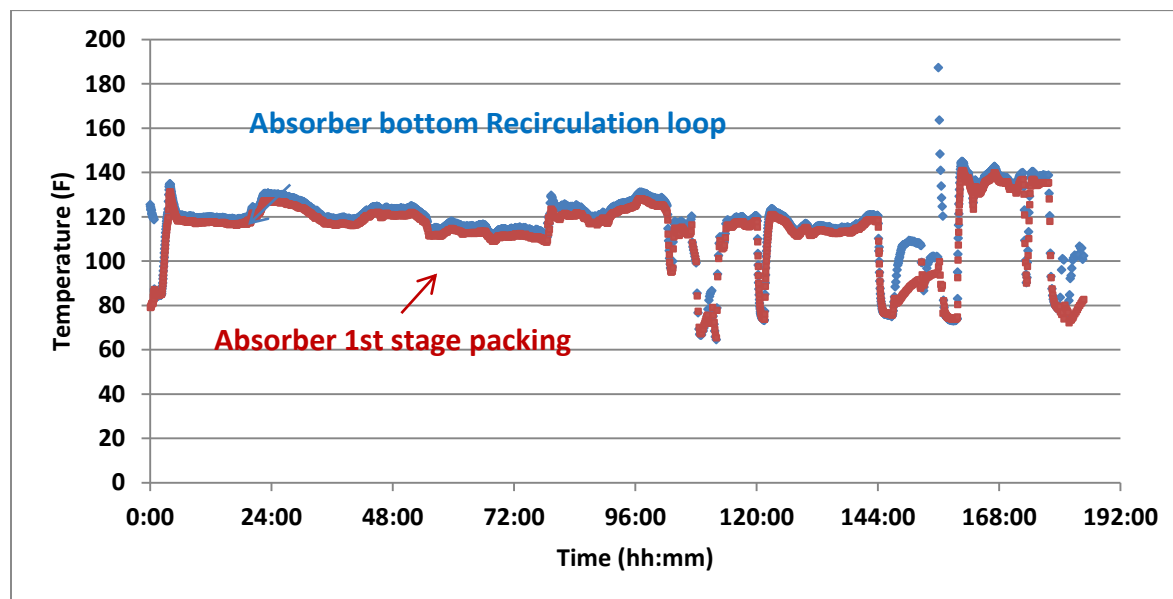


Figure 60. Absorber bottom-stage temperature profile (Run # 10).

Both the absorber and regenerator were operated at similar pressures (~ 350 psig) to reduce pumping needs across pressure boundaries. High-pressure absorption results in reduced ammonia emission and thus lowers the operating cost by minimizing solvent make-up costs.

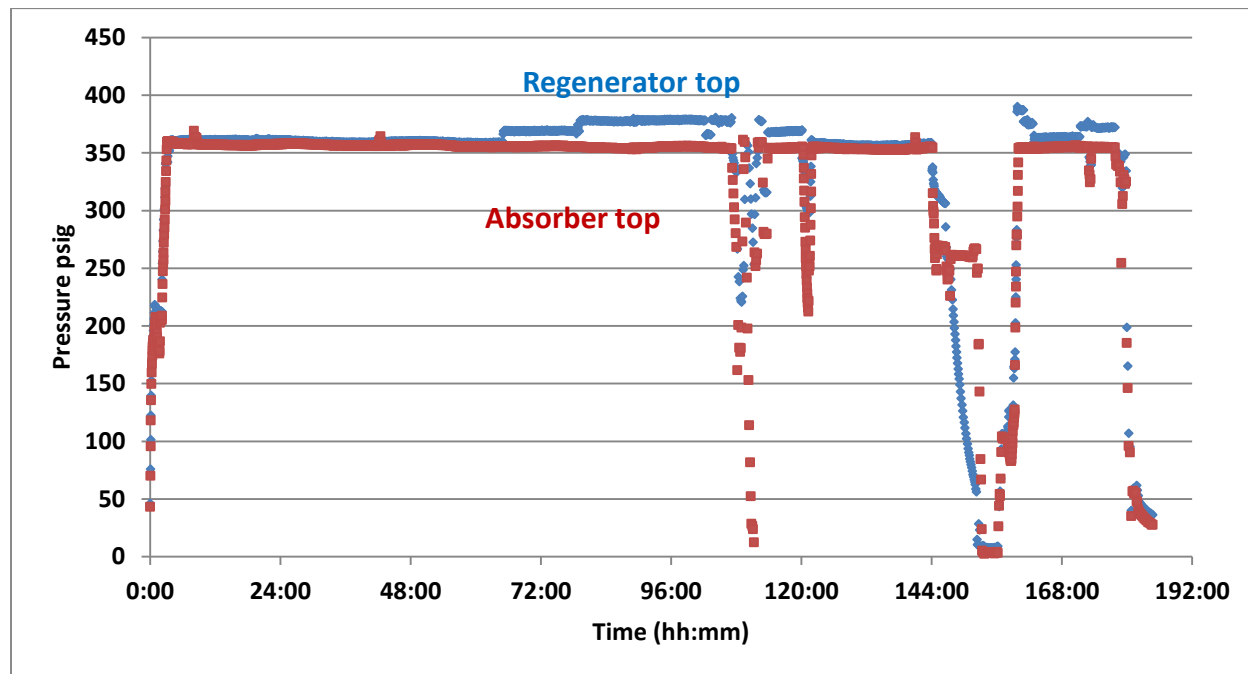


Figure 61. Absorber and regenerator pressure (Run #10).

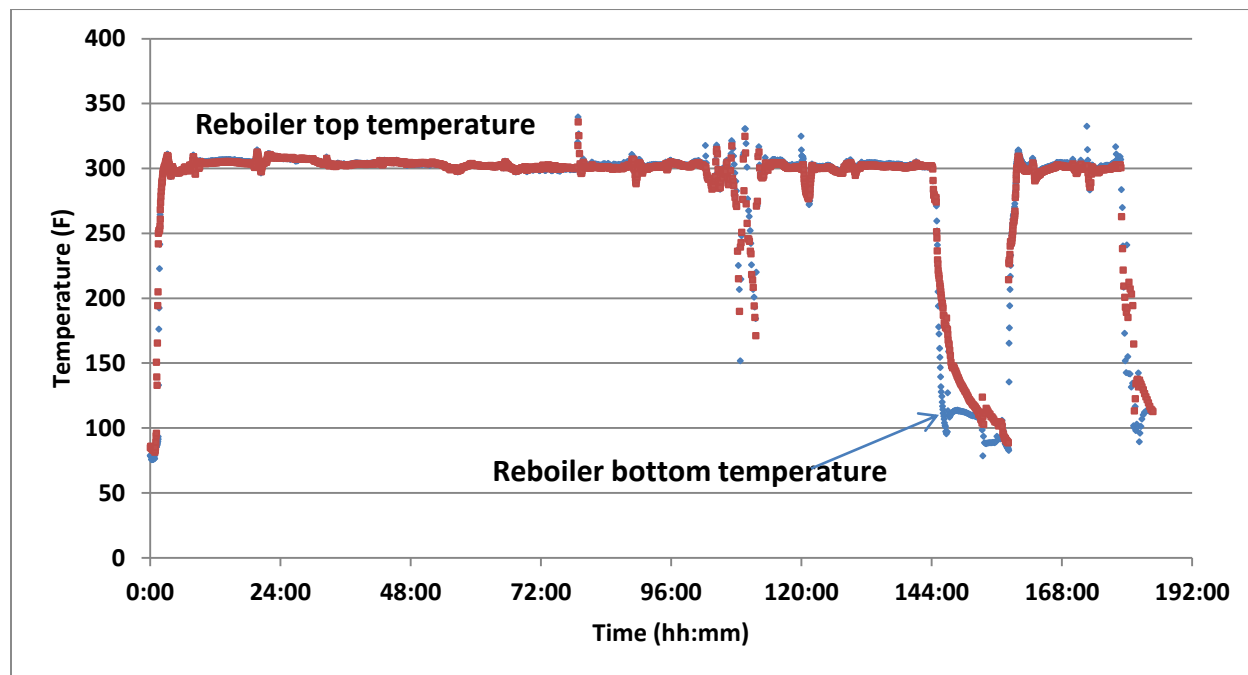


Figure 62. Reboiler temperature for thermal siphon (Run #10).

A vertical reboiler was used to regenerate rich solution using steam in a counter-current heat exchanger at moderate pressure. The temperature in the regenerator was maintained by controlling the steam flow in the reboiler. It was determined that both CO₂ and H₂S can be

regenerated in a single vessel, and lean solution is recirculated back to the absorber. In a commercial system, the heat source in the reboiler can be syngas and this can potentially result in significantly increased efficiency and reduced operating expenses. It may be noted that ammonia does not degrade at the operating temperature of reboiler. The higher the reboiler temperature, the higher the pressure of regenerated streams of CO_2 and H_2S —thereby reducing the compression needs of CO_2 stream after converting H_2S to elemental sulfur in the BPSC.

The regenerated stream was tested for composition. Grab samples from the regenerated gas stream were taken in a pressure vessel and analyzed with a GC. It is evident that the solubilities of fuel species like H_2 , CO , and CH_4 in solvent are very low; thus, there is minimal loss of fuel species.

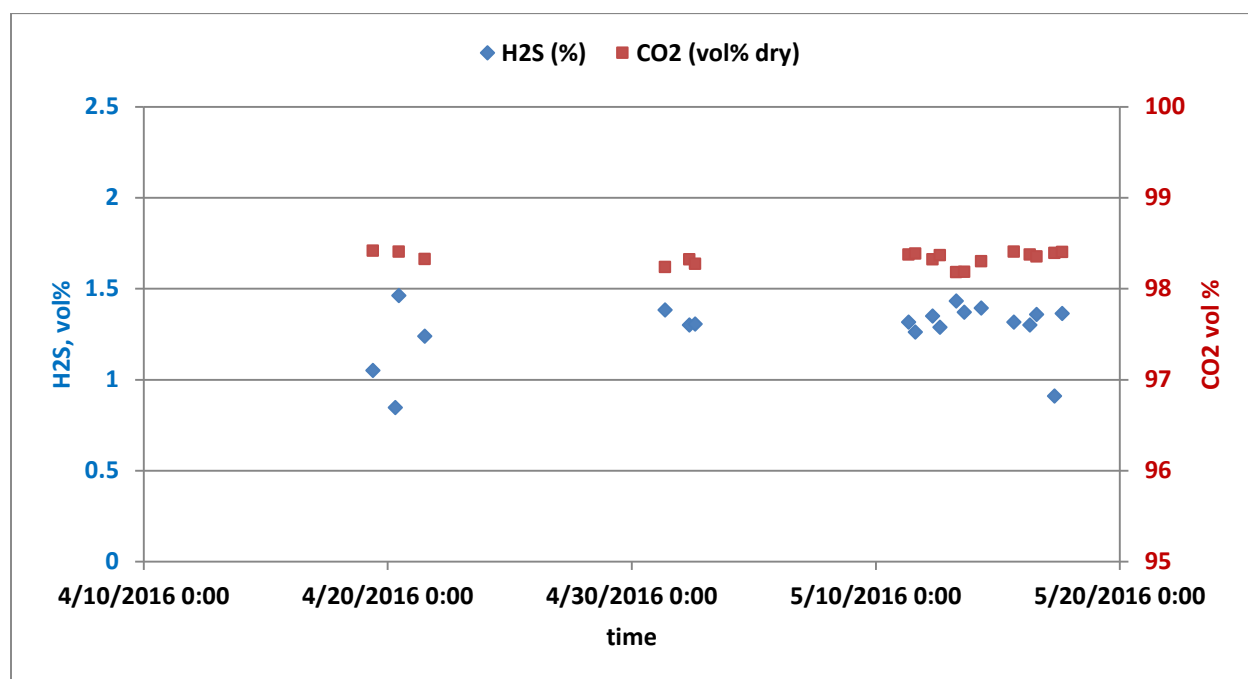


Figure 63. Regenerated gas stream main constituents.

Solubility of methane and carbon monoxide was below the detection limit of the GC. Figure 64 shows the GC measurement results for CH_4 and CO in the regenerated gas stream and Figure 65 shows the GC measurement results of hydrogen and argon in the regenerated gas stream.

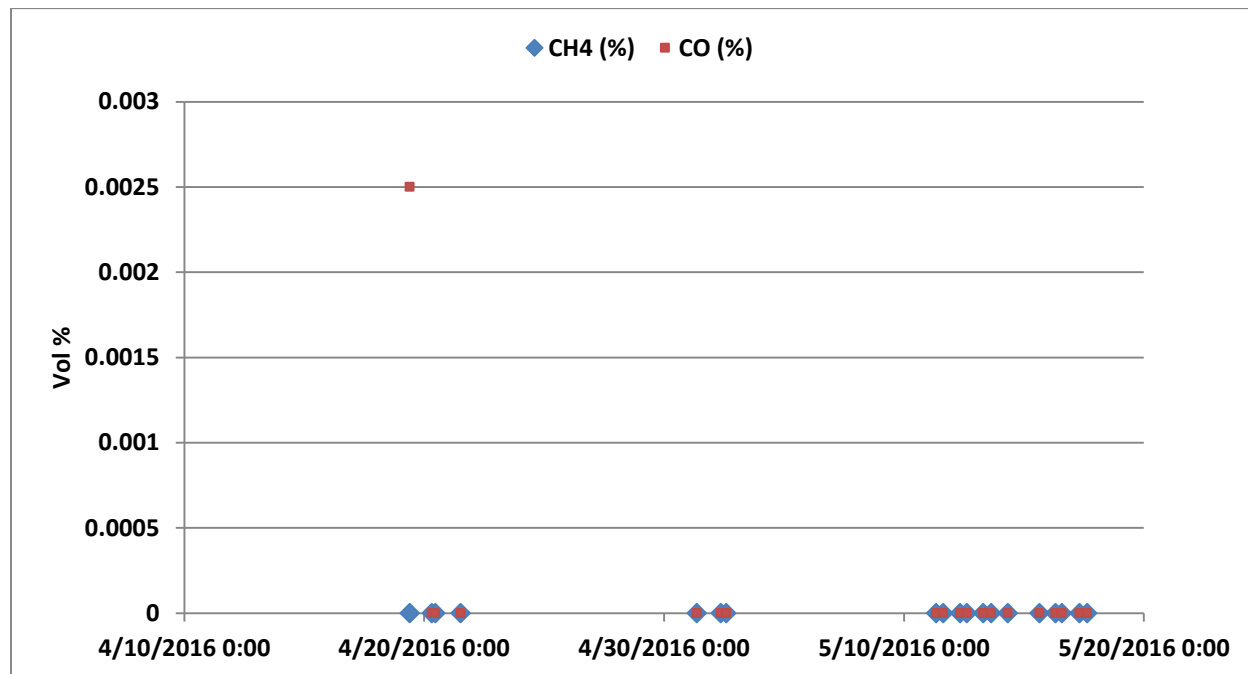


Figure 64. Methane and carbon monoxide in the regenerated stream.

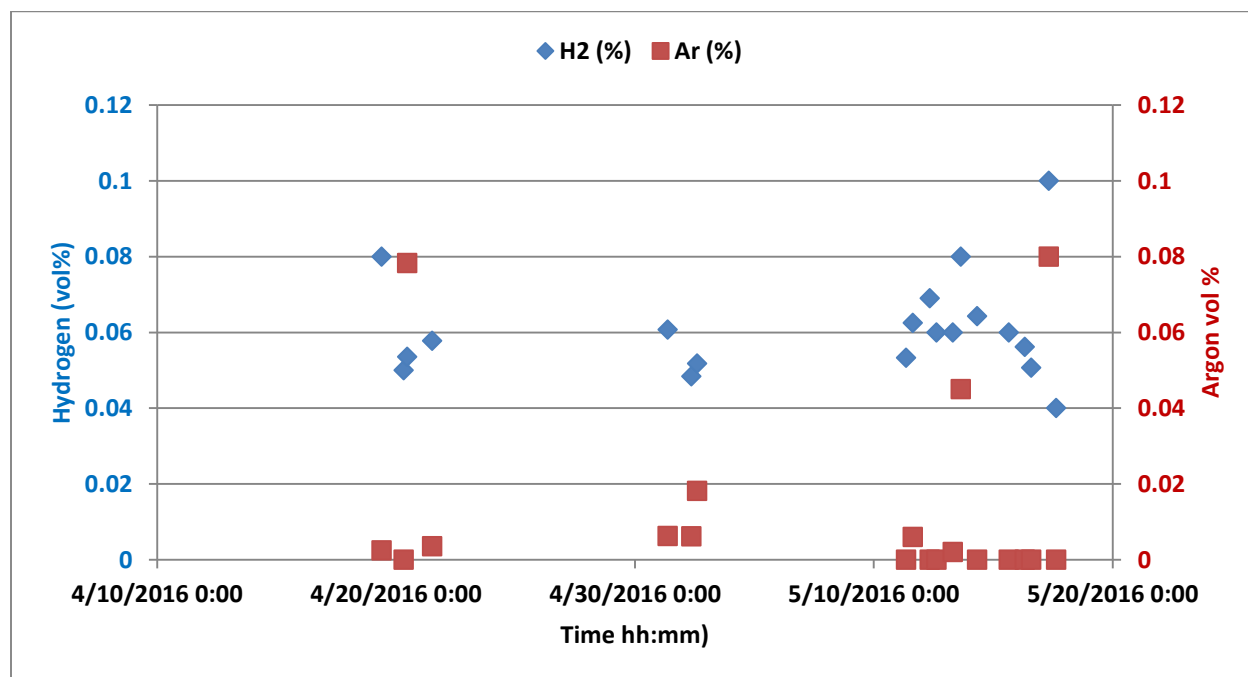


Figure 65. Hydrogen and argon in the regenerated gas stream.

Coriolis meters were used to measure various gas flows in the process system, including the inlet raw syngas flow, clean syngas return flow, and regenerated gas stream flow. Figure 66 shows a mass balance between product and inlet gas flow rates.

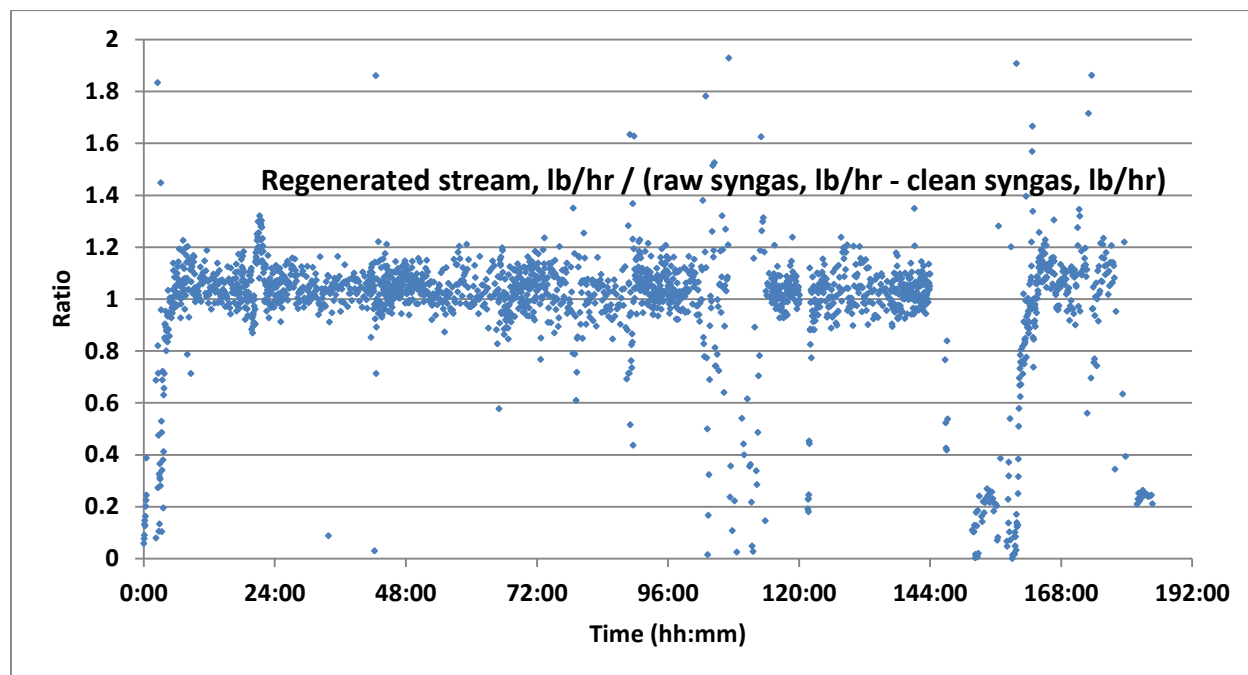


Figure 66. Gas mass balance (Run #10).

The AC-ABC / BPSC system setup at the NCCC is rated for ~ 150,000 scfd syngas flowrate. The absorber and regenerator columns are 8-in ID and 40-feet tall. This is a relatively small system to measure heat of reaction. ASPEN Plus was used to model the system and to calculate the heat of reaction. Based on the modelling results, the program predicted the heat of reaction for CO₂ and H₂S absorption and regeneration as ~ 690 BTU/l b or 1.45 GJ/ton of regenerated gas stream.

The measured heat input was higher than calculated due to heat losses in a small system. Figure 67 shows the heat of reaction based on steam input to the system during the 7-day steady-state run.

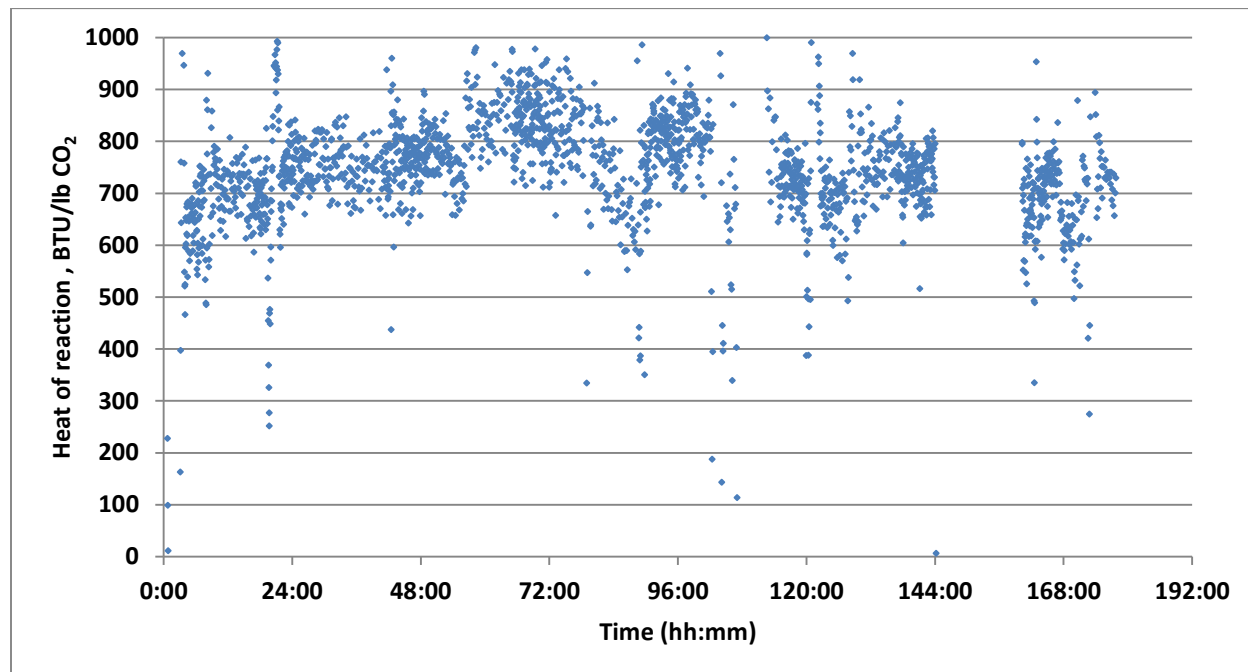


Figure 67. Energy input to reboiler (Run #10).

Corrosion

During the second test campaign, some dark solids were observed in the solvent. Four samples were collected and sent for analysis to an outside lab. X-ray diffraction (XRD) analysis showed iron and sulfides.

The waste collected during the test campaign included spent solvent, rinse water, and stream from two water-wash columns. As per the report provided by the NCCC, the spent solvent contained 28 mg/kg of chromium (the specification for disposal is 5), the rinse water had 3.6 mg/kg, and the waste water from water-wash columns contained 0.154 mg/kg.

The above tests indicate possible corrosion in the system; however, it is not yet clear where this corrosion may be happening. The regenerator and reboiler are the hottest parts of the system, but the solvent is lean in H₂S and CO₂ in these vessels and rich in ammonia. Another possibility is in the bottom of absorber, where rich solution is circulated at 120 - 140°F. Both the absorber and regenerator were constructed out of 316 steel. According to one study of sour-water strippers in refineries, SS316 is more prone to corrosion than carbon steel, especially in ammonia-rich environments due to ammonia-metal complex formation.

During the first test campaign in September/October 2015, water samples were collected at the beginning and end of each of five runs. Some chromium was reported in the water samples of the first two of the five test runs during the test campaign. Solids transported with syngas

during the first two test runs (as shown by the presence of calcium and magnesium) were assumed to be the sources of chromium during the first test campaign. There was no chromium recorded in test Runs #3, 4, and 5 of the first test campaign.

The location of corrosion is not determined.

H₂S to Sulfur

Bechtel holds U.S. Patent 7,374,742 for what is now known as the Bechtel Pressure Swing Claus (BPSC) technology. Proof of concept was achieved at the Idaho National Energy and Engineering Laboratory (INEEL), and the subsequent tests in pilot plants were conducted in 2015 and 2016 and are the subject of the text below. The purpose of the technology is to recover sulfur from a high-pressure gas (CO₂, syngas, or hydrocarbons) as liquid sulfur using SO₂ as an oxidant. Multiple sub-dew-point reactors are used in rotation (Lead/Lag/Regeneration) similar to a molecular sieve dehydration unit (Mole-Sieve), a pressure swing absorption unit (PSA), or a low pressure sub-dew-point Claus.

In this process, SO₂ is introduced to the acid gases (“feed gas”) and they are heated indirectly by steam in the “reactor feed heater”. Then the mixture is fed to the first or primary on-line reactor (“primary reactor”), where most of the H₂S, COS, and SO₂ are converted to sulfur and adsorbed on the catalyst. Based on the bench-scale testing, the primary reactor is expected to produce a sweet gas of about 100 ppmv total sulfur (including residual elemental sulfur vapor). The gas flows through a cooler (“reactor intercooler”), where it is cooled by generating steam. Provisions are made to accommodate any sulfur that may condense at this location. Any recovered sulfur drains to a sulfur pit, and the vapor goes to the next reactor (“secondary reactor/sulfur trap”), which acts as a sulfur trap/guard bed. Here, it is expected that residual sulfur vapor will be adsorbed and most of the remaining residual H₂S, COS, and SO₂ will be converted to sulfur and/or adsorbed. The second reactor is expected to reduce the sulfur in the product gas to less than 20 ppmv total sulfur. The product gas is returned to the facility for compression. After about 8-12 hours online, the primary reactor is rotated to regeneration, the secondary reactor moves up to the primary position, and the regenerated reactor is switched to the secondary reactor position. The “regen reactor” is shown in regeneration in Figure 78. The sulfur-loaded bed is partially regenerated by pressure let down. Flash gas passes through a sulfur condenser (“sulfur condenser”) and is recompressed (“regen recycle compressor and regen gas compressor”) prior to being mixed into the BPSC feed stream. There is a heating and cooling cycle (“regeneration heater and cooler”) using recycled sweep gas to complete the reactor

regeneration. High-pressure SO_2 is produced from some of the product sulfur by reacting it with oxygen from a proprietary reactor or a third-party vendor.

BPSC allows recovery of sulfur species as elemental sulfur while maintaining system pressure. Due to the higher pressures compared to traditional Claus units, equipment size is reduced.

Bechtel Pressure Swing Claus

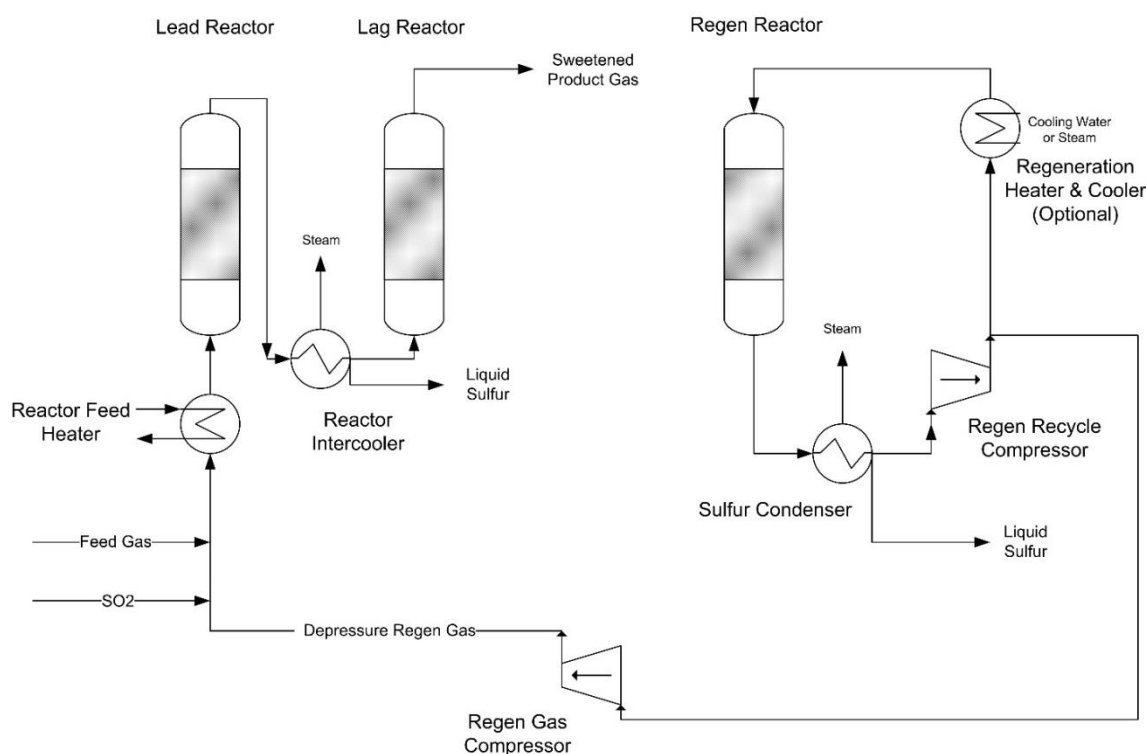


Figure 68. BPSC diagram.

The 2008 INEEL work, documented in report INEEL/EXT-05-02663 and sponsored by a Bechtel Technical Grant, showed proof-of-concept for high-pressure sub-dew-point operation of Claus catalyst using typical γ -activated alumina. At INEEL, the reaction between H_2S and SO_2 was accomplished at pressures between 220-420 psig and 270-600 F, with H_2S concentrations of 0.2-0.9 volume %. After sitting overnight at atmospheric pressure, the catalyst was found to be “regenerated”, meaning no sulfur was found on the catalyst, and it was reused. Both nitrogen and laboratory-synthesized syngas were used as the carrier gases. The initial “direct oxidation”

approach using O_2 failed due to side reactions with the syngas components ($CO + H_2$), but success was seen when SO_2 was used as an oxidant.

The objectives of the pilot plant efforts were to:

- A. Test overall recoveries of sulfur from the feed gas.
- B. Measure catalyst capacity for sulfur during high-pressure, sub-dew-point operation.
- C. Evaluate catalyst capacity as it ages during operation (absorption and regeneration cycles).
- D. Test different sulfur condenser design parameters.

These parameters are well known for sub-dewpoint Claus operations conducted at near atmospheric pressure but are not known when operating at elevated pressures.

Some of the initial objectives had to be sacrificed due to the size of the plant and the time available. Measurement of the effects of recycling the regeneration gas into the process feed is one example, as a recycle compressor was not commercially available in this size range. Similarly, supplementing the H_2S concentration available at the facility was ultimately not allowed due to concerns about potential H_2S releases.

The BPSC pilot plant was offered at a total flow rate of ~ 111 lb/hr, although only 60%-80% of that rate was typically received. Typical scale-up for pilot plant activities is a factor of no more than 100x the size of the pilot plant. Therefore, Bechtel was aware that additional work would be needed before making a commercial offering. However, a commercial demonstration unit would be within reach.

A total of eight regenerations were executed during the second campaign, with two showing “on-spec” sulfur recovery when the reactor was returned to service. The regeneration efficiency appears to be a function of the pressure used, catalyst temperature, the composition of the regeneration gas, the flow rate of the regeneration gas, and duration of the regeneration step. The other six regenerations had difficulties, which are understood and can be corrected. Such difficulties ranged from inconsistently maintained catalyst temperatures, test interruptions due to problems with the host facility, test interruptions due to problems with the upstream AC-ABC units, and valves/piping plugged with elemental sulfur.

Table 11. Regenerations #1-#4.

Reactor	1	1	2	3
Date	5/1/2016	5/3/2016	5/11/2016	5/12/2016
Start Time	10:22	10:36	14:18	17:55
Prev Run, hr	15.6	21.8	15.0	19.8-21.5
Final H ₂ S (Lead)		800-1500	400-750	1000
Final SO ₂ (Lead)		300	1200	400
Final H ₂ S (Lag)	>900	1-3	BDL	2
Final SO ₂ (Lag)	unclear (0?)	0	150	15
REGENERATION				
Pressure	12-33	9-50	11-13	15
Notes:	FIRST LEAD RUN		FIRST LEAD RUN	FIRST LEAD RUN
	later, RX-2 = 140 H ₂ S			

Table 12. Regenerations #5-#8.

Reactor	2	3	2	1
Date	5/13/2016	5/13-5/15	5/15-5/16	5/15/2016
Start Time	1:00	5/13/2016 0:00	18:22	23:53
Prev Run, hr	7.7	45 (<16.5)	12.2	
Final H ₂ S (Lead)	900	600 (200)	2000+	RX-1&3 solo
Final SO ₂ (Lead)	10	600 (1500)	300	RX-1&3 solo
Final H ₂ S (Lag)	200	600	1900	RX-1&3 = 1000+
Final SO ₂ (Lag)	10	500	300	RX-1&3 = 1000+
REGENERATION				
Pressure	5-10	5-8	7-25	6-8
Notes:				

As can be seen in Table 11's first data column, Reactor #1 saturated after 15.6 hours using virgin catalyst. Although the reactor outlet concentrations of H₂S and SO₂ were not directly measured, the outlet of the lag reactor was over 900 ppmv H₂S, with an unclear amount of SO₂. Immediately after, the subsequent measurements of Reactor 2 when put into the lead position showed a decreasing H₂S concentration from several hundred to 140 ppmv H₂S, thus showing the need for a regeneration of the lead bed – in this case, Reactor #1.

As can be seen in Table 11's second data column, subsequent operation of Reactor #1 in the lead position was successful. Because this was early in our data collection, the focus was on the outlet of the lag reactor and sufficient inter-reactor data was not taken to prove how efficient the regeneration was for the lead reactor. The second run through Reactor #1 saturated with sulfur after 21.8 hours of operation. The increase in run time (vs. 15.6 hours in the virgin run) is attributed to fluctuations in flow and H₂S concentration in the feed gas, as well as imperfect process control of SO₂. As the overall quality of process control during that period of operation actually decreased, one would expect net sulfur recovery to decrease as well, which is reflected in an artificially extended run time. Ideally, we would have taken additional readings between the reactors, as was done for data regarding Reactors #2 and #3. However, we were able to measure Reactor #1 outlet concentrations while in the lag position (after a subsequent regeneration), and they were below detectable limits (BDL) for H₂S and 65 ppmv SO₂. A catalyst bed that was still saturated with sulfur would not be able to produce these levels of sulfur species. That is, H₂S and SO₂ would have desorbed in much higher concentrations (several hundred) based on subsequent observations during the pilot.

Reactor #1 was not reused in the lead position due to concerns about sulfation of the catalyst from off-spec pilot operation. The other two reactors were not in the lead position of service during this off-spec operation; thus, there was no concern about sulfation of those reactors.

As can be seen in Table 11's third data column, Reactor #2 saturated after 15.0 hours using virgin catalyst. The outlet of Reactor #2 was 400-750 ppmv H₂S and 1200 ppmv SO₂ before saturation was declared. After regeneration at the conditions shown, Reactor #2 was placed into the lead position and provided 20 ppmv H₂S and 20 ppmv SO₂ product, reflecting a successful regeneration. That run lasted 7.7 hours. The decrease in performance is closer to meeting our expectations compared to that of Reactor #1. The decrease in operating time before saturation is believed to better reflect on-spec operation realized by improved process control in both the BPSC unit (SO₂ delivery) as well as upstream units (H₂S fed to the BPSC unit).

Figure 69 shows Reactor #2 temperature profile during regeneration. The reactor flow was top to bottom, which is reflected in the temperatures shown, with hotter temperatures at the top of the beds at steady state.

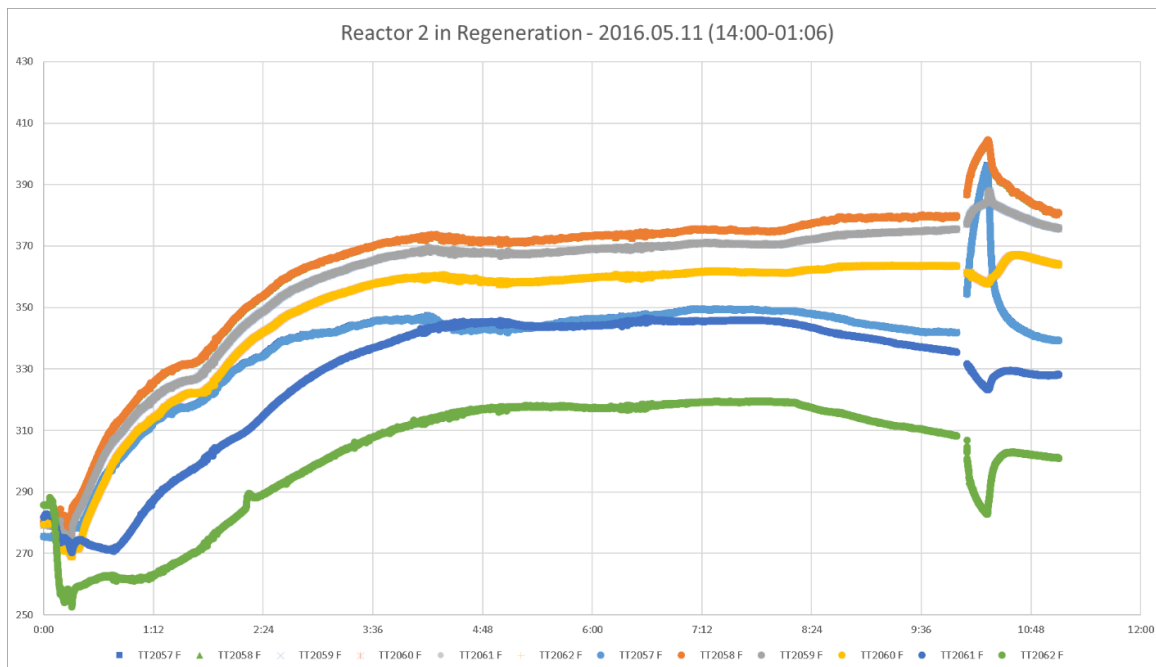


Figure 69. The graph shows good regeneration and different temperatures at various catalytic reactor locations. Multiple temperature levels (once stabilized) show significant heat loss from the reactor vessel.

The last data column of Table 11 and several of those in Table 12 show “suspect data” followed by a number. Because of the questionable nature of the data, it cannot be taken too seriously. The Draeger apparatus in question had two needle valves in series fed to a gas-filled glass bottle. The gas sample then flowed out of that glass bottle, past a check valve, and to a twin glass bottle filled half-way with 10 wt% caustic. After bubbling through caustic, the gas sample was passed through a color changing adsorbent (based on H_2S and CO_2 adsorbed) and then discharged to the local atmosphere. Because the process gas was primarily CO_2 , sodium carbonate was generated in the caustic bottle in sufficient quantities to plug the vapor path through the liquid. Back pressure was generated sufficiently to cause wildly inaccurate measurements as taken by the operator. After discovery, a subsequent measurement of H_2S was reduced from 6,000 ppmv to 200 ppmv. Thus, false readings for H_2S were recorded; they were too high by several fold.

A simultaneous error during the second test campaign resulted in SO_2 readings being low compared to the actual value. The samples from the middle reactor had significant quantities of water, as the water had not yet been removed by the process. As the sample was cooled (so as not to melt the plastic tubing associated with the Draeger apparatus), the water also condensed and was eventually collected in the first glass bottle. In retrospect, nearly all of the SO_2 was condensed in this stream, causing an erroneously low measurement in the gas phase. After

discovery (at the same time as the carbonate salts were discovered), the reading went from 30 ppmv SO₂ to 1500 ppmv.

At that time, we were aware of a potential sulfating problem on the remaining beds of catalyst. However, as mechanical difficulties began to resurface, we were unable to observe or test the effects on proper regeneration before the conclusion of the second test campaign.

Looking at overall sulfur removal, the data in Table 13 were collected using Draeger tubes from the second of two reactors operating in series. The dividing line represents a change in the lead reactor and lag reactor.

Table 13. Near complete removal of sulfur in BPSC.

Date	Time	Feed Rx	Feed H ₂ S mole %	Prod H ₂ S mole %	Prod SO ₂ mole %	Notes
2-May	2300	1	1.1	0.0040	0.0010	
3-May	100	1	1.2	0.0020	0.0030	
	300	1	1.3	0.0005	0.0050	
	500	1	1.0	0.0005	0.0110	Process upset seen in H ₂ S inlet.
	806	1	0.65	0.0002	0.0000	
10-May	2300	2	1.3	0.0020	0.0060	
11-May	1200	2	1.6	BDL	0.0150	H ₂ S below detectable limits.
	1500	3	0.9	BDL	0.0060	H ₂ S below detectable limits.
	1700	3	1.3	0.0010	0.0040	
	1900	3	1.3	0.0002	0.0010	
	2100	3	1.2	0.0002	0.0015	
	2300	3	1.4	0.0001	0.0010	
12-May	300	3	0.5	0.0001	0.0015	
	500	3	1.5	0.0002	0.0020	
	700	3	1.5	0.0001	0.0025	
12-May	1800	2	1.3	0.0050	0.0005	Reactor 2 on second use.
	1900	2	1.1	0.0006	0.0010	
	2100	2	1.2	0.0005	0.0010	
	2300	2	1.2	0.0200	0.0010	Breakthrough in the bed or bad data (unclear).

As can be seen from the data, each reactor set was able to achieve the stated DOE target of 0.01 volume % (100 ppmv) H₂S and was frequently much lower than that—sometimes below the detectable limit (BDL) of 1 ppmv H₂S.

Regarding the objectives of the BPSC skid:

- A. **Test overall recoveries of sulfur from the feed gas:** This objective was met. On multiple occasions, residual H₂S levels (after passing through two catalytic reactor beds in series) were below detectable limits (< 0.5 ppmv H₂S) as measured by Draeger tubes. Typical guarantee levels are expected to be between 4-100 ppmv for two reactors in series.
- B. **Measure catalyst capacity for sulfur during high-pressure, sub-dewpoint operation:** This objective was partially met. Fresh catalyst capacity was measured at 15-22 hours of operation before break-through at the given volumes. Multiple regenerations on the same catalyst were difficult to obtain due to various mechanical problems within the unit and within upstream units. Naturally, increased catalyst volumes would result in longer periods before break-through. The measured saturation points were significantly longer than expected and may have allowed for decreasing the required reactor volume, which reduces capex. Increased catalyst volumes would result in longer periods before saturation of the bed.
- C. **Evaluate catalyst capacity as it ages during operation (absorption and regeneration cycles):** This objective was only partially met. Again, multiple regenerations on the same catalyst were difficult to obtain due to various mechanical problems within the unit and within upstream units. However, each of two reactor beds was regenerated with subsequent operation meeting specifications for several hours. This needs to be studied further in the next stage of development.
- D. **Test different sulfur condenser design parameters:** This objective was partially met. Because of the various problems encountered, sulfur condenser design parameters were not optimized. The data collected indicates that the values used in the pilot plant sulfur condenser design are sufficient to move forward to the next phase, where they can be optimized further.

Process Modelling

Description of the Selexol Process: A schematic of the Selexol process for CO₂ and H₂S capture from syngas is shown in Figure 70. The system treats cooled syngas from a GE gasifier after the sour shift so that the main species in the gas are CO₂ and H₂, and the minor species are CO, CH₄, H₂S, Ar, N₂, and H₂O. Due to the relatively low efficiency of CO₂ capture and the need to achieve 90% carbon capture, the system requires a deep shift reaction to reduce the CO concentration to below 1%. To achieve the low CO concentration, a large amount of high-

pressure steam is injected upstream of the shift system and a few stages of shift reactors with inter-cooling are required.

The syngas pressure entering the acid gas removal (AGR) is at about 750 psi and is treated in a H₂S absorber and then in a CO₂ absorber. The H₂S absorber captures a lot more CO₂ than H₂S. To improve the H₂S/CO₂ ratio of the solution and to make the stripped gas suitable for Claus plant feed, the solution from the H₂S absorber is first heated to an intermediate temperature and sent to the H₂S enrichment tower, where CO₂ is stripped from the solution by clean and treated syngas. After enrichment, the solution is sent to an H₂S/CO₂ stripper, and the H₂S-rich stream from the stripper is sent to the Claus plant. The Claus plant in the current system is an oxygen-blown plant; the tail gas is compressed and sent to the Selexol absorber.

The CO₂ is regenerated by a pressure swing in which the solution is flashed in a series of steps to atmospheric pressure. The pressurized Selexol solution from the absorber is first flashed from 770 psi to about 250-300 psi to strip and recover H₂, CO, and CH₄, which dissolve into the solution in the absorber. The stripped gas from the first flash chamber contains 70-90% CO₂, and it is recompressed in compressor C1 and sent back to the process. The main stripping of the CO₂ is accomplished in few flashing steps including (optionally) a below-atmospheric-pressure stripping step to reduce the CO₂ content of the solution and increase its net CO₂ loading. The CO₂ gas from the flashing chambers is compressed to 2,200 psig for sequestration or for enhanced oil recovery. The high compression ratio of the CO₂ requires 5-6 compression stages with inter-cooling.

The power required for the compressor when treating 1,000,000 lb/CO₂ (compressor stages C4-C7 in Figure 70 is estimated at 30-40 MWe, depending on the average pressure of the stripped CO₂). The power required to pump about 50,000 gpm Selexol solution (based on absorbing the 1,000,000 lb/hr CO₂ at net load of 40 g/L using pump P1 from atmospheric pressure to 800 psi) is about 20 MWe. The pumps P2-P4 and the compressors C1-C3 add significant power consumption to the process. In addition, chilling of the solution to 41°F is required for removing H₂S and CO₂ to low concentration levels, and this requires additional power consumption.

The H₂S stripping is performed at low pressure and high temperature. Typically, 150 psig steam is used for the stripping; heat consumption per lb of H₂S is high due to the low concentration of H₂S in the feed solution to the stripper and the need to generate H₂S-free solution in order to achieve low H₂S emissions in the syngas. Recent data obtained from an operating Selexol plant show that the actual heat consumption of the H₂S stripper is 8,500 btu/lb of H₂S stripped.

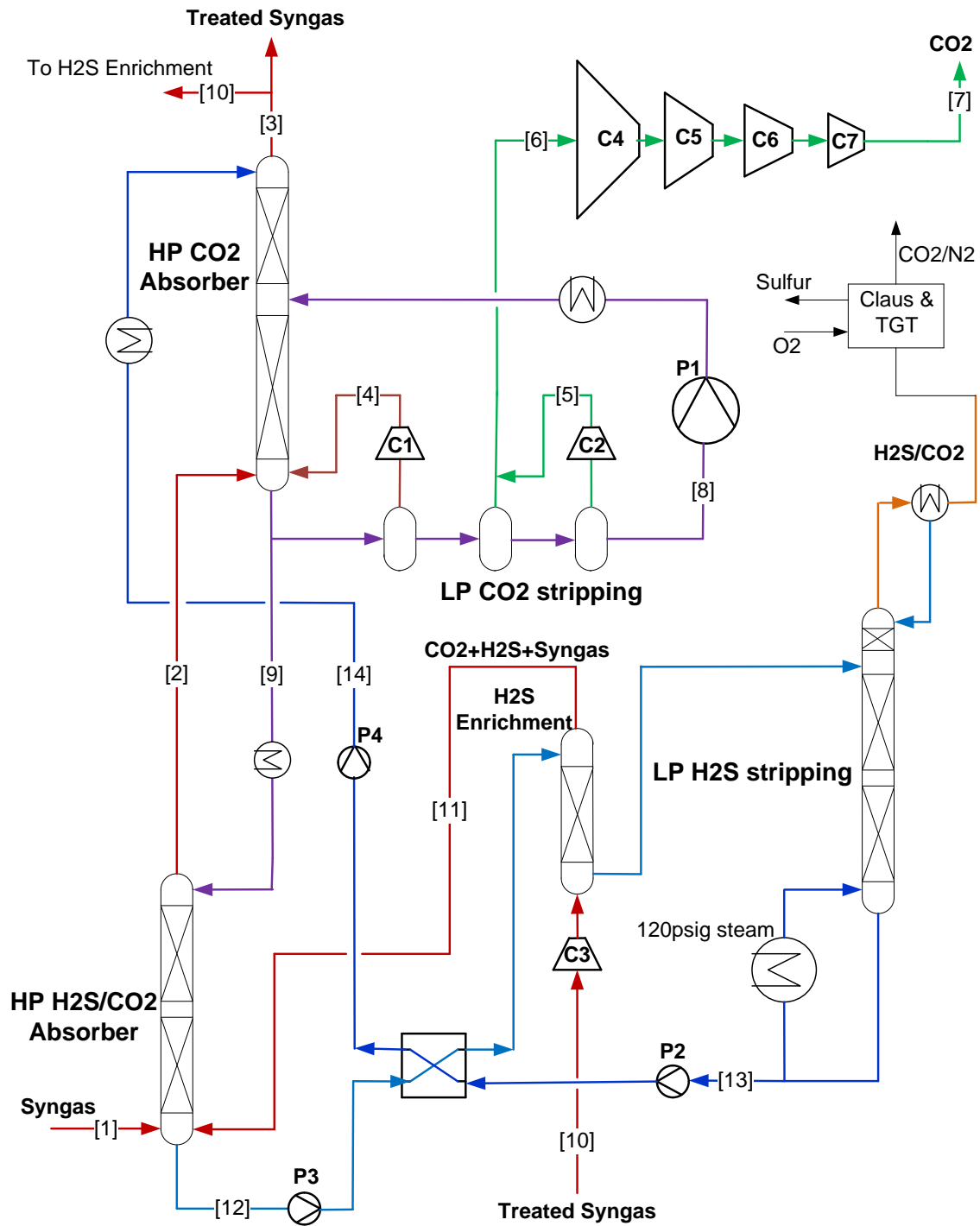


Figure 70. Schematic of the Selexol process for 90% CO₂ capture and sequestration at 2,200 psi; H₂S outlet is 10 ppm.

Description of the AC-ABC Process. A schematic of the AC-ABC process for CO₂ and H₂S capture from syngas is shown in Figure 71. The system treats cooled syngas from a GE gasifier after the sour shift and cooling. The system is designed for > 99% CO₂ capture and complete H₂S capture. Since practically all the CO₂ is captured in the absorber and 90% capture of carbon is required, the residual carbon (< 10%) can be in the form of CO in the clean syngas. This translates to about 4% CO in the raw syngas (dry basis) from the water-gas shift reactor. As a result, only a moderate shift is required, and significantly less steam is injected into the syngas compared to the Selexol case. After the shift, the main species in the gas are CO₂, CO, and H₂, and the minor species are CH₄, H₂S, Ar, N₂, and H₂O. The gas pressure is about 750 psi, and it is sent to the AGR for CO₂ and H₂S capture. The simultaneous capture of CO₂ and H₂S dramatically simplifies the process and significantly reduces its capital cost.

The absorber is a multistage vessel in which CO₂ and H₂S are captured by using a high-concentration aqueous ammoniated solution. The top stage of the absorber is a polishing step in which residual CO₂, H₂S, and ammonia vapor are captured in water and in the weak ammoniated solution from the sour water stripper.

The CO₂ and H₂S are regenerated at elevated temperature and pressure; the CO₂-rich solution is first heated in a regenerative heat exchanger in a counter current flow with the CO₂-lean solution and is then sent to the stripper. A polishing stage at the top of the regenerator using water from the sour water stripper for the gas wash ensures that the CO₂/H₂S gas stream is practically ammonia free.

The heat source in the CO₂/H₂S stripper can be steam. Alternatively, the heat source can be hot syngas, which can be used directly in the reboiler since the ammoniated solution does not decompose at high temperature. In the reboiler, the syngas is cooled and a fraction of its water condensed while boiling the CO₂ and H₂S from the rich solution. Significant energy efficiency and capital cost advantages can be achieved by using hot syngas as the source of heat in the process compared to using hot syngas to generate steam in a boiler and heat the reboiler. For the purpose of this study, intermediate pressure (IP) steam was used to regenerate the rich solution.

The higher the reboiler temperature, the higher the regenerator pressure, the resultant CO₂ pressure, and the lean solution pressure can be. Higher CO₂ pressure results in a much lower CO₂ compressor power, and higher lean solution pressure results in lower pumping power for pumping the lean solution to the absorber.

The CO₂/H₂S gas from the stripper is sent to a BPSC system. The BPSC is a low-cost and simple process for in-situ reduction of H₂S to elemental sulfur at high gas pressure. Oxygen is used to convert sulfur to SO₂ and then, through the classical Claus reaction, to convert the H₂S to

sulfur. The clean CO₂ gas stream from the BPSC is compressed from 300 to 750 psi to 2,200 psig for sequestration or for enhanced oil recovery. The compression of the CO₂ requires 1-2 compression stages with inter-cooling.

The power required for the compressor when treating 1,000,000 lb/CO₂, (compressor stages C1-C2 in Figure 14) is estimated at 15-20 MWe for CO₂ stripped at 300-750 psi. The power required to pump ~ 17,000 gpm lean solution (based on absorbing the 1,000,000 lb/hr CO₂ at net load of 120 g/lit) using pump P1 from 300-750 psi to 800 psi is in the range of 2-4 MWe. There is no need for refrigeration, since there is efficient removal of H₂S and CO₂ such that low concentrations of these gases are achieved at ambient temperature conditions.

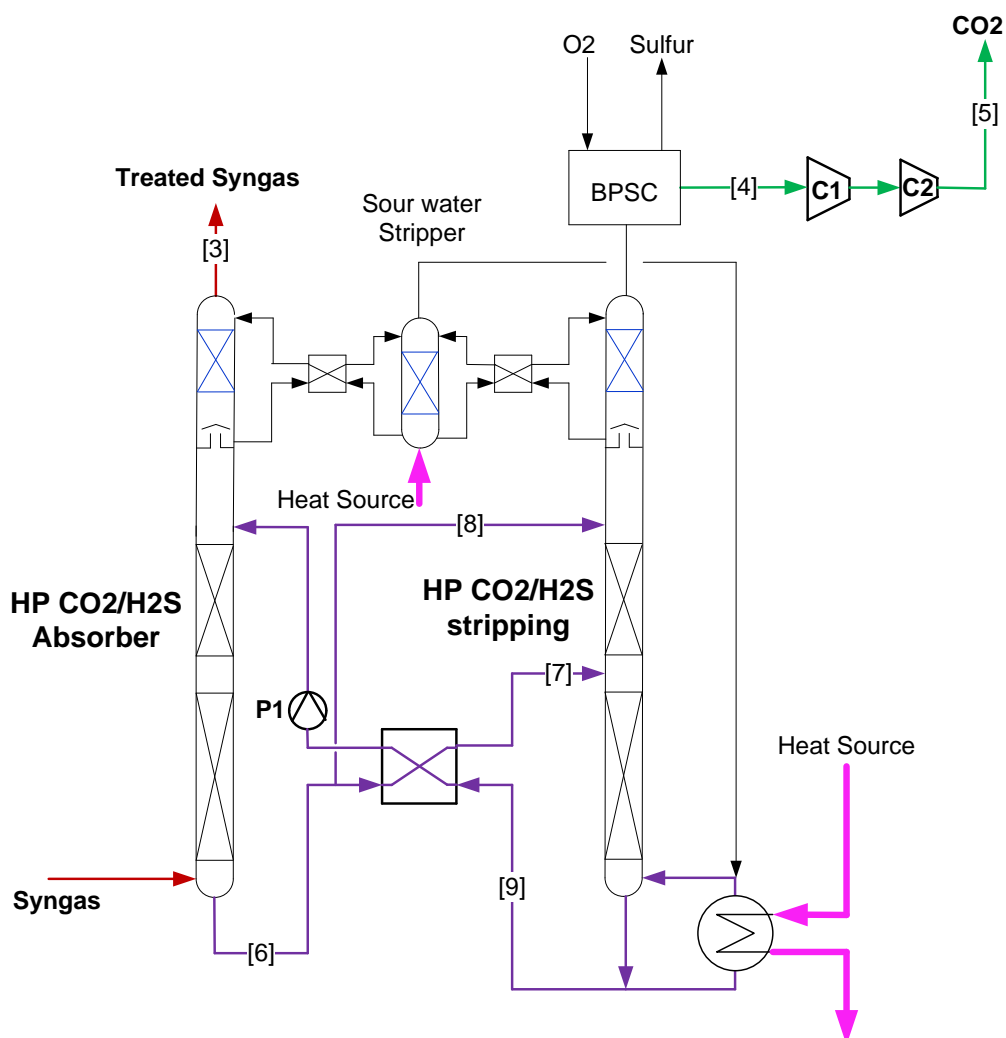


Figure 71. Schematic of the AC-ABC process for 90% CO₂ capture and sequestration at 2,200 psi; the emissions at the H₂S outlet are 10 ppm.

Power for CO₂ Compression: About 500 st/h of CO₂ is captured in the CO₂ absorber. The CO₂ is stripped from the solution in the CO₂ stripper. The CO₂ must be delivered at a pressure of 2,215 psia for sequestration or for enhanced oil recovery and is compressed from the stripper outlet pressure using a multistage CO₂ compressor with inter-cooling between each stage. The power required for the CO₂ compression as a function of the compressor inlet pressure and assuming 84% compression efficiency (DOE estimate for future highly efficient compressor) and inter-cooling to 130°F is shown in Figure 72.

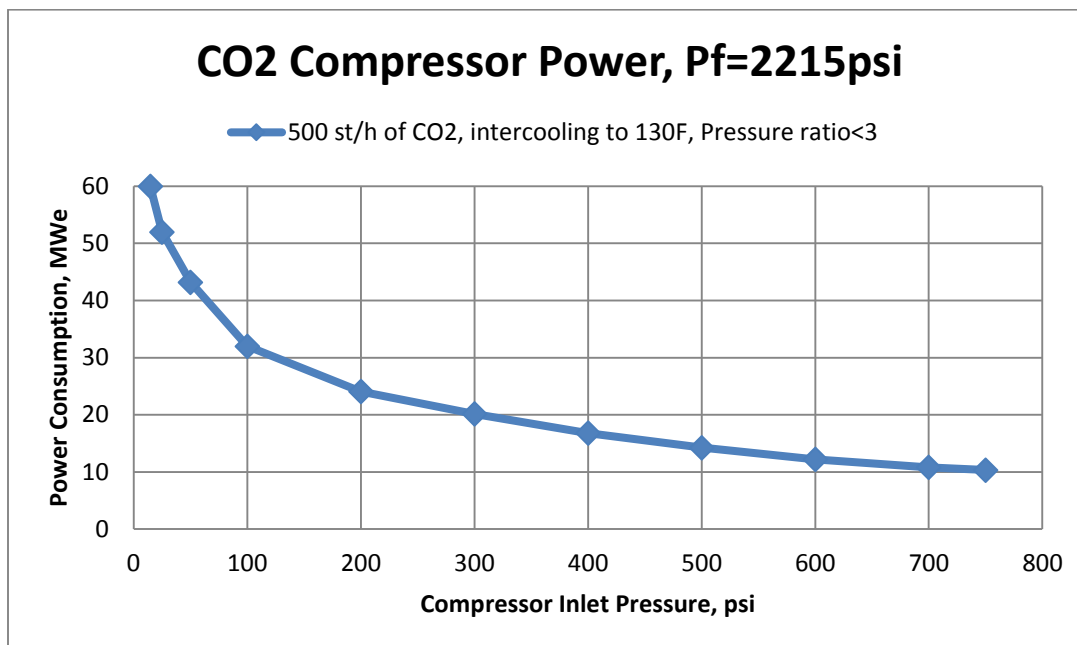


Figure 72. CO₂ compressor power for compression of 500 st/h of CO₂ to 2,215 psia.

As shown in Figure 72, stripping the CO₂ at atmospheric pressure results in power consumption of 60 MWe and requires a 5-stage compressor with very large first stage and an inlet of about 250,000 NM₃/hr of CO₂ at atmospheric pressure. Stripping the CO₂ gas at 300 psi pressure requires a two-stage compressor and results in a 20-MWe power consumption. Stripping the CO₂ gas at 750 psi requires only a one-stage compressor and results in 10 MWe of power consumption.

In most commercial operating Selexol systems, the CO₂ is stripped from the solution in a few stages with average pressures in the range of 15-50 psi. The Coffeeville Selexol plant generates 1/6 of its total CO₂ at 150 psia, and the balance is vented to the atmosphere at about 20 psia, which is an average of slightly over 40 psia. However, the higher pressure CO₂ stream contains as much as 2-5% H₂ and as much as 0.5% CO and CH₄, which represents losses from the plant and requires purification of the CO₂ via oxidation step.

It can be concluded from Figure 72 that power consumption for CO₂ compression in the Selexol process is 45-60 MWe, while the CO₂ compression power in the AC-ABC process is significantly lower. In addition, multistage compressors need a significant amount of water for inter-stage cooling.

Power for Pumping Solution between CO₂ Absorber and CO₂ Stripper: The 500 st/hr of CO₂ captured in the absorber is transferred to the CO₂ stripper in a CO₂-rich solution. The returning lean solution has to be pumped from the pressure of the CO₂ stripper to that of the absorber, and the power required is a function of the flow rate and of the pressure increase across the pump.

The flow rate is determined by the net CO₂ loading of the solution, which depends on many optimization considerations. Typical net CO₂ loading for the Selexol process is 40-50 gm per liter, requiring 40,000 to 50,000 gpm of solution to be pumped around the system. Typical net CO₂ loading for the AC-ABC is 120-150 gm per liter, requiring 13,500 to 17,000 gpm of solution to be pumped around the system. The power required for pumping is shown in Figure 73.

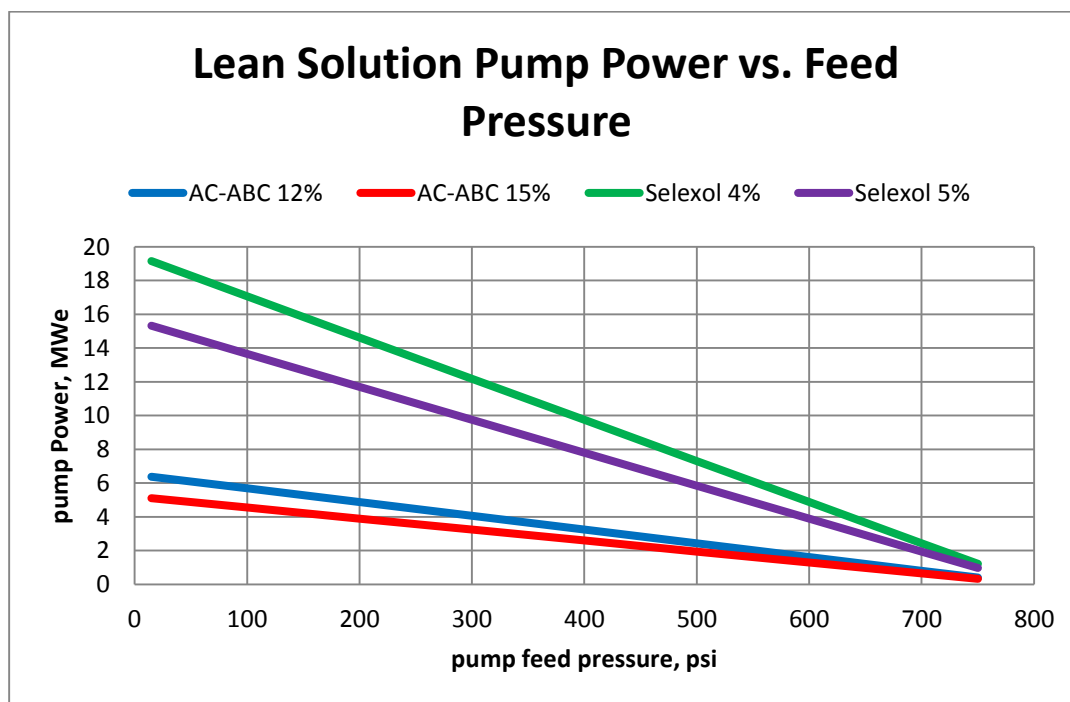


Figure 73. Pump power for pumping lean solution to the CO₂ absorber as a function of the CO₂ stripper operating pressure (pump feed pressure).

In the Selexol process, the last stage of the CO₂ release is at atmospheric pressure, requiring 15 MWe and 19 MWe of electric power to pump the lean solution back to the absorber

when the net CO₂ loadings are 5% and 4%, respectively. In the AC-ABC process, the CO₂ stripper operates in the range of 300 to 750 psi, and pumping power is about 4 MWe at the low-pressure range and less than 1 MWe at the high end of the pressure range.

Steam Consumption for the Shift Reaction: The Selexol and the AC-ABC processes are designed for an overall removal of 90% of the carbon input so that the carbon content of the CO₂ in the turbine flue gas is 10% of the carbon content of the coal input to the gasifier.

In the Selexol process, CO₂ capture efficiency is limited to 90-95%, and higher efficiency requires refrigerating the top of the absorber at high cost, operating the last stage of CO₂ flash at negative pressure, and utilizing a high rate of solution recycle between the absorber and stripper, i.e., low CO₂ loading and high pumping cost. To comply with the requirements for 90% capture of carbon, the system has to be installed with deep shift to reduce CO concentration in the syngas to below 1% and increase the CO₂ concentration of the gas. This deep shift requires steam injection to the syngas upstream of the shift reactors and multiples of shift reactors with inter-cooling.

The steam injected to the syngas has to be at a pressure above the syngas pressure and is high-quality steam. In the current study, the injected steam is at a temperature of 615°F and 875 psia. A total of about 240,000 lb/hr of steam is required. While a portion of the heat content of the steam is recovered in the form of lower-pressure steam, the energy loss and reduction in the plant efficiency amounts to a loss of about 15 MWe in steam turbine power production.

The AC-ABC process is designed to capture practically all the CO₂ in the gas stream with minimal additional cost relative to 90-95% capture efficiency. In addition, the use of the BPSC for the H₂S capture results in no CO₂ venting from the system. As a result of the high efficiency of CO₂ capture, almost 10% of the carbon in the syngas can be fed to the gas turbine as CO. This means that the CO content of the syngas can be about 4%. Achieving the limited CO shift conversion to CO₂ requires no steam injection to the syngas and additional production of about 5 MWe power in the steam turbine relative to the Selexol deep-shift case. The limited shift also results in significant cost savings.

Effect of Steam Quality and Consumption Rate on Steam Turbine Power: The operating pressure of CO₂ depends mainly on the reboiler temperature. When steam is used in the reboiler, the entire heat input is at the top required temperature.

The heat source temperature required to achieve the stripping of CO₂ pressure in the range of 100-700 psi to generate lean solution containing CO₂/NH₃= 0.35 mole ratio based on vapor-liquid equilibrium (VLE) models and experiments conducted at SRI is given in Figure 74.

It takes only a 276°F heat source (steam at 50 psia pressure) to generate the CO₂ at 100 psi, a 314°F heat source (steam at 85 psia pressure) to generate the CO₂ at 300 psi, and a 350°F heat source (steam at 140 psia pressure) to generate the CO₂ at 700 psia.

There is no thermal degradation of the solution, and the high-temperature heat source—such as hot syngas or hot combustion gas from a coal-fired boiler or from a gas turbine exhaust—can be used directly in the reboiler. When syngas is used as the heat source in the reboiler, an innovative design for boiling CO₂ from ammoniated solutions requires that only the top temperature is as shown in Figure 74. As a result, a very efficient and effective utilization of the heat content of the syngas can be applied.

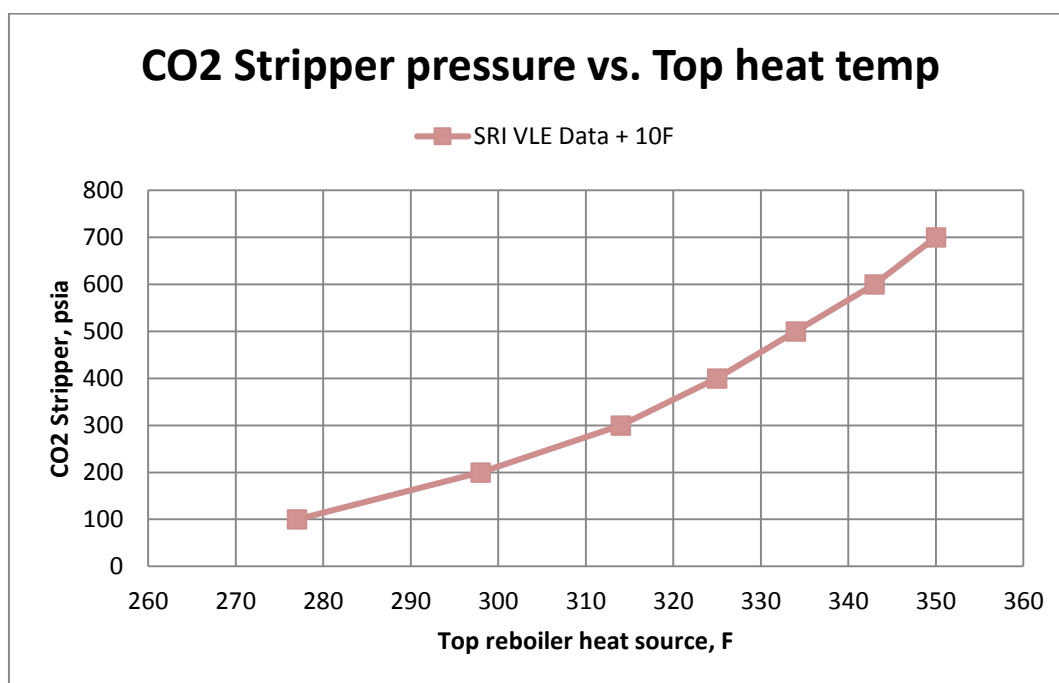


Figure 74. Saturated steam temperature required for the stripping of CO₂.

Steam Consumption for H₂S stripping: About 12,500 lb/hr of H₂S is captured in the process. The stripping of the H₂S in the H₂S stripper in the Selexol process is energy intensive and requires 8,500 btu/lb of H₂S stripped (together with CO₂) using 150 psia steam. It amounts to more than 100 MMbtu/hr of MP steam use in the H₂S reboiler and significant loss of power production in the steam turbine.

The AC-ABC process has no separate stripper for the H₂S. Rather, the H₂S is stripped together with the CO₂ in the CO₂/H₂S stripper. **The** marginal heat consumption for the H₂S stripping is 1,100 btu/lb and a total of less than 14 MMbtu/hr.

SRI used the Aspen Plus Model in combination with GT Pro to evaluate the power loss due to the use of steam and additional heat extraction from the process and to calculate total power production and efficiency. The results are summarized in Table 14.

Table 14. Net power output and relative efficiency in CO₂ capture.

	Net Power, MWe	Relative Efficiency, %
Base case - no capture	622.05	100
Selexol capture	543.25	87.3
AC-ABC with limited shift and BPSC	551.63	88.7

TECHNO-ECONOMIC ANALYSIS OF AC-ABC PROCESS: SUMMARY

Tables 15 and 16 summarize the costs of CO₂ capture from coal-fired power plants using the AC-ABC process. Case B5A from (NETL 2015), a non-capture IGCC plant with a GE gasifier, is used as the reference case. The CO₂ capture costs using the AC-ABC process are compared to the costs of using a dual-stage Selexol process (Case B5B from Ref. 1). CO₂ capture costs are 25-32% lower using the AC-ABC process than the Selexol process, and the capital costs required to implement the AC-ABC process are 48% lower than the Selexol capital costs.

Table 15. CO₂ capture costs compared to IGCC base case (Case B5A).

Power Plant Inputs		DOE Case B5A: Baseline GEE IGCC- No Capture	DOE Case B5B: Selexol Capture	AC-ABC CO ₂ & H ₂ S Capture
Heat Rate (BTU/kWh)		8,756	10,458	10,299
Gross Power, kWe		747,800	734,000	714,173
Net Power, kWe		622,050	543,250	551,634
Total Overnight Cost (\$/net-kW)		\$3,036	\$4,195	\$3,701
Annual Output at	Net Power (GWH/year)	5,449	4,759	4,832
	CO ₂ Captured (million metric tons per year)	-	4.0	4.0
Cost of Electricity				
COE (\$/MWh)	Power Plant Capital	53.7	74.3	65.6
	Power Plant Fuel	25.8	30.8	30.3
	Power Plant O&M	23.1	30.5	28.7
	CO ₂ Transport, Storage, and Monitoring	-	9.2	9.2
	Total	102.6	144.8	133.7
COE (% Increase)			41.2%	30.4%
Avoided Cost (cost of CO₂ capture, \$/metric ton)			\$50.21	\$37.89
Cost of CO₂ Captured, \$/metric ton			\$39.26	\$26.71

Table 16. Capital cost comparison to IGCC base case (Case B5A).

Capital Cost, 2011 (x \$1,000)	DOE Case B5A: Baseline GEE IGCC- No Capture	DOE Case B5B: Selexol Capture	AC-ABC CO ₂ & H ₂ S Capture
Selexol		\$251,145	
SRI AGR			\$121,104
CO₂ Compression		\$84,088	\$17,212
Water-Gas Shift Reactors		\$21,370	\$17,981
Claus		\$40,699	
Pressure Swing Claus			\$49,615
Subtotal (WGS, AGR, H₂S Conversion, and CO₂ Compression steps only)		\$397,302	\$205,912
Total Overnight Cost (TOC) of Complete IGCC Plant	\$1,888,393	\$2,278,752	\$2,041,739

IGCC REFERENCE CASE

Capturing CO₂ from coal-fired power plants is a critical step in carbon sequestration. In the IGCC process, coal is reacted with steam and O₂ under pressure in the range of 300 to 1,000 psi to form a fuel gas containing mainly CO, H₂, H₂S, CO₂, and residual steam. The CO in the gas stream is converted to CO₂ and H₂ by using the water-gas shift reaction at about 200° to 285°C. The gas stream leaving the water-gas shift reactor (WGSR) contains mainly H₂, CO₂, H₂S, and H₂O. An H₂-rich fuel gas suitable for combustion in a gas turbine is produced by condensing the steam and removing the CO₂ and H₂S. The current “best-case” option for carbon capture is using a liquid solvent such as Selexol or Rectisol to absorb CO₂ and H₂S at elevated pressures.

Case B5B of the DOE/NETL report “Cost and Performance Baseline for Fossil Energy Plants, Volume 1b: Bituminous Coal (IGCC) to Electricity,” Revision 2b, July 2015, was used as a reference case for this analysis (NETL 2015). Case B5B was an IGCC plant with a GE gasifier and CO₂ and H₂S capture using a dual-stage Selexol process and production of elemental sulfur from H₂S using the Claus process. A block flow diagram of this process is shown below.



IGCC CASE WITH AC-ABC CO₂ AND H₂S CAPTURE

The AC-ABC process for capture of CO₂ and H₂S in the pre-combustion gas stream offers many advantages over other solvent-based technologies. The process relies on the simple chemistry of the NH₃-CO₂-H₂O-H₂S system and on the ability of the aqueous ammoniated solution to absorb CO₂ at near ambient temperatures and to release it as a high-pressure gas at a moderately elevated temperature. The AC-ABC process exhibits several advantages over the Selexol process in the IGCC application, which are listed below. These advantages have been validated by several hundred hours of pilot-scale testing at the NCCC in Wilsonville, AL.

The AC-ABC process exhibits CO₂ capture efficiencies greater than 99%.

- CO₂ and H₂S stripping can be accomplished at elevated pressures, greatly reducing the costs required to compress the exiting CO₂ stream to pipeline pressure. H₂S recovery from the regenerated gas stream is accomplished with the BPSC process, which allows the CO₂ stream to remain at elevated pressure.
- The solubility of fuel gases such as H₂, CO, and CH₄ in the aqueous ammoniated solutions is very low, which eliminates the need for a flash step to recover these gases from the solution.
- The low solubility of the fuel gases and the high efficiency of CO₂ absorption allow the overall target of 90% carbon capture to be achieved without needing to convert all of the CO in the syngas to CO₂. Allowing lower conversion in the water-gas shift reactors eliminates the need to add steam to the unshifted syngas, which preserves more of the steam for power generation. It has been confirmed with shift catalyst vendors Johnson-Matthey and Haldor-Topsoe that the shift reactions can theoretically be run at such a low conversion, though the efficacy of this has yet to be tested at large scale.
- The capital cost of the AC-ABC process can be significantly lowered in comparison to the Selexol process due to: (i) absorption of the H₂S and the CO₂ in the same absorber vessel, resulting in the elimination of a separate H₂S absorber vessel and its auxiliary equipment; (ii) elimination of H₂S enrichment vessel and clean gas stripping compressor; (iii) smaller shift reactors for achieving reduced level of water gas shift reaction; (iv) the stripping of the H₂S together with the CO₂, which eliminates the need for a separate H₂S stripper and its auxiliary equipment; and (v) a much smaller CO₂ compressor.
- The parasitic electric power consumption is low for the AC-ABC process because the CO₂ is stripped at elevated pressures, high CO₂ loadings can be attained in the solution, and the absorber and stripper can be operated at nearly the same pressure. Capital costs for pumps and compressors are reduced as well.
- The AC-ABC steam consumption to strip the H₂S is a small fraction of the heat consumption of the Selexol process for H₂S stripping. In addition, recovering some heat from the hot syngas, either directly or using IP steam as an intermediary to be used as a heat source for CO₂/H₂S stripping, reduces the steam usage and thus the power output penalty.

A block flow diagram for the GEE IGCC process using AC-ABC instead of Selexol is shown below.

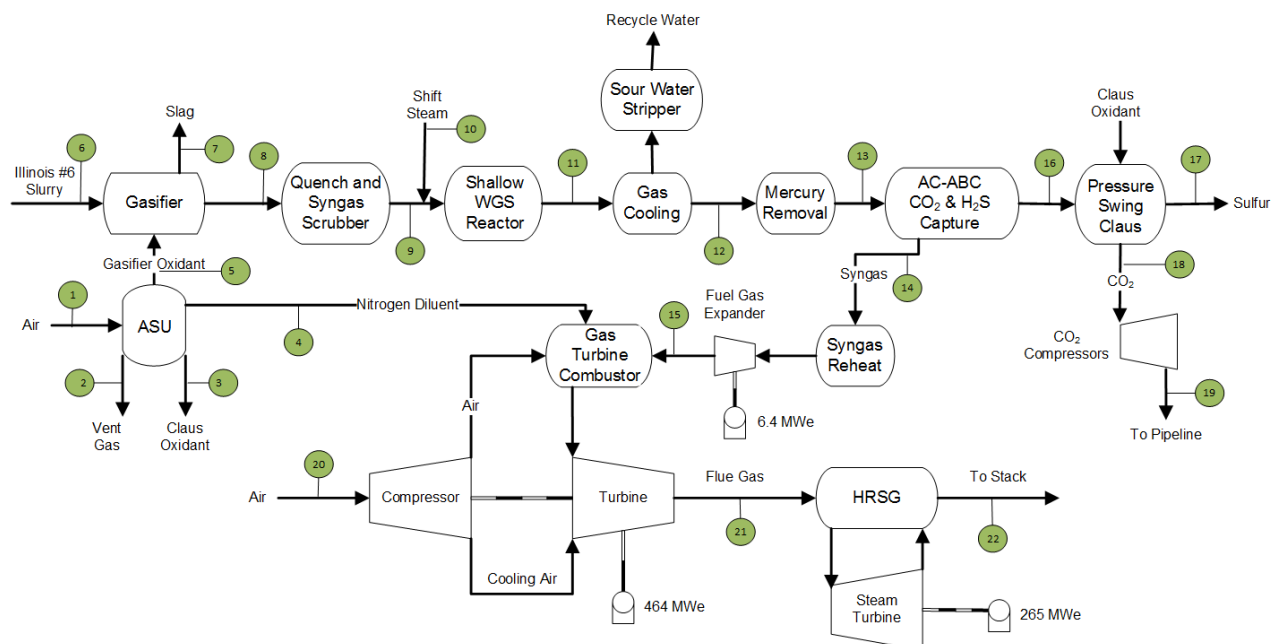


Figure 76. GEE IGCC block flow diagram with AC-ABC and BPSC.

The IGCC plant with AC-ABC was modeled in Aspen Plus, version 8.8. Figure 76 shows the process flow diagram and stream compositions; properties for the major streams within the IGCC plant are provided in Table 17. The Peng-Robinson property method was used for most of the IGCC plant, with the exception of the steam turbines and heat recovery steam generator (HRSG) power, which were modeled with the STEAM-NBS property method as in the DOE base cases. The AC-ABC process was modeled with the OLI Systems (OLI) property method, which better accounts for an aqueous electrolyte system such as the NH_3 - CO_2 - H_2S - H_2O system that is the basis of the AC-ABC CO_2 / H_2S capture method. Using the OLI property method requires the purchase of the OLI Engine for Aspen Plus. The most recent version of OLI, Version 9.2, was used in this analysis. The power island was modeled in GT-PRO.

Table 17. Stream tables: GEE IGCC with AC-ABC and BPSC.

	1	2	3	4	5	6	7	8	9	10	11
Temperature F	59	70	90	385	90	60	410	2400	410	0	450
Pressure psia	14.4	16.4	145	450	125	14.4	797.7	814.7	797.7	0	770
Enthalpy Btu/lb	-81.74	-76.29	0.024	93.99	1.14	0	0	-1884.62	-4281.33	0	-4523.86
Density lb/cuft	0.075	0.101	0.791	1.393	0.682	0	0	0.537	1.697	0	1.563
Mole Flow scfm	397976	15262	1677	276461	80117	0	0	322718	416857	0	416857
V-L Mass Flow lb/hr	1815330	64658	8531	1226680	407652	0	0	1041360	1308800	0	1308800
Solids Mass Flow lb/hr	0	0	0	0	0	487005	53457	0	0	0	0
V-L Mole Fraction											
Ar	0.009	0.024	0.029	0.002	0.032	0	0	0.008	0.006	0	0.006
CH ₄	0	0	0	0	0	0	0	992 PPM	768 PPM	0	768 PPM
CO	0	0	0	0	0	0	0	0.344	0.266	0	0.038
CO ₂	295 PPM	0.008	0	0	0	0	0	0.152	0.117	0	0.345
COS	0	0	0	0	0	0	0	188 PPM	146 PPM	0	38 PPM
H ₂	0	0	0	0	0	0	0	0.335	0.26	0	0.488
H ₂ O	0.011	0.249	0	0	0	0	0	0.142	0.337	0	0.108
HCl	0	0	0	0	0	0	0	0	0	0	0
H ₂ S	0	0	0	0	0	0	0	0.007	0.006	0	0.006
N ₂	0.772	0.503	0.011	0.992	0.018	0	0	0.009	0.007	0	0.007
NH ₃	0	0	0	0	0	0	0	0.002	0.001	0	0.001
O ₂	0.208	0.217	0.96	0.005	0.95	0	0	trace	trace	0	trace
SO ₂	0	0	0	0	0	0	0	0	0	0	0
	12	13	14	15	16	17	18	19	20	21	22
Temperature F	73	95	72.6	311.3	176	601.1	328.1	246.6	59	1053.1	270
Pressure psia	745	740	739.7	460	364.7	356.2	356.2	2215	14.7	15.24	15.24
Enthalpy Btu/lb	-3985.64	-3985.64	-127.04	-67.19	-3888.32	3.72	-3904.20	-3860.63	-317.26	-1854.91	-1854.91
Density lb/cuft	2.621	2.568	0.602	0.255	2.312	6.02	1.801	17.744	0.076	0.026	0.026
Mole Flow scfm	372000	372000	224772	224772	150343	398	151353	144890	1544750	1936640	1936640
V-L Mass Flow lb/hr	1181050	1181050	165097	165097	1024820	12102	1023120	1004710	7046210	8437990	8437990
Solids Mass Flow lb/hr	0	0	0	0	0	0	0	0	0	0	0
V-L Mole Fraction											
Ar	0.007	0.007	0.011	0.011	51 PPM	0	370 PPM	386 PPM	0.009	0.009	0.009
CH ₄	861 PPM	861 PPM	0.001	0.001	6 PPM	0	6 PPM	7 PPM	0	0	0
CO	0.042	0.042	0.07	0.07	209 PPM	0	0	0	0	0	0
CO ₂	0.387	0.387	64 PPM	64 PPM	0.957	0	0.952	0.995	295 PPM	0.009	0.009
COS	43 PPM	43 PPM	70 PPM	70 PPM	211 PPB	0	10 PPB	11 PPB	0	0	0
H ₂	0.547	0.547	0.903	0.903	0.003	0	0.003	0.003	0	0	0
H ₂ O	0.001	0.001	0.001	0.001	0.022	0	0.043	0	0.011	0.114	0.114
HCl	0	0	0	0	0	0	0	0	0	0	0
H ₂ S	0.006	0.006	856 PPB	856 PPB	0.016	0	5 PPM	6 PPM	0	0	0
N ₂	0.008	0.008	0.013	0.013	19 PPM	0	0.002	0.002	0.772	0.759	0.759
NH ₃	837 PPM	837 PPM	15 PPM	15 PPM	0.002	0	45 PPM	47 PPM	0	2 PPM	2 PPM
O ₂	trace	trace	trace	trace	0	0	0	0	0.208	0.11	0.11
SO ₂	0	0	0	0	0	0	25 PPM	26 PPM	0	8 PPM	8 PPM

COST ESTIMATING METHODOLOGY AND ASSUMPTIONS

General Site Assumptions

- **Site characteristics:** Same as in (NETL 2015): Greenfield, Midwestern USA.
- **Coal:** Same as in (NETL 2015): Illinois No. 6 coal with a cost of \$2.78/GJ or \$2.94/MMBtu.
- **Emissions:** The IGCC case with AC-ABC CO₂/H₂S capture meets all emissions limits described in the baseline IGCC cases in (NETL 2015) (PM, SO₂, NO_x, mercury).
- **CO₂ captured/avoided costs:** Calculated using the below equations from (NETL 2015).

$$\text{Cost of CO}_2 \text{ Captured} = \frac{(COE_{CCS} - COE_{Non\ CCS})}{CO_2 \text{ Captured}}$$

$$\text{Cost of CO}_2 \text{ Avoided} = \frac{(COE_{CCS\ with\ T\ \&\ S} - COE_{Non\ CCS})}{CO_2 \text{ Emissions}_{Non\ CCS} - CO_2 \text{ Emissions}_{CCS}}$$

- **Capacity factor:** Same as in (NETL 2015) for IGCC cases: 80%.
- **Raw water withdrawal and consumption:** Same as in (NETL 2015).

Capital Cost Calculations and Assumptions

Bare erected cost (BEC), total plant cost (TPC), and total overnight cost (TOC) were calculated as “overnight” costs and expressed in 2011 dollars. For the purposes of our comparison, it was not necessary to calculate a total as-spent cost (TASC). The BEC includes process equipment, supporting facilities, and both direct and indirect labor. The TPC includes BEC plus the engineering, construction, & contractor’s fee (EPC), process contingency, and project contingency. The TOC includes TPC plus preproduction costs, inventory capital, financing costs, and other owner’s costs.

Summary of BEC, TPC, and TOC Calculations

The TPC for sections of the process other than CO₂/ H₂S capture was assumed to be the same as in Case B5B of (NETL 2015). Two exceptions to this were: (1) the water-gas shift reactors, whose costs were scaled back based on the decreased capacity requirement since no added steam is present; and (2) the CO₂ compression and drying costs, which were scaled back based on the decreased compression power requirement due to regenerating CO₂ at high pressure. To account for the capital costs of the CO₂/ H₂S capture processes, the capital costs related to the dual-stage Selexol process and the elemental sulfur plant in the DOE Case B5B were deleted (at the TPC level) and replaced by the TPC of the AC-ABC system and the BPSC system. The TPC estimates for AC-ABC were generated by: (1) simulating the full AC-ABC

process in Aspen Plus; (2) using the stream flows, column sizes, equipment power, and heat transfer requirements calculated by Aspen to size the process equipment; (3) costing the equipment based on correlations from Peters et al. 2013 and Towler et al. 2013; (4) using the delivered-equipment ratio factor method from Peters, et al. 2013, to calculate the BEC from the delivered equipment cost; and (5) using factors from (NETL 2015) for the EPC, process contingency, and project contingency to calculate the TPC from the BEC. The factors from Peters et al. 2013 and (NETL 2015) are shown in Table 18 below.

Table 18. Factors for calculating BEC and TPC from delivered equipment cost.

Factors included in BEC	Percent of delivered equipment cost for fluid processing plant
Purchased equipment delivered	100
Purchased-equipment installation	47
Instrumentation and controls (installed)	36
Piping (installed)	68
Electrical systems (installed)	11
Buildings (including services)	18
Yard improvements	10
Service facilities (installed)	70
Total direct plant cost (bare erected cost)	3.6 x delivered equipment cost
Factors included in TPC	Percent of delivered equipment cost for fluid processing plant
Engineering, construction, & contractor's fee (EPC)	10
Contingency (process)	20
Contingency (project)	30% of the sum of delivered equipment cost, process contingency and EPC fees
Total indirect plant cost	Project contingency + process contingency + EPC fees
Fixed Capital Investment (Total Plant Cost)	TPC = BEC plus total indirect plant cost

Other Capital Cost Assumptions

- **Plant maturity, contracting strategy, and estimate scope:** Same as in (NETL 2015).
- **Exclusions:** Same as in (NETL 2015): taxes (except payroll and property), site-specific considerations, labor incentives in excess of 5-10%, and additional EPC premiums are excluded from the capital cost estimate.
- **Process contingency:** Same as (NETL 2015) for Selexol IGCC case: 20%. This 20% value is reasonable based on the Association for the Advancement of Cost Engineering (AACE) guidelines for process contingency, which recommend 20-35% for technologies with small pilot-plant data.
- **Project contingency:** The guideline for project contingency given in (NETL 2015) was 15-30% of the sum of BEC, EPC fees, and process contingency; 20% was used here.
- **Owner's costs and TASC/TOC ratio:** Same as in (NETL 2015), Case B5B.
- **Capital charge factor:** Same as in (NETL 2015): a first-year capital charge factor of 0.1243 was assumed.

Based on the above assumptions, the TPC for the IGCC plant with AC-ABC and BPSC CO₂/H₂S capture was calculated and compared to the Selexol case (Case B5B). Results are summarized in Table 19. Detailed equipment costs are provided in Appendix A.

Table 19. Difference in Selexol and AC-ABC total plant cost.

Item from DOE Case B5B Cost Details:	(All Costs in \$ x 1000)		
	DOE Cost*	Action	Cost with AC/ABC-BPSC
5A.1 Double-Stage Selexol	\$251,145	Delete All	\$0
5A.2 Elemental Sulfur Plant	\$40,699	Delete All	\$0
5A.4 Shift Reactors	\$21,370	Reduce by 13.3%	\$17,981
5B.2 CO ₂ Compression and Drying	\$84,088	Reduce	\$17,212
New.1 AC/ABC System single stage		Add	\$121,104
New.2 BPSC System		Add	\$49,615
Sub-totals	\$397,302		\$205,912
Total Plant Cost *	\$1,840,115		\$1,648,725
Delta	\$191,390		
% Cost Reduction:	10.40%		

*DOE Costs from “Cost and Performance Baseline for Fossil Energy Plants, Volume 1b: Bituminous Coal (IGCC) to Electricity,” Revision 2b. DOE/NETL, July 2015. Does not include owner's costs, financing costs, and TASC multiplier.

Operations and Maintenance Cost Calculations and Assumptions

- **Operating labor:** Total operating labor requirements and costs are assumed to be the same as in DOE Case B5B.
- **Maintenance material and labor:** Labor costs are assumed to be the same as in DOE Case B5B. Maintenance material costs were scaled from Case B5B based on the capital cost.
- **Consumables:** Consumables not related to CO₂/H₂S removal were scaled based on flow-rate differences from DOE Case B5B. Consumables for CO₂/H₂S removal were calculated based on the Aspen Plus and GT Pro simulation results. Since an oxygen-blown Claus plant was used in the base case, the oxygen stream required for the BPSC sulfur recovery process (which replaces the Claus plant) was assumed to have no additional cost.
- **Waste disposal:** Waste disposal not related to CO₂/H₂S removal was scaled based on flow-rate differences from DOE Case B5B. No additional waste disposal costs were incurred from the AC-ABC process.
- **Co-products and by-products:** Same as in (NETL 2015). No credit was taken for any potential salable value of byproducts such as sulfur.

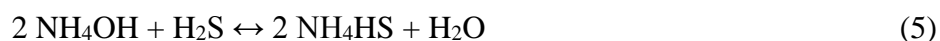
- **CO₂ transport, storage, and monitoring (TS&M):** Same as in (NETL 2015), Case B5B.

AC-ABC PROCESS DETAILS AND ASSUMPTIONS

AC-ABC Process Details

A schematic of the AC-ABC process for CO₂ and H₂S capture from syngas is shown in Figure 77. Stream tables from the Aspen simulation of the AC-ABC process are provided in Table 20. The system treats cooled syngas from a GE gasifier after the sour water-gas shift reactors. The system is designed for 99+% CO₂ capture and near-complete H₂S capture. Since practically all of the CO₂ in the shifted syngas is captured in the absorber and 90% capture of carbon is required to meet the DOE target, the residual 10% carbon can be in the form of CO that is not converted in the shift reactors. This translates to about 4% CO in the syngas (dry basis). No additional steam needs to be injected into the syngas if the CO does not need to be completely converted ("shallow shift"). After the shift, the main species in the syngas are CO₂, CO, and H₂ and the minor species are CH₄, H₂S, Ar, N₂, and H₂O. The gas pressure is about 750 psi, and it is sent to the AGR for CO₂ and H₂S capture. The AC-ABC process allows simultaneous capture of the CO₂ and H₂S in a single absorber vessel and regeneration of the CO₂ and H₂S in a regenerator vessel operating at high pressure.

The absorber is a multistage vessel in which the bulk of CO₂ and H₂S are captured at the bottom stages using high-concentration (6-12 molal) ammoniated solution from the high-pressure CO₂/H₂S regenerator. Following the absorber is a water-wash step in which residual ammonia vapor is captured and sent to a sour-water stripper for recovery. The following reversible aqueous phase reactions occur between NH₃, CO₂, and H₂S in the absorber:



The CO₂ and H₂S regeneration is performed at elevated temperature and pressure; the CO₂-rich solution is first heated in a regenerative heat exchanger in counter current flow with the CO₂-lean solution and is then sent to the stripper. The reactions listed above proceed in reverse

order in the regenerator. A polishing water-wash stage at the top of the regenerator ensures that the CO₂/H₂S gas stream is free of ammonia (< 10 ppm).

The heat of reaction for CO₂, which depends on temperature, molality, and the CO₂/NH₃ loading, is in the range of 300-700 Btu/lb CO₂. The heat of reaction for H₂S is in the range 800-1,100 Btu/lb H₂S. The heat source in the CO₂/H₂S stripper can be steam. Alternatively, the heat source could be hot syngas, which can be cooled and a fraction of its water condensed while boiling CO₂ and H₂S from the rich solution in the reboiler.

The higher the reboiler temperature, the higher the regenerator pressure and the resultant CO₂ pressure and the lean solution pressure. Higher CO₂ pressure results in a much lower CO₂ compressor power, and higher lean solution pressure results in lower power for pumping the lean solution to the absorber. However, steam usage in the reboiler is greater.

The CO₂/H₂S gas from the stripper is sent to a BPSC system. The BPSC is a low-cost and simple process for in-situ reduction of H₂S to elemental sulfur at high gas pressure. Oxygen is used to convert sulfur to SO₂ and then through the classical Claus reaction to convert the H₂S to sulfur. The clean CO₂ gas stream from the BPSC is compressed from 300 to 750 psi to 2,200 psig for sequestration or for enhanced oil recovery. The compression of the CO₂ requires only one or two compression stages with inter-cooling.

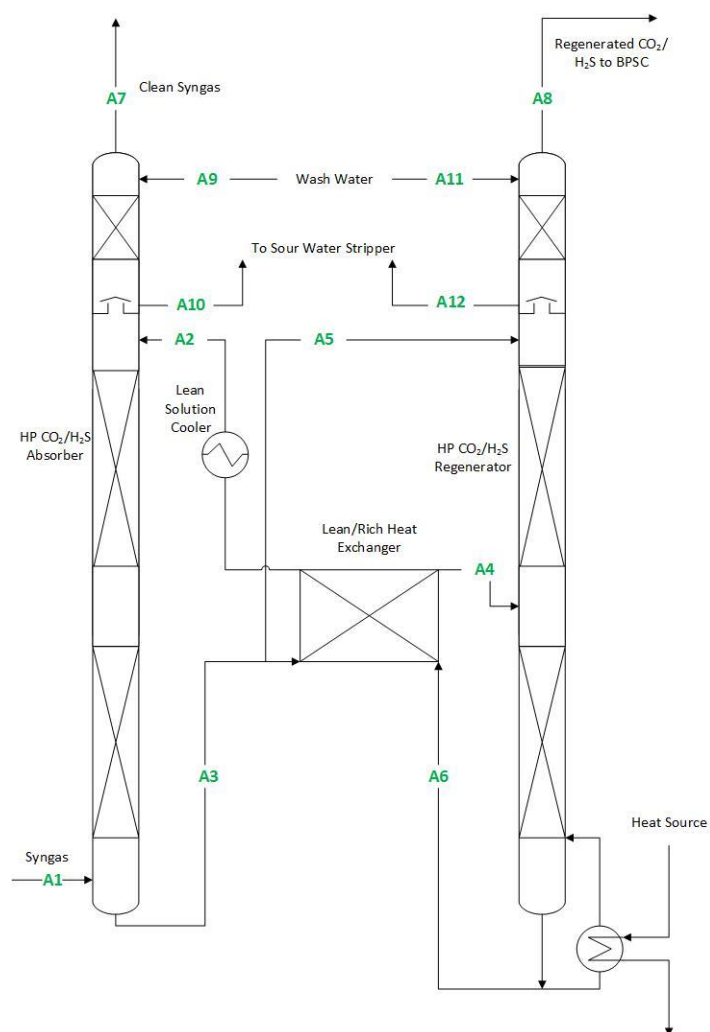
AC-ABC Process Block Flow Diagram and Stream Tables**Figure 77.** AC-ABC block flow diagram.

Table 20. AC-ABC process stream tables.

	A1	A2	A3	A4	A5	A6
Temperature F	98.6	85	159.6	250.9	159.6	85
Pressure psia	740	739.7	741.7	727.7	741.7	357.7
Enthalpy Btu/lb	-3981.1	-43413	-47459.2	-42531.4	-4081.5	-43375
Density lb/cuft	2.50	68.40	69.49	38.66	69.49	68.38
Mole Flow lbmol/h	58814	375813	399046	364728	34318	375403
V-L Mass Flow lb/hr	1181050	7143800	8157680	7456120	701561	7137970
Solids Mass Flow lb/hr						
V-L Mole Fraction						
Ar	0.007	0	3 PPM	3 PPM	3 PPM	trace
CH ₄	867 PPM	0	330 PPB	330 PPB	330 PPB	trace
CO	0.043	0	14 PPM	14 PPM	14 PPM	trace
CO ₂	0.387	0.042	0.097	0.097	0.097	0.042
COS	43 PPM	0	14 PPB	14 PPB	14 PPB	0
H ₂	0.547	0	183 PPM	183 PPM	183 PPM	trace
H ₂ O	999 PPM	0.836	0.787	0.787	0.787	0.836
HCl	0	0	0	0	0	0
H ₂ S	0.006	0.001	0.002	0.002	0.002	0.001
N ₂	0.008	0	2 PPM	2 PPM	2 PPM	trace
NH ₃	835 PPM	0.121	0.114	0.114	0.114	0.121
O ₂	0	0	0	0	0	0
SO ₂	0	0	0	0	0	0
	A7	A8	A9	A10	A11	A12
Temperature F	77.6	176	75	78	80	179
Pressure psia	739.7	364.7	14.7	739.7	14.7	364.7
Enthalpy Btu/lb	-125.8	-3874.8	-681.8	-678.2	-119.1	-122.2
Density lb/cuft	0.58	2.49	62.25	62.34	62.20	65.75
Mole Flow lbmol/h	35578	23593	5543	5533	969	1018
V-L Mass Flow lb/hr	166699	1017350	99859	99729	17462	19827
Solids Mass Flow lb/hr						
V-L Mole Fraction						
Ar	0.012	46 PPM	0	7 PPM	0	11 PPB
CH ₄	0.001	6 PPM	0	863 PPB	0	1 PPB
CO	0.071	231 PPM	0	31 PPM	0	47 PPB
CO ₂	331 PPB	0.958	0	533 PPM	0	0.058
COS	71 PPM	237 PPB	0	56 PPB	0	trace
H ₂	0.901	0.003	0	311 PPM	0	712 PPB
H ₂ O	0.001	0.023	1	0.995	1	0.879
HCl	0	0	0	0	0	0
H ₂ S	831 PPB	0.015	0	216 PPM	0	0.001
N ₂	0.013	27 PPM	0	4 PPM	0	4 PPB
NH ₃	16 PPM	4 PPM	0	0.003	0	0.062
O ₂	0	0	0	0	0	0
SO ₂	0	0	0	0	0	0

AC-ABC-Specific Cost Estimation Assumptions

- The operating pressure for the AC-ABC absorber in this cost analysis was assumed to be 725 psig, and the regenerator pressure 350 psig—although regeneration should be feasible up to at least 725 psig as well.
- The lean AC-ABC solvent in the model consisted of 8 molal aqueous ammonia with a CO_2/NH_3 molar ratio (CO_2 loading) of 0.35. The rich solution CO_2/NH_3 loading was 0.85.
- Operating parameters such as the recycle rates within the absorber and water-wash columns were based on the operating conditions of the AC-ABC pilot plant at the National Carbon Capture Center in Wilsonville, AL.
- Steam used in the regenerator reboiler was assumed to be at 458°F and 458 psia, as extracted from the IP steam turbine.
- Flow rates of clean water into the water-wash column and the regenerator water wash were optimized to minimize water usage while achieving targets of 30 ppm NH_3 in the clean syngas and 10 ppm NH_3 in the regenerated $\text{CO}_2/\text{H}_2\text{S}$ stream.
- No additional sour-water stripper was included in the AC-ABC capital cost estimation because the amount of sour water produced from AC-ABC is less than the amount of sour water avoided by not adding additional steam to the water-gas shift reactors. Therefore, the sour water from the AC-ABC water washes can be sent to the existing sour-water stripper within the IGCC plant without adding any new capacity.
- Equipment in the AC-ABC process was assumed to be constructed of 316 stainless steel for the purpose of resisting corrosion.

Heat requirements: The following sources of heat were considered to be available for supplying regeneration heat to the AC-ABC reboiler (in the form of IP steam, as in the reference cases):

- The hot syngas exiting the first sour-gas shift (SGS) stage. In the Selexol case, this heat was used to generate the steam added before the SGS reactors, but in the AC-ABC case this additional steam stream can be used to supply the reboiler.
- The hot syngas exiting the second SGS stage. In the DOE cases, this was used to preheat unshifted syngas or used to generate IP steam sent to the heat recovery steam generator (HRSG). For the AC-ABC case, this IP steam was used to supply the reboiler, so no credit was taken for recycling this heat back to the HRSG.
- Further cooling of the hot syngas prior to the mercury removal stage. Some of the steam raised from the heat removed here was used to reheat the clean syngas prior to expansion.

IP steam directly from the HRSG was used to provide the remainder of the steam required in the AC-ABC reboiler. Because the AC-ABC solvent does not degrade at high temperatures, high-temperature process streams such as the hot syngas could potentially be used for direct heat exchange to regenerate the rich AC-ABC solvent, rather than using IP steam as an intermediary. This would provide cost savings and reduce the steam usage requirement.

Bechtel Pressure-Swing Claus Process: Bechtel Hydrocarbon Technology Solutions, Inc. is developing an alternate process to convert H_2S to elemental sulfur at elevated pressures (Figure 78). This process can use the $\text{CO}_2\text{-H}_2\text{S}$ stream produced in the regenerator of the AC-ABC process to produce elemental sulfur and a CO_2 gas stream that is suitable for sequestration.

Bechtel Pressure Swing Claus

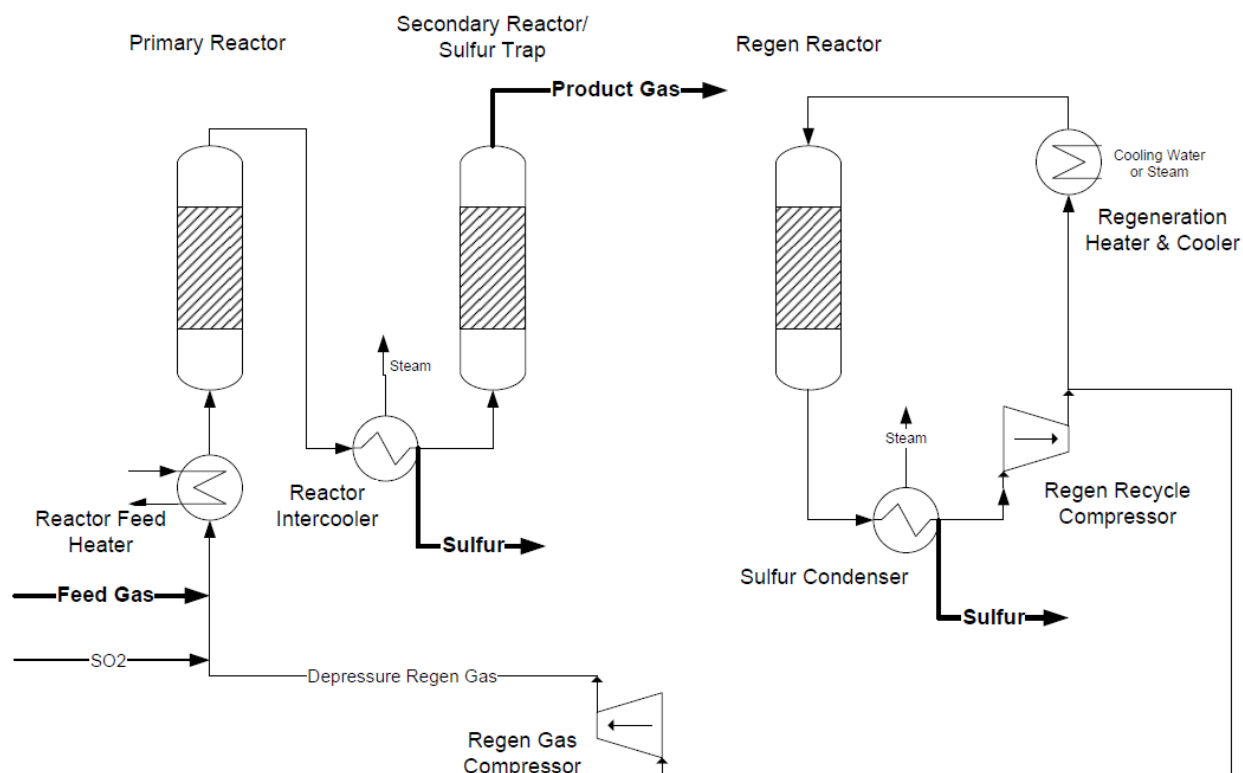


Figure 78. Bechtel pressure-swing Claus process to convert H_2S to elemental sulfur.

In this process, SO_2 is introduced to the acid gases (“feed gas”) and they are heated indirectly by steam in the “reactor feed heater”. Then the mixture is fed to the first or primary on-line reactor (“primary reactor”), where most of the H_2S , COS , and SO_2 are converted to sulfur and adsorbed on the catalyst. Based on the bench-scale testing, the primary reactor is expected to produce a sweet gas of about 100 ppmv total sulfur (including residual elemental sulfur vapor). The gas flows through a cooler (“reactor intercooler”), where it is cooled by generating steam. Provisions are made to accommodate any sulfur that may condense at this location. Any recovered sulfur drains to a sulfur pit, and the vapor goes to the next reactor (“secondary reactor/sulfur trap”), which acts as a sulfur trap/guard bed. Here, it is expected that residual sulfur vapor will be adsorbed and most of the remaining residual H_2S , COS , and SO_2 will be converted to sulfur and/or adsorbed. The second reactor is expected to reduce the sulfur in the

product gas to less than 20 ppmv total sulfur. The product gas is returned to the facility for compression. After about 8-12 hours online, the primary reactor is rotated to regeneration, the secondary reactor moves up to the primary position, and the regenerated reactor is switched to the secondary reactor position. The “regen reactor” is shown in regeneration in Figure 78. The sulfur-loaded bed is partially regenerated by pressure let down. Flash gas passes through a sulfur condenser (“sulfur condenser”) and is recompressed (“regen recycle compressor and regen gas compressor”) prior to being mixed into the BPSC feed stream. There is a heating and cooling cycle (“regeneration heater and cooler”) using recycled sweep gas to complete the reactor regeneration. High-pressure SO₂ is produced from some of the product sulfur by reacting it with oxygen from a proprietary reactor or a third-party vendor.

BPSC allows recovery of sulfur species as elemental sulfur while maintaining system pressure. Due to the higher pressures compared to traditional Claus units, equipment size is reduced.

PLANT PERFORMANCE SUMMARY WITH AC-ABC CO₂ AND H₂S CAPTURE

The gas turbine, steam turbine, and HRSG were modeled in GT Pro. Given the composition of the clean syngas as an input, GT Pro calculates the amount of clean syngas needed to achieve the specified gas turbine power of 464 MW. Given the process steam requirements and conditions, the gross steam turbine power and auxiliary power requirements are calculated. Table 21 summarizes the gross and net power plant outputs for the three IGCC cases: no CO₂ capture, Selexol capture, and AC-ABC capture.

Table 21. Plant performance summary.

	DOE Case B5A: Baseline, No CO ₂ Capture	DOE Case B5B: Selexol CO ₂ Capture	AC-ABC CO ₂ & H ₂ S Capture	
GROSS POWER PLANT OUTPUT				
Gas Turbine Power	464,000	464,000	464,000	kWe
Sweet Gas Expander Power	7,500	6,500	6,359	kWe
Steam Turbine Power	276,300	263,500	243,814	kWe
TOTAL POWER	747,800	734,000	714,173	kWe
AUXILIARY LOAD				
Coal Handling	460	470	470	kWe
Coal Milling	2,180	2,270	2,270	kWe
Coal Slurry Pumps	180	190	190	kWe
Slag Handling and Dewatering	1,120	1,160	1,160	kWe
Air Separation Unit Auxiliaries	1,000	1,000	1,000	kWe
ASU Main Air Compressor	53,820	67,330	67,330	kWe
Oxygen Compressor	10,260	10,640	10,640	kWe
Nitrogen Compressor	33,340	35,640	35,640	kWe
Other Auxiliaries ³	17,290	18,330	17,406	kWe
Quench Water Pump	520	540	540	kWe
Ground Water Pump	430	530	530	kWe
Scrubber Pumps	220	230	230	kWe
AGR Removal	2,590	19,230	-	kWe
AC-ABC CO ₂ & H ₂ S Capture	-	-	3,576	kWe
Claus Plant/TGTU Auxiliaries	250	250	-	kWe
Pressure Swing Claus Auxiliaries	-	-	4,697	kWe
Tail Gas Recycle Compressor	2,090	1,780	-	kWe
CO ₂ Compressor	-	31,160	16,861	kWe
TOTAL AUXILIARIES	125,750	190,750	162,539	kWe
Net Plant Performance				
Auxiliary Load	125,750	190,750	162,539	kWe
NET PLANT POWER	622,050	543,250	551,634	kWe
Net Plant Efficiency (HHV)	39.0%	32.6%	33.1%	
CONSUMABLES				
Coal Feed Flowrate	466,898	487,005	487,005	lb/hr
Thermal Input ¹	1,596,309	1,665,074	1,665,075	kWth
CO₂ CAPTURE PERFORMANCE				
CO ₂ Captured	-	1,005,720	1,000,970	lb/hr
CO ₂ Removal	-	90%	90.1%	

1 – HHV of as-received Illinois No. 6 coal is 27,135 kJ/kg (11,666 Btu/lb)

2 – Includes plant control systems, lighting, HVAC, and miscellaneous low-voltage loads

3 – Includes boiler feed-water pumps, condensate pumps, circulating water pump, cooling tower fans, gas turbine auxiliaries, steam turbine auxiliaries, miscellaneous balance of plant and transformer losses.

COST ADVANTAGES OF AC-ABC PROCESS

In summary, the AC-ABC process has many advantages over Selexol-based processes.

1. The advantage of parasitic electric power consumption with the AC-ABC process over the Selexol process is considerable as described below.
 - a. The CO₂ stripping in the AC-ABC process can be accomplished at elevated pressures in the range of 300-750 psig, resulting in a 3 to 7.5 pressure ratio to compress the gas to the pipeline pressure of 2,215 psia. In the Selexol process, the pressure ratio of the CO₂ compressor is 100-150, requiring five stages of compression to achieve the pipeline pressure and consuming a significant amount of electrical energy.
 - b. The AC-ABC process does not require compressors other than the CO₂ compressor. The Selexol process deploys additional high-pressure-ratio compressors to return flashed syngas to the main syngas stream in both the CO₂ absorber and in the sulfur enrichment step prior to H₂S stripping.
 - c. High CO₂ loading and high-pressure CO₂ strippers in the AC-ABC process reduce the pumping power between the absorber and the regenerator compared to the Selexol process, in which lower CO₂ loading is combined with pumping the solvent from almost-ambient pressure in the CO₂ stripping to the higher absorber pressure.
 - d. The AC-ABC process has these characteristics:
 - No steam injection is required to enhance the shift reaction.
 - The steam consumption to strip the H₂S is a small fraction of the heat consumption of the Selexol process for H₂S stripping.
 - The heat consumption for CO₂ stripping is high compared to no steam for CO₂ stripping in the Selexol process. However, using the hot syngas as the main heat source for the CO₂ stripping instead of using IP steam would reduce the power output penalty.
2. The net power production in the case of CO₂ capture by the AC-ABC process with limited shift and BPSC is 8.4 MWe higher compared to the case in which Selexol solvent is used.
3. The capital cost of an IGCC plant using the AC-ABC process for AGR is 10.4% lower than the same IGCC plant using the Selexol process due to reduced equipment sizes and complexity.
 - Absorption of the H₂S and the CO₂ in the same absorber vessel allows for the elimination of the separate H₂S absorber vessel and its auxiliary equipment.
 - H₂S enrichment is eliminated in the vessel and clean gas-stripping compressor.
 - Stripping of the H₂S together with the CO₂ results in the elimination of H₂S stripper and its auxiliary equipment.
 - Using the pressure-swing Claus process results in the elimination of the Claus plant and the tail gas treatment, which are replaced with a simple, low-cost, and low-energy system to convert the H₂S to elemental sulfur in-situ in the high-pressure CO₂ stream.

- High-pressure CO₂ stripping results in a simple, low-cost, and low-power CO₂ compressor with single-stage intercooling compared to a large, costly compressor with multiple intercoolers for the Selexol CO₂ compressor.
 - There is virtually no hydrogen dissolution in the AC-ABC solvent, resulting in no hydrogen loss and no need for recycling of gas streams by using compression back into the syngas.
4. Considering only the capital costs of the sour gas shift, CO₂ removal and compression, and H₂S capture and recovery steps, the AC-ABC/BPSC process is only 52% of the cost of the Selexol/Claus process.

SENSITIVITY ANALYSES

Several sensitivity analyses were carried out to determine the effect on net plant power output, capital cost, cost of electricity (COE), and CO₂ avoided and captured costs of process variables such as syngas composition in the inlet to AC-ABC, CO₂ capture efficiency, and process steam usage. Each sensitivity case was modeled in Aspen Plus, with the power island modeled in GT Pro. The contributions to costs from the BPSC process for H₂S recovery were assumed to be constant in each of the sensitivity cases. Capital costs were calculated using the same methods described earlier. The cases studied are listed below, and results are summarized in Table 22.

Case 1: Increased (50 mol%) CO₂ concentration in inlet syngas to AC-ABC

Case 2: Increased H₂S concentration (1.5 mol%) in inlet syngas to AC-ABC

Case 3A: AC-ABC captures only 99% of CO₂ in inlet syngas

Case 3B: AC-ABC captures only 90% of CO₂ in inlet syngas

Case 4A: Steam usage 20% lower than expected

Case 4B: Steam usage 20% higher than expected

Table 22. Summary of sensitivity analysis results.

	Net Power (kWe)	Total Overnight Cost (2015 \$)	COE (% increase over GEE IGCC Without Capture)	Avoided Cost (\$/metric ton)	Cost of CO ₂ Captured (\$/metric ton)
Base Case	551,634	\$2,043,373	30.5%	\$37.96	\$26.79
Case 1	545,248	\$2,078,030	33.1%	\$38.50	\$28.08
Case 2	551,639	\$2,043,945	30.5%	\$38.57	\$27.22
Case 3A	557,364	\$2,043,778	29.2%	\$36.51	\$25.31
Case 3B	546,530	\$2,055,559	32.1%	\$40.29	\$29.02
Case 4A	560,372	\$2,043,373	28.6%	\$36.17	\$24.81
Case 4B	544,056	\$2,043,373	32.2%	\$39.52	\$28.50

Case 1: Effect of CO₂ Concentration of Inlet Syngas to AC-ABC

Case 1 considers the effect of increasing the CO₂ concentration in the syngas exiting the water-gas shift reactors and entering the AC-ABC process from 38 to 50 mol percent. The total flow rate of the syngas was assumed to remain constant, so the flow rates of the non-CO₂ components were reduced proportionally. It was assumed for this case that the processes upstream of AC-ABC (i.e., the water-gas shift reactors) remained unchanged.

The main effects of the increased CO₂ concentration were that: (1) the capital costs of the process increased by 1.6% due to the need for a larger regenerator and reboiler, and (2) the net power output of the plant decreased by 1.2% due to the greater steam requirements to regenerate the extra CO₂ within the AC-ABC process. Overall, this case resulted in an 8.5% increase in COE and a 4.8% increase in the cost of CO₂ captured.

Case 2: Effect of H₂S Concentration of Inlet Syngas to AC-ABC

Case 2 considers the effect of increasing the H₂S concentration in the syngas exiting the water-gas shift reactors and entering the AC-ABC process from 0.6 to 1.5 mol percent. The total flow rate of the syngas was assumed to remain constant, so the flow rates of the non-H₂S components were reduced proportionally. It was assumed for this case that the processes upstream of AC-ABC (i.e., the water-gas shift reactors) remained unchanged.

Increasing the H₂S concentration had an insignificant effect on the net power output of the plant and the capital costs. The AC-ABC solvent easily absorbs the additional H₂S, and the heat required for regeneration is not much more than in the base case because the amount of H₂S in the rich solution is still small compared to the amount of CO₂. The avoided cost and cost of CO₂ captured are higher in Case 2 than in the base case only because of the assumption that the total flow rate of the inlet syngas to AC-ABC remains unchanged, which leads to a lower flow rate of CO₂ through AC-ABC, which in turn decreases the total CO₂ captured by the process.

Case 3: Effect of AC-ABC CO₂ Capture Efficiency

Case 3A considers what would happen if the AC-ABC process were only able to capture 99% of the CO₂ in the syngas instead of the > 99.9% capture in the base case. In order to meet the 90% carbon capture target if only 99% of the CO₂ can be captured by AC-ABC, the conversion of CO to CO₂ in the water-gas shift reactors must be higher than in the base case. The base case did not require the addition of high-pressure steam before the water-gas shift reactors, but in order to increase the CO to CO₂ conversion in Case 3A it was necessary to add a small steam stream (800 psia, 20,000 lb/h). This stream is much smaller than the added steam in Case 3B or the Selexol case (Case B5B in the DOE reports).

The main effects of the decreased capture efficiency were: (1) the capital costs of the process increased very slightly due to larger water-gas shift reactors, and (2) the net power output of the plant increased by 1.0% due to the larger flow rate and higher heat capacity of the syngas that resulted from the steam addition, yielding a greater amount of heat that could be recovered from the syngas between/after the water-gas shift reactors. This increased heat recovery decreased the amount of intermediate-pressure steam that needed to be taken from the turbine and used in the AC-ABC reboiler substantially, which was enough to offset the power output penalty that resulted from the need to take the small high-pressure steam stream from the steam turbine. Overall, this case resulted in a 4.3% decrease in COE and a 5.4% decrease in the cost of CO₂ captured.

Case 3B considers what would happen if the AC-ABC process were only able to capture 90% of the CO₂ in the syngas instead of the > 99.9% capture in the base case. In order to meet the 90% carbon capture target if only 90% of the CO₂ can be captured by AC-ABC, a near-complete conversion of CO to CO₂ in the water-gas shift reactors is required. Therefore, the elimination of added steam to the water-gas shift reactor in the base case is no longer valid. As in the Selexol case (Case B5B in the DOE reports), a high-pressure steam stream (800 psia, 285,691 lb/h) must be taken from the steam turbine and fed to the first water-gas shift reactor.

The main effects of the decreased capture efficiency were: (1) the capital costs of the process increased by 0.6% due to larger water-gas shift reactors, and (2) the net power output of the plant decreased by 1.0% due to the high-pressure steam stream that was taken from the steam turbine, reducing plant power output. Part of this steam usage penalty, however, was made up for by the increased amount of heat that could be recovered from the syngas between/after the water-gas shift reactors due to the larger flow rate and higher heat capacity of the syngas that resulted from the steam addition. Overall, this case resulted in an 8.3% increase in COE and a 5.2% increase in the cost of CO₂ captured.

Case 4: Effect of Steam Usage

Case 4A considers what would happen if the AC-ABC process required 20% less steam than currently predicted in the base case to regenerate the captured CO₂. It was assumed that equipment sizes and costs were unchanged from the base case. The only change from the base case is that 20% less steam is extracted from the IP turbine.

The effect of the decreased steam usage was that the power plant output increased by 1.6%, which resulted in a 6.2% lower COE and a 7.4% lower CO₂ capture cost as compared to the base case.

Case 4B considers what would happen if the AC-ABC process required 20% more steam than currently predicted in the base case to regenerate the captured CO₂. It was assumed that equipment sizes and costs were unchanged from the base case. The only change from the base case is that 20% more steam is extracted from the IP turbine.

The effect of the decreased steam usage was that the power plant output decreased by 1.4%, which resulted in a 6.6% higher COE and a 6.4% higher CO₂ capture cost as compared to the base case.

APPENDIX A

Equipment Cost List for AC-ABC Process

Table 23. Equipment costs for AC-ABC and BPSC process.

Equipment	Size	Unit	Cost, 2011
Absorber			
<u>Column</u>			
316 SS column	64	height (ft)	\$5,898,640
	20	diameter (ft)	
Packing (3.5" SS pall rings)	8	stages	\$4,022,114
<u>Cooler on top absorber recycle stream</u>			
Cooling duty - top absorber recycle cooler	-1.92E+08	Btu/h	
Plate and frame exchanger area	112815	sqft	\$2,989,006
<u>Pumps on absorber recycle loops</u>			
Pump duty (lower absorber recirculation pump)	171	hp	
Electrical usage (kW)	127	kW	\$1,056,646
Pump duty (upper absorber recirculation pump)	806	hp	
Electrical usage (kW)	601	kW	\$744,449
Regenerator			
<u>Column</u>			
316 SS column	40	height (ft)	\$2,764,283
	14	diameter (ft)	
Trays (316 SS valve trays)	8	trays	\$77,005
<u>Reboiler</u>			
Reboiler duty	7.65E+08	Btu/h	
Reboiler (316 SS floating head exchanger)	31250	sqft	\$1,781,318
Lean/Rich Recirculation Equipment			
<u>Lean/Rich Heat Exchanger</u>			
Exchanger duty	8.46E+08	Btu/h	
Exchanger area (316 SS, plate and frame exchanger)	254626	sqft	\$6,473,162
<u>Rich/Lean circulation pump (from regenerator to absorber)</u>			
Pump duty	3673	hp	
Electrical usage (kW)	2739	kW	\$156,205
<u>Cooler on lean stream</u>			
Cooling duty - lean stream cooler	-5.59E+08	Btu/h	
Exchanger area (316 SS, plate and frame exchanger)	73834	sqft	\$1,599,425
Water Washes			
<u>Absorber Water Wash Column</u>			
316 SS column	14	height (ft)	\$625,636
	6.8	diameter (ft)	
Trays (316 SS valve trays)	2	trays	\$5,177

<u>Cooler on water wash recycle stream</u>			
Cooling duty - water wash recycle cooler	-4.12E+05	Btu/h	
Exchanger area (316 SS, floating head exchanger)	203	sqft	\$49,388
<u>Absorber Water Wash Pumps</u>			
Pump duty (water wash recirculation pump)	30	hp	
Electrical usage (kW)	23	kW	\$49,854
Pump duty (water wash inlet water pump)	106	hp	
Electrical usage (kW)	79	kW	\$14,869
<u>Regenerator Water Wash Column</u>			
316 SS column	20	height (ft)	\$860,803
	7.9	diameter (ft)	
Trays (316 SS valve trays)	4	trays	\$13,468
<u>Regenerator Water Wash Pumps</u>			
Pump duty (regenerator water wash inlet water pump)	9.1	hp	
Electrical usage (kW)	6.8	kW	\$12,196
Sum of Equipment Costs			\$29,193,643
CAPITAL COST ESTIMATES			
Direct Costs			
Purchased equipment delivered	1		\$29,193,643
purchased equipment installation	0.47		\$10,554,625
Instrumentation & controls	0.36		\$8,084,393
Piping	0.68		\$19,851,677
Electrical	0.11		\$2,470,231
Buildings	0.18		\$4,042,197
Yard improvements	0.1		\$2,245,665
Service facilities	0.7		\$15,719,654
Total Direct Plant Cost (~bare erected cost in (NETL 2015))			\$92,162,084
Indirect Costs			
Engineering, construction, & contractor's fee	0.1		\$2,919,364
Contingency (Process)	0.2		\$5,838,729
Contingency (Project)	0.2		\$20,184,035
Total indirect plant cost			\$28,942,128
Fixed Capital Investment (~Total plant cost in (NETL 2015), AC-ABC Only)			\$121,104,212
BPSC Equipment Costs			
Fixed capital investment (~Total Plant Cost in (NETL 2015), BPSC Only)			\$49,614,853
Other Changed Equipment Costs in IGCC Plant			
Water-Gas Shift Reactors (84% of base-case throughput)	1,308,800	Throughput (lb/h)	\$17,980,565
CO₂ Compressor	22610 16861	hp kW	\$17,212,379
Fixed capital investment (~Total Plant Cost in (NETL 2015), WGS Reactors and CO₂ Compressor Only)			\$35,192,943

Operating and Maintenance Cost Summary

Table 24. GEE IGCC with AC-ABC/ BPSC: initial/annual operating and maintenance costs.

INITIAL & ANNUAL O&M EXPENSES				Cost Base	2011
GEE Radiant 550 MW IGCC w/ SRI CO2 Capture and BPSC Sulfur Removal				Heat Rate-net (Btu/kWh):	9,636
				MWe-net	552
<u>OPERATING & MAINTENANCE LABOR</u>				Capacity Factor (%):	80
<u>Operating Labor</u>					
Operating Labor Rate (base):	39.70	\$ /hour			
Operating Labor Burden:	30.00	% of base			
Labor O-H Charge Rate:	25.00	% of labor			
Operating Labor Requirements (O.J.) per Shift:				<u>1 unit/mod.</u>	<u>Total Plant</u>
Skilled Operator				2.0	2.0
Operator				10.0	10.0
Foreman				1.0	1.0
Lab Techs, etc.				<u>3.0</u>	<u>3.0</u>
TOTAL-O.J.'s				16.0	16.0
					<u>Annual Unit Cost</u>
				<u>Annual Cost \$</u>	<u>\$/kW-net</u>
Annual Operating Labor Cost				\$7,233,658	\$13.316
Maintenance Labor Cost				\$18,843,231	\$34.687
Administrative & Support Labor				\$6,519,222	\$12.001
Property Taxes & Insurance				\$36,802,296	\$67.747
TOTAL FIXED OPERATING COSTS				\$69,398,406	\$127.751
<u>VARIABLE OPERATING COSTS</u>					<u>\$/kWh-net</u>
Maintenance material cost					\$31,671,981
<u>Consumables</u>	<u>Initial Fill</u>	<u>/day</u>	<u>unit cost</u>	<u>initial fill cost</u>	
Water (/1000 gallons)		3412.6	1.67		\$1,664,120
Chemicals					\$0.00044
MU & WT Chem. (lb)	0	24994	0.27	\$0	\$1,970,525
Carbon (Mercury Removal) (lb)	135009	231	5.5	\$742,550	\$370,511
COS Catalyst (m3)	0	0	2397.36	\$0	\$0
WGS Catalyst (ft3)				\$4,057,07	
	5255	4	771.99	0	\$811,778
Selexol Solution (gal)	0	0	36.79	\$0	\$0
BPSC Catalyst (m3)	0	0	0	\$0	\$266,667
Ammonia (19% NH3) (ton)	441	1	263	\$116,045	\$56,215
Claus Catalyst (ft3)	w/equip	0	203.15		\$0
Subtotal-Chemicals				\$4,915,664	
				4	\$5,139,816
Other					\$0.00091
Supplemental Fuel (Mbtu)	0	0	0	\$0	\$0
Gases, O2, N2 etc. (/100 scf)	0	0	0	\$0	\$0

LP Steam (/1000 pounds)	0	0	0	\$0	\$0	\$0.00000
Subtotal-Other				\$0	\$0	\$0.00000
Waste Disposal						
Spent Mercury Catalyst (lb)	0	231	0.65	\$0	\$43,788	\$0.00001
Fly-ash (ton)	0	0	0	\$0	\$0	\$0.00000
Slag (ton)	0	640	25.11	\$0	\$4,693,875	\$0.00123
Subtotal Waste Disposal				\$0	\$4,737,662	\$0.00125
Byproducts & Emissions	0	0	0	\$0	\$0	\$0.00000
Sulfur (ton)	0	0	0	\$0	\$0	\$0.00000
Subtotal Byproducts				\$0	\$0	\$0.00000
TOTAL VARIABLE OPERATING COSTS				\$4,915,664	\$41,549,459	\$0.00260
Fuel (ton)	0	5837	68.54	\$0	\$116,810,277	\$0.03070

Table 25. DOE Case B5B: initial and annual operating and maintenance costs (NETL 2015).

Case:	B5B – GEE Radiant IGCC w/ CO ₂			Cost Base:	Jun 2011	
Plant Size (MW _{net}):	543	Heat Rate-net (Btu/kWh):	10,459	Capacity Factor (%):	80	
Operating & Maintenance Labor						
Operating Labor			Operating Labor Requirements per Shift			
Operating Labor Rate (base):	39.70	\$/hour	Skilled Operator:	2.0		
Operating Labor Burden:	30.00	% of base	Operator:	10.0		
Labor O-H Charge Rate:	25.00	% of labor	Foreman:	1.0		
			Lab Tech's, etc.:	3.0		
			Total:	16.0		
Fixed Operating Costs						
				Annual Cost		
				(\$)	(\$/kW-net)	
Annual Operating Labor:				\$7,233,658	\$13.316	
Maintenance Labor:				\$18,843,231	\$34.687	
Administrative & Support Labor:				\$6,519,222	\$12.001	
Property Taxes and Insurance:				\$36,802,296	\$67.747	
Total:				\$69,398,406	\$127.751	
Variable Operating Costs						
				(\$)	(\$/MWh-net)	
Maintenance Material:				\$35,348,580	\$9.28526	
Consumables						
	Consumption				Cost (\$)	
	Initial Fill	Per Day	Per Unit	Initial Fill		
Water (/1000 gallons):	0	4,201	\$1.67	\$0	\$2,053,253	\$0.53934
Makeup and Waste Water Treatment Chemicals (lbs):	0	25,026	\$0.27	\$0	\$1,957,230	\$0.51412
Carbon (Mercury Removal) (lb):	135,182	231	\$5.50	\$743,501	\$371,751	\$0.09765
Shift Catalyst (ft ³):	6,246	4.28	\$771.99	\$4,822,025	\$964,405	\$0.25333
Selexol Solution (gal):	298,498	95	\$36.79	\$10,982,126	\$1,020,094	\$0.26796
Claus Catalyst (ft ³):	w/equip	2.01	\$203.15	\$0	\$119,487	\$0.03139
Subtotal:				\$16,547,652	\$6,486,219	\$1.70378
Waste Disposal						
Spent Mercury Catalyst (lb.):	0	231	\$0.65	\$0	\$43,941	\$0.01154
Flyash (ton):	0	0	\$0.00	\$0	\$0	\$0.00000
Slag (ton):	0	641	\$25.11	\$0	\$4,701,292	\$1.23492
Subtotal:				\$0	\$4,745,232	\$1.24646
By-Products						
Sulfur (tons):	0	146	\$0.00	\$0	\$0	\$0.00000
Subtotal:				\$0	\$0	\$0.00000
Variable Operating Costs Total:				\$16,547,652	\$46,580,031	\$12.23551
Fuel Cost						
Illinois Number 6 (ton):	0	5,844	\$68.54	\$0	\$116,961,258	\$30.72304
Total:				\$0	\$116,961,258	\$30.72304



Figure 79. A photograph of the AC-ABC pilot plant at the NCCC.



Figure 80. A photograph of the AC-ABC process skids.



Figure 81. A photograph of sulfur recovery reactors.



Figure 82. A photograph of skid B-1 with sulfur condensers.

CONCLUSIONS

Based on the test results from the two test campaigns and the techno-economic analysis results, the AC-ABC technology is able to meet DOE's performance goal of 90% CO₂ capture with a cost of CO₂ capture much lower than the DOE goal of \$40/ton of CO₂ and with significant system availability even at the small pilot-scale level.

The following conclusions can be drawn:

- The ammoniated solution is very effective in rapid absorption of CO₂ with high CO₂ loading at elevated pressure. CO₂ capture efficiency greater than 99% was demonstrated, with 12% CO₂ effective loading.
- H₂S can be simultaneously absorbed along with CO₂ in a single absorber column. The H₂S capture efficiency was greater than 99%.
- The absorption and thus loss of fuel gas species like H₂, CO, and CH₄ were shown to be very low.
- There was low ammonia loss from the system.
- Both the absorber and regenerator were operated at similar elevated pressure, thus reducing the need for pumping solvents across pressure boundaries.
- Simultaneous stripping of CO₂ and H₂S was demonstrated in a single column at elevated pressure and moderate temperature.
- The Bechtel Pressure-Swing Claus Process (BPSC) process demonstrated conversion of H₂S to high-purity elemental sulfur, and a clean CO₂ gas stream at elevated pressure was available for sequestration or transportation.
- Availability of regenerated CO₂ at elevated pressure significantly reduced the compressor requirements for CO₂ sequestration.
- The techno economic analysis showed the cost of CO₂ capture using AC-ABC/BPSC process from IGCC gas stream was less than \$30/metric ton of CO₂

Solvent-based technologies have proven themselves to be effective and relatively easy to operate compared to some of the newer technologies for CO₂ capture. The equipment for solvent technologies, i.e., pumps, valves, heat exchangers, etc., is readily available, and the scale-up factors and challenges are well understood in the industry. We do not envision any new custom-built equipment, which will increase the likelihood of success at larger-scale demonstration level. System modeling tools, property methods, and solvent performance data are well developed and

documented and are readily available and require few assumptions and extrapolations. The ammoniated solution used in this process is readily available. The low cost of the solvent coupled with demonstrated low losses from the process significantly reduced the operating costs of the plant. There is a vast industrial experience in ammonia-based processes including operation of sour-water strippers across refineries and other industries. With the long-term goal to sequester and/or utilize CO₂ instead of venting it to the atmosphere, the availability of high-pressure CO₂ from this process offers a unique benefit over the currently available technologies. Although the commercial interest in the IGCC for power generation has declined over the past few years, there is a potential for this technology to be used for other syngas applications such as the production of ammonia and other chemicals, for acid gas removal from biomass gasification, and for acid gas removal from natural gas and other hydrocarbon streams.

REFERENCES

- Environmental Protection Agency (EPA) proposed new source performance standard on April 13, 2012, for emission of carbon dioxide for a new fossil fuel fired electric utility generating unit.
- Field, J. H., G. E. Johnson, H. E. Benson, and J. S. Tosh, "Removing Hydrogen Sulfide by Hot Potassium Carbonate Solution," U.S. Bureau of Mines Reports of Investigation No. 5660 (1960).
- Nagar, A., SRI International. *CO2 Capture from IGCC Gas Streams using the AC-ABC Process. Quarterly Progress Report 27 (April-June 2016)*. SRI International, July 2016.
- National Energy Technology Laboratory (NETL). "*Cost and Performance Baseline for Fossil Energy Plants, Volume 1b: Bituminous Coal (IGCC) to Electricity*," Revision 2b. DOE/NETL, July 2015.
- National Energy Technology Laboratory (NETL). "*Cost and Performance Baseline for Fossil Energy Plants, Volume 1: Bituminous Coal and Natural Gas to Electricity*," Final Report, Revision 2. DOE/NETL, 2010.
- National Energy Technology Laboratory (NETL). "*Quality Guidelines for Energy Systems Studies*."
- National Energy Technology Laboratory (NETL). "*Quality Guidelines for Energy Systems Studies – Process Modeling Design Parameters*." DOE/NETL, May 2014.
- Perry, J. Chemical Engineering Handbook, 5th edition, pp 3-101 to 3-103 (1973).
- Peters, M., Timmerhaus, K., and West, R., *Plant Design and Economics for Chemical Engineers*, McGraw Hill, 2003.
- Shoor, S. K., R. D. Walker, and K. E. Gubbins, "Salting out of Nonpolar Gases in Aqueous Potassium Hydroxide solution," *J. Phys. Chem.*, 73, 312-317 (1966).
- Towler, G., and Sinnott, R., *Chemical Engineering Design: Principles, Practice and Economics of Plant and Process Design*, Elsevier, 2013.